

Effect of Heat Stress on Reproductive Development of Wheat (*Triticum aestivum* L.)

by

Kumarapeli Arachchige Dinithi Vishvanie Kumarapeli

A thesis submitted in partial fulfillment of the requirements for the degree of

Master of Science

in

Plant Science

Department of Agricultural, Food and Nutritional Science
University of Alberta

© Kumarapeli Arachchige Dinithi Vishvanie Kumarapeli, 2021

Abstract

Rising global atmospheric temperature can negatively affect the reproductive development of crops including wheat (*Triticum aestivum* L.) which can ultimately lead to a reduction in seed set and yield. The aim of this study was to determine the effect of moderate heat stress (35 °C for 6 h per day for 8 days) imposed during early flowering (beginning at BBCH 37 stage; when the flag leaf is just visible) on the reproductive morphology, pollen viability, and grain yield in selected heat-sensitive and heat-resistant recombinant inbred lines (RILs) of wheat derived from a 'CDC Go' X 'Attila' RIL population where the parents segregate for heat resistance with respect to grain yield. A general response to heat stress across the RILs and parental lines was to reduce the growth of the main tiller and anthers potentially allowing the sensitive stages of reproductive development to complete with reduced exposure to the negative effects of heat stress. Reduction of tiller growth under heat stress could also facilitate an adequate supply of photoassimilate to developing grains. The most heat-sensitive RIL assessed (RIL 131) exhibited reduced pollen viability and an increase in ovule size under heat stress conditions at anthesis indicating abnormal reproductive development. The spike and spikelet length at anthesis were also greater in RIL 131 under heat stress conditions suggesting a more favorable partitioning of assimilates to the tissues that will surround the developing grain which may negatively affect grain development. Heat-resistant RILs maintained grain yield under heat stress by maintaining pollen viability and ovule size indicative of normal reproductive development. Reduced spikelet length also appeared to be a common trait in heat-resistant lines, indicative of more favorable partitioning of assimilates to the developing grain than the surrounding floral structures.

The application of 4-Cl-IAA prior to heat stress in RIL 137 increased grain yield under heat stress conditions but did not affect any morphological parameters assessed. These data suggest that auxin potentially facilitated photoassimilate partitioning to the developing grains thereby maintaining grain yield under heat stress conditions.

The presence of *Rht-B1b* mutant allele in the heat-sensitive RIL 131 and parent ‘CDC Go’ may enhance the photoassimilate supply to developing florets under control conditions by reducing stem elongation, but this alone did not improve grain yield under heat stress in these lines. Overall, these data confirm previous studies that heat stress can negatively affect reproductive development in wheat reducing grain yield. Heat-resistant RILs maintained normal grain yield under heat stress by maintaining pollen viability, reducing the growth of tillers and anthers potentially to complete development more rapidly to minimize exposure heat stress, and reducing growth in other tissues peripheral to the developing grains to facilitate adequate photoassimilate supply to the latter.

Key words; Grain yield, Heat stress, Reproductive development, RIL

Preface

All the experiments in this thesis were designed by Dr. Jocelyn A. Ozga (Plant BioSystem Group, Department of Agricultural, Food and Nutritional Science, University of Alberta). The auxin (4-Cl-IAA) and adjuvant (Agral) solutions used in this study were prepared by Dr. Dennis M. Reinecke (University of Alberta). I performed the experiments, and collected, organized, and analysed the data for all experiments presented in this thesis except for the *Rht* PCR experiment. For the *Rht* PCR experiment, Dr. Harleen Kaur (University of Alberta) performed the genomic DNA extractions, chose the PCR primers, and assisted in setting up the PCR experiment. I ran the PCR reactions and the gels for this experiment.

Acknowledgement

I would like to thank number of peoples who have helped me to successfully complete this research project. First and foremost, I am extremely grateful to my supervisor Dr. Jocelyn Ozga for valuable guidance, continuous support, and encouragement during my master's project. My gratitude extends to Dr. Stephen Strelkov and Dr. Boyd Mori for being on my graduate committee and their insightful comments and valuable inputs to this research project. My sincere gratitude also goes to Dr. Dennis Reinecke for preparing the solutions required for hormone application. Besides that, I would like to thank Dr. Rong-Cai for his kind support for statistical analysis. I would also like to thank Dr. Dean Spaner and his group for initially providing the wheat seeds required for this project. My gratitude also goes to Dr. Sheri Strydhorst for taking the time to provide me with the pictures that I requested for my thesis. Further, I would like to thank Dr. Harleen Kaur for helping me to setting up the PCR experiment and numerous other ways.

I would also like to thank Arlene Oatway for taking the time and effort to help me out with troubleshooting the problems that I have encountered during the microscopy studies. My gratitude also goes to Bin Shan for technical assistance and providing an extra pair of hands during this project. I would specially like to thank Nikki-Karyssa Scott, Kelly Dunfield, Urmila Basu, and Holly Horvath for friendly support through out my studies. I am also thankful to Dhanuja Abeysingha for providing me with the initial data required for this project and helping me to carried out the hormone applications. I also would like to appreciate Dhanuja Abeysingha and Dr. Charitha Jayasinghege for taking time to provide comments on this thesis. Thank you my lab group for all your help, friendship and lovely companionship which made this journey easy.

Further, I would like to sincerely acknowledge the financial support provided by the Natural Sciences and Engineering Research council of Canada and Alberta Wheat Commission to my supervisor for this project. I am also grateful for the Robert Simonet graduate scholarship and Michael R Bevan graduate scholarship received from the Faculty of Graduate Studies and Research at University of Alberta and Alberta Wheat Commission Graduate Research scholarship in Crop Science.

Finally, my heartfelt gratitude goes to my loving parents for their constant love and support and keep me motivated and confident to achieve best in my life. I cannot begin to express my gratitude and appreciation for all my Sri Lankan friends. I am grateful beyond words to Dilini, Dilhara, Dakshina, Charitha, Dhanuja, Nimesh for taking care of me and helping me to adjust new environment in Canada. Special thanks go to Dilini and Dilhara for providing me accommodation for last month of my degree program. Last but not least, I would like to thank all my friends Brasathe, Ranithri, Anusha and Chandila, Kethmi and Dinuka, Shakila and Ravindra, Lalani and Chandana, Dilrukshi and Ishan, Iswarya for your kindness and supportive hands.

Table of Contents

Abstract.....	ii
Preface.....	iv
Acknowledgement	v
List of Tables	x
List of Figures	xv
List of Abbreviations	xvii
1. INTRODUCTION	1
1.1 Bread wheat origin and production	1
1.2 Reproductive development of wheat.....	3
1.3 Role of plant hormones during reproductive development.....	9
1.4 Effect of heat stress on plant reproductive development	12
1.4.1 Impact of heat stress on anther and pollen development.....	13
1.4.2 Impact of heat stress on hormonal regulation of anther and pollen development.....	15
1.4.3 Impact of heat stress on female reproductive development and early grain set	16
1.4.4 Wheat grain growth and development.....	17
1.4.5 Effect of heat stress on grain growth and development.....	18
1.5 Breeding for heat tolerance in wheat.....	21
1.6 Recombinant inbred lines (RIL).....	22
1.7 <i>Rht</i> alleles	23
1.8 Thesis hypothesis	24
Specific Thesis Objectives	24
2. MATERIALS AND METHODS.....	25
2.1 Morphological characterization of the effect of heat stress on reproductive development	25
2.1.1 Plant material.....	25
2.1.2 Plant growth conditions, heat stress treatment, and morphological trait sample collection	26
2.1.3 Assessment of auricle distance, spike length and spikelet length	27
2.1.4 Pollen viability and anther length.....	28
2.1.5 Ovule measurements.....	29
2.1.6 Grain yield parameters.....	31
2.1.7 Histology	31

2.2 Effect of 4-Cl-IAA application on grain yield	33
2.3 <i>Rht</i> allele identification	33
2.3.1 Plant growth conditions and sample collection	33
2.3.2 Genomic DNA extraction	34
2.3.3 Primers	35
2.3.4. PCR amplification	35
2.4 Statistical analyses	35
3. RESULTS	37
3.1 Morphological characterization of the effect of heat stress on wheat reproductive development	37
3.1.1 Effect of heat stress on auricle distance and spike length	37
3.1.2 Effect of heat stress on spikelet length	39
3.1.3 Effect of heat-stress on pollen viability	42
3.1.4 Effect of heat stress on anther length	45
3.1.5 Effect of heat stress on pollen morphology	48
3.1.6 Wheat carpel structure prior to fertilization	50
3.1.7 Effect of heat stress on ovule and embryo sac size	51
3.1.8 Effect of heat stress on grain yield	55
3.2 Effect of 4-Cl-IAA application on grain yield	66
3.3 <i>Rht-B1</i> allele determination	70
4. DISCUSSION	71
4.1 Reduction of auricle distance is a general response to heat stress in wheat	71
4.2 Spikelet length, a potential indicator of developing grains within the spikelet grown under heat stress conditions	72
4.3 Reduction in anther length, a general response to heat stress in wheat lines	73
4.4 Pollen viability decreased with heat stress	73
4.5 Enlargement in ovule tissue with heat-stress was observed in heat-sensitive RIL 131	74
4.6 Heat-resistant RIL 123 maintained normal pollen viability and ovule size, and reduced spikelet growth facilitating normal grain yield under heat stress, and the heat-sensitive RIL 131 did not	74
4.7 The application of 4-Cl-IAA increased the grain weight in RIL 137 without affecting other morphological parameters tested	75
4.8 The presence of <i>Rht</i> mutant allele in ‘CDC Go’ and RIL 131 did not confer higher grain yield under heat stress	76

4.9 Summary	78
5. CONCLUSIONS.....	79
5.1 Heat stress reduces tiller and anther length in wheat	79
5.2 The negative effects of heat stress on pollen viability, and ovule size could lead to a reduction in grain yield in lines highly sensitive to heat stress.....	80
5.3 Increased growth of spikelets could decrease photoassimilate partitioning to developing grains	81
5.4 Auxin application increases the grain yield of RIL 137.....	81
5.5 Future perspectives.....	81
References.....	83
Appendix.....	98

List of Tables

Table	Page
2.1	Average days to anthesis of selected heat-resistant and heat-sensitive RILs and parents grown in a growth chamber at 20 °C/17 °C (light /dark),16 h photoperiod.....25
2.2	List of primer sequences35
3.1	Effect of heat stress on auricle distance and spike length of the main tiller of selected heat-resistant and heat-sensitive RILs and parents.....38
3.2	The effect of heat-stress on spikelet length from the basal, central, and distal regions of the main tiller of selected heat-resistant RILs and parent ‘Attila’40
3.3	The effect of heat-stress on spikelet length from the basal, central, and distal regions of the main tiller of selected heat-sensitive RILs and parent ‘CDC Go’41
3.4	The effect of heat stress on percentage pollen viability in the basal, central, and distal regions of the main spike of selected heat-resistant RILs, and parent ‘Attila’43
3.5	The effect of heat stress on percentage pollen viability in the basal, central, and distal regions of the main spike of selected heat-sensitive RILs, and parent ‘CDC Go’44
3.6	The effect of heat stress on anther length in the basal, central, and distal regions of the main spike of selected heat-resistant RILs and parent ‘Attila’46
3.7	The effect of heat stress on anther length in the basal, central, and distal regions of the main spike of selected heat-sensitive RILs and parent ‘CDC Go’47
3.8	The effect of heat stress on the area and length of ovules from florets at the basal, central, and distal positions of the main tiller spike of heat-resistant and heat-sensitive RILs, and parents.....53
3.9	The effect of heat stress on the number of spikelets and fertile spikelets on the main tiller spike of heat-resistant and heat-sensitive RILs and parental lines.....57
3.10	The effect of heat stress on the number of fertile spikelets at the basal, central, and distal positions on the main tiller spike of heat-resistant RILs, and parent ‘Attila’58
3.11	The effect of heat stress on the number of fertile spikelets at the basal, central, and distal positions on the main tiller spike of heat-sensitive RILs, and parent ‘CDC Go’ ...59

3.12	The effect of heat stress on total grain weight and number of the main tiller spike of heat-sensitive and heat-resistant RILs and parental lines.....	60
3.13	The effect of heat stress on grain number at the basal, central, and distal regions of the main tiller spike of heat-resistant RILs, and parent ‘Attila’.....	61
3.14	The effect of heat stress on grain number at the basal, central, and distal regions of the main tiller spike of heat-sensitive RILs, and parent ‘CDC Go’.....	62
3.15	The effect of heat stress on grain weight at basal, central, and distal regions of the main tiller spike of heat-resistant RILs and parent ‘Attila’.....	63
3.16	The effect of heat stress on grain weight at basal, central, and distal regions of the main tiller spike of heat-sensitive RILs and parent ‘CDC Go’.....	64
3.17	The effect of 4-Cl-IAA application and heat stress on auricle distance, spike length, total grain weight and number, and number of spikelets and fertile spikelets per spike at the basal, central, and distal regions of the main tiller spike of RILs 80 and 137.....	67
3.18	The effect of 4-Cl-IAA application and heat stress on pollen viability, anther length, spikelet length, and grain weight and number at the basal, central, and distal regions of the main tiller spike of RIL 80.....	68
3.19	The effect of 4-Cl-IAA application and heat stress on pollen viability, anther length, spikelet length, and grain weight and number at the basal, central, and distal regions of the main tiller spike of RIL 137.....	69
A.1	The internode length of the main tiller of ‘Attila’ and ‘CDC Go’ plants at the flag-leaf emerging stage.....	99
A.2	Auricle distance ANOVA analysis degrees of freedom, F values, and probability for the temperature and RIL ID main effects, and temperature x RIL ID interaction presented in Table 3.1 of the thesis.....	104
A.3	Spike length ANOVA analysis degrees of freedom, F values, and probability for the temperature and RIL ID main effects, and temperature x RIL ID interaction presented in Table 3.1 of the thesis.....	104
A.4	Spikelet length ANOVA analysis degrees of freedom, F values, and probability for the temperature and spike region main effects, and temperature x spike region interaction presented in Tables 3.2 and 3.3 of the thesis.....	105

A.5	Pollen viability ANOVA analysis degrees of freedom, F values, and probability for the temperature and spike region main effects, and temperature x spike region interaction presented in Tables 3.4 and 3.5 of the thesis.....	106
A.6	Anther length ANOVA analysis degrees of freedom, F values, and probability for the temperature and spike region main effects, and temperature x spike region interaction presented in Tables 3.6 and 3.7 of the thesis.....	107
A.7	Ovule area and length ANOVA analysis degrees of freedom, F values, and probability for the temperature and spike region main effects, and temperature x spike region interaction presented in Table 3.8 of the thesis.....	108
A.8	Number of spikelets per spike ANOVA analysis degrees of freedom, F values, and probability for the temperature and RIL ID main effects, and temperature x RIL ID interaction presented in Table 3.9 of the thesis.....	108
A.9	Number of fertile spikelets per spike ANOVA analysis degrees of freedom, F values, and probability for the temperature and RIL ID main effects, and temperature x RIL ID interaction presented in Table 3.9 of the thesis.....	109
A.10	Number of fertile spikelets per spike ANOVA analysis degrees of freedom, F values, and probability for the temperature and spike region main effects, and temperature x spike region interaction presented in Tables 3.10 and 3.11 of the thesis.....	109
A.11	Total grain weight ANOVA analysis degrees of freedom, F values, and probability for the temperature and RIL ID main effects, and temperature x RIL ID interaction presented in Table 3.12 of the thesis.....	110
A.12	Total grain number ANOVA analysis degrees of freedom, F values, and probability for the temperature and RIL ID main effects, and temperature x RIL ID interaction presented in Table 3.12 of the thesis.....	110
A.13	Grain number ANOVA analysis degrees of freedom, F values, and probability for the temperature and spike region main effects, and temperature x spike region interaction presented in Tables 3.13 and 3.14 of the thesis.....	111

A.14	Grain weight ANOVA analysis degrees of freedom, F values, and probability for the temperature and spike region main effects, and temperature x spike region interaction presented in Tables 3.15 and 3.16 of the thesis.....	112
A.15	Total grain number and grain weight ANOVA analysis degrees of freedom, F values, and probability for the temperature and hormone treatment main effects, and temperature x hormone treatment interaction presented in Table 3.17 of the thesis.....	113
A.16	Auricle distance ANOVA analysis degrees of freedom, F values, and probability for the temperature and hormone treatment main effects, and temperature x hormone treatment interaction presented in Table 3.17 of the thesis.....	113
A.17	Spike length ANOVA analysis degrees of freedom, F values, and probability for the temperature and hormone treatment main effects, and temperature x hormone treatment interaction presented in Table 3.17 of the thesis.....	113
A.18	Number of spikelets per spike ANOVA analysis degrees of freedom, F values, and probability for the temperature and hormone treatment main effects, and temperature x hormone treatment interaction presented in Table 3.17 of the thesis.....	114
A.19	Number of fertile spikelets per spike ANOVA analysis degrees of freedom, F values, and probability for the temperature and hormone treatment main effects, and temperature x hormone treatment interaction presented in Table 3.17 of the thesis.....	114
A.20	Pollen viability ANOVA analysis degrees of freedom, F values, and probability for the temperature, hormone treatment, and spike region main effects, and temperature x hormone treatment, temperature x spike region, temperature x hormone treatment x spike region interaction presented in Tables 3.18 and 3.19 of the thesis.....	115
A.21	Anther length ANOVA analysis degrees of freedom, F values, and probability for the temperature, hormone treatment, and spike region main effects, and temperature x hormone treatment, temperature x spike region, temperature x hormone treatment x spike region interaction presented in Tables 3.18 and 3.19 of the thesis.....	115

- A.22 Spikelet length ANOVA analysis degrees of freedom, F values, and probability for the temperature, hormone treatment, and spike region main effects, and temperature x hormone treatment, temperature x spike region, temperature x hormone treatment x spike region interaction presented in Tables 3.18 and 3.19 of the thesis116
- A.23 Grain number ANOVA analysis degrees of freedom, F values, and probability for temperature, hormone treatment, and spike region main effects, and temperature x hormone treatment, temperature x spike region, temperature x hormone treatment x spike region interaction presented in Tables 3.18 and 3.19 of the thesis.....116
- A.24 Grain weight ANOVA analysis degrees of freedom, F values, and probability for the temperature, hormone treatment, and spike region main effects, and temperature x hormone treatment, temperature x spike region, temperature x hormone treatment x spike region interaction presented in Tables 3.18 and 3.19 of the thesis.....117

List of Figures

Figures	Page
1.1 Terminal spikelet initiation stage of wheat RIL 28.....	4
1.2 The structure wheat floral spike.....	5
1.3 Late boot stage of wheat with swollen flag leaf sheath, BBCH 45.....	5
1.4 Transverse sections of anthers from wheat cultivars Halberd and Cranbrook over development (stages 1-15)	7
1.5 Developing wheat anther at stage 11 (vacuolated pollen stage) of ‘Attila’	8
1.6 Grain development using the BBCH scale.....	18
2.1 Wheat ovule at anthesis after pistil clearing.....	30
3.1 Representative micrographs of the cross sections of anthers at approximately stage 11 from heat-sensitive RIL 131 and heat-resistant RIL 123.....	49
3.2 Wheat floret and carpel structure prior to anthesis.....	50
3.3 Representative micrographs of ovules within the carpels from heat-resistant and heat-sensitive RIL obtained from the central region of the spike grown under control or heat stress conditions	52
3.4 Representative micrographs of ovules from florets at anthesis just prior to anther dehiscence with the area of the embryo sac delineated from carpels of heat-resistant and heat-sensitive RIL obtained under control and heat-stress conditions.....	54
3.5 Amplification profiles for <i>Rht-B1a</i> and <i>Rht-B1b</i> dwarfing alleles present in selected heat-resistant and heat-sensitive RILs and parental lines.....	70
4.1 Schematic overview of the comparison of the effect of heat stress on morphological and yield parameters of heat-resistant parent ‘Attila’ and heat-sensitive parent ‘CDC Go’	76
4.2 Schematic overview of the comparison of the effect of heat stress on morphological and yield parameters of heat-resistant RIL 123 and heat-sensitive RIL 131	77
A.1 Longitudinal sections of the main tiller of ‘Attila’ and ‘CDC Go’ plants at the flag-leaf emerging stage (BBCH 37)	98

A.2	The first floral spike at anthesis.....	100
A.3	Diagrams depicting the floral morphological measurements.....	101
A.4	Pollen grains imaged after staining with modified Alexander staining solution under a light microscope at 10X magnification.....	102
A.5	Representative images of the developmental stage of the main tiller spike from the control and heat stress-treated plants of RIL 123 and RIL 131 at the time of tissue.....	103

List of Abbreviations

Abbreviation	Definition
4-Cl-IAA	4-chloroindole-3-acetic acid
AD	Auricle distance
An	Anther
ANOVA	Analysis of Variance
ARFs	Auxin response factors
BBCH	Biologische Bundesanstalt, Bundessortenamt and Chemische Industrie (a scale used to identify the phenological development stages of a plant)
C	Connective Tissue
CC	Central Callose
Ch	Chalazal region
Cv	Cultivar
D	Dorsal
DAA	Days after anthesis
DIC	Differential contrast microscopy
DNA	Deoxyribonucleic acid
DPG	Degraded Pollen Grain
E	Epidermis
EtOH	Ethanol
En	Endothecium
FAA	Formaldehyde-acetic acid-alcohol
Fg	Female gametophyte
Gas	Gibberellins
HS	Heat Stress
HSPs	Heat shock proteins
IAA	Indole-3-acetic acid
II	Inner integument
IPA	Indole-3-pyruvate
IPG	Intact pollen grain
JA	Jasmonic acid
L	Lacunae
LSD	Least Significant Difference test
M	Micropylar region
MAS	Marker-assisted selection
MC	Meiotic cells

ML	Middle Layer
MMC	Microspore Mother Cells
N	Node
Nu	Nucellus
O	Ovary
OI	Outer integument
Ov	Ovule
OVL	Ovule length
OVA	Ovule area
Pa	Parietal Tissue
PCR	Polymerase chain reaction
PG	Pollen Grains
PIPES	Piperazine-N, N'-bis (2-ethanesulfonic acid)
Pvb	Provascular bundle
QTL	quantitative trait loci
RIL	Recombinant Inbred Line
ROS	Reactive oxygen species
SNP	Single nucleotide polymorphism
Sp	Sporogenous Tissue
St	Style/Stigma
StR	Stomium Region
T	Tapetum
TAA	Tryptophan aminotransferases
Tds	Tetrads
TN	Tillering Node
Trp	Tryptophan
V	Vascular Region
Vn	Ventral
VM	Vacuolate Microspores
VP	Vacuolated Pollen grains
YM	Young Microspores

1. INTRODUCTION

1.1 Bread wheat origin and production

Wheat is one of the important staple crops belonging to the Poaceae family, and it provides 20% of the total available calories and proteins to most of the world population (Venske et al., 2019). It is grown under diverse climatic conditions in more than 40 countries including China, India, Russian Federation, USA, France, Canada, Ukraine, Pakistan, Germany and Argentina (Tshikunde et al., 2019). Wheat is a widely cultivated crop that occupies about 215 million hectares of land all over the world (FAOSTAT, 2019). The total wheat production in 2019 was 756 million tonnes with an average yield of 3546.8 kg/ha (FAOSTAT, 2019). The first cultivation of wheat dates back to 10,000 years ago in the south-eastern part of Turkey as part of the Neolithic revolution (Shewry, 2009). Among the different species of wheat cultivated, the allohexaploid bread wheat (*Triticum aestivum* L., $2n = 42$, AABBDD) is the most widespread and it accounts for 95% of all the wheat cultivated in the world (Venske et al., 2019). Allohexaploid bread wheat was first thought to originate as a result of a two-step hybridization between three wild ancestors, each with a unique genome. First, hybridization occurred between *Triticum urartu* ($2n=14$, AA) and *Aegilops speltoides* ($2n=14$, BB) which gave rise to *Triticum turgidum* ($2n=28$, AABB) also known as wild emmer wheat. Later on, a second hybridization occurred approximately 8000 to 10,000 years ago in Northern Iran between *Aegilops tauschii* ($2n=14$ DD) and *Triticum turgidum*, giving rise to allohexaploid bread wheat (*Triticum aestivum* L., $2n=42$, AABBDD; Venske et al., 2019; Byrne, 2020).

Wheat is successfully adapted to grow in subtropic and temperate climate zones between the latitudes of 30° and 60°N and 27° and 40°S. However, in tropical and subtropical regions, it is also cultivated in high elevations (FAO 2002; Shewry, 2009). Wheat is successfully grown across a wide range of environments including dry and high rainfall areas, and from warm-humid to dry-cold environments (FAO, 2002). The optimum temperature required for wheat plant growth and development ranges from 17 °C and 23 °C. The germination of wheat seeds occurs at the minimum temperature between 3 °C to 4 °C, and flowering occurs above 14 °C. Temperature above the optimum range can have a significant negative effect on wheat yield (Porter and Gawith, 1999). The moisture requirement can vary depending on the variety, growth stage and climatic conditions (AGRI-FACTS, 2011). It can be grown in areas where average annual

precipitation ranges from 250 mm to 1750 mm. The genetic diversity of the wheat genome allows it to adapt to diverse environments. The high environment adaptability and yield, and unique elastic property of gluten, makes bread wheat one of the most successful among other temperate crops (Shewry, 2009; Venske et al., 2019).

Primary wheat production areas in Canada are the prairie provinces of Manitoba, Saskatchewan, and Alberta (McCallum and DePauw, 2008). In 2021, Saskatchewan accounted for 12 million acres of wheat harvested area, followed by 6.9 million acres of wheat from Alberta and 2.9 million acres from Manitoba (Canada Statistics, 2021). However, a relatively small percentage of area in British Columbia and eastern Canada also contribute to total wheat production (McCallum and DePauw, 2008). The total area of wheat harvested in 2021 in Canada was 23.4 million acres, with an average production of 22.9 million tonnes and an average yield of 37.2 bushels per acre (Canada Statistics, 2021). Allohexaploid spring bread wheat (*Triticum aestivum* L.) was the prominent type of wheat grown in the western prairie region. In addition, a small portion of allohexaploid winter bread wheat (*Triticum aestivum* L.) and durum wheat (*Triticum turgidum* L. ssp.) were also grown (McCallum and DePauw, 2008).

Wheat is categorized into several classes depending on its agronomic and end-use quality. Based on the hardness of the seed, it is divided into two classes, hard and soft. Wheat is categorized as red and white in reference to the colour of the outer layer (bran) of the kernel. Wheat is also classified into two classes according to the growing season, spring, and winter (Bushuk and Rasper, 1994). The growth cycle of wheat can be divided into two phases, the vegetative and reproductive phases. Various growth scales have been developed to standardise the growth stages of wheat during its development. In this thesis, the BBCH scale is used that describes the phenological development of cereals to identify specific growth stages of the wheat plant (Lancashire et al., 1991).

1.2 Reproductive development of wheat

The reproductive development of wheat begins when the vegetative shoot apical meristem transforms into reproductive inflorescence meristem. This occurs due to a series of morphological changes that occur in the shoot apex in response to the intrinsic signals from the plant and extrinsic signals from the environment (Feng et al., 2017; Koppolu and Schnurbusch, 2019). Wheat reproductive development is commonly categorized into two stages, the early reproductive phase when spikelet primordia are initiated, and the late reproductive phase when the stem internodes elongate, and the floret primordia develop into flowers. The length of the vegetative and early reproductive phases determines the number of spikelet primordia initiated on the shoot apex. The late reproductive phase determines how many spikelet primordia will develop into fertile florets (Gol et al., 2017). During the early stages of reproductive development, the young inflorescence meristem differentiates into the double ridge stage by forming a series of ridges along the elongating shoot apex. The double ridge consists of a lower leaf ridge and the upper spikelet ridge. The lower leaf ridge often suppresses its growth during early development while the upper spikelet ridge differentiates into spikelets (Bowden et al., 2008; Feng et al., 2017). Spikelet development first starts from the most advanced ridges in the center of the spike and later develops progressively towards either side of the spike central region (the basal and distal sections). This spikelet formation occurs on the opposite sides of the central axis called the rachis. The wheat floral shoot apex is determinate. Usually, after producing about 20 spikelet primordia in the shoot apex, the last initiating primordia develop into floret primordia to form the terminal spikelet (Fig. 1.1; Kirby, 2002). The final number of spikelets per spike is determined at this stage depending on the length of transition from the vegetative to early reproductive stage (Kirby, 2002). Starting from the double ridge stage various floral structures are formed within each spikelet. First, the spikelet ridge initiates the formation of glume primordia to protect the spikelet. Then, lemma and palea form within the glume covering the outer and inner sides of the florets (Kirby, 2002; Bowden et al., 2008). Generally, around 6-11 floret primordia are produced per spikelet depending on their position along the spike, with each adjacent spikelet positioned on opposite sides of the spikelet axis (rachilla) (Fig. 1.2 A and B; Gonzalez et al., 2005). The development of the florets within the spikelet occurs starting from the basal extending to the distal region; therefore, the more mature florets are found in the base of each spikelet. The distal florets within the spikelet are often less developed and

eventually die. Each floret of the spikelet is comprised of a carpel, three stamens and two lodicules (Fig. 1.2C; Kirby, 2002).

Rapid stem elongation and floret differentiation occur during the late stage of wheat reproductive development, which normally begins after forming the terminal spikelet. Most of the floret primordia will degenerate during the stem elongation phase before reaching a mature floret at anthesis. This occurs mainly due to the competition between the florets for nutrients and moisture at this developmental stage (González et al., 2005). The duration of the late reproductive phase determines the final number of fertile florets per spikelet (Gol et al., 2017). The rapid growth of the peduncle causes the well-developed head (Fig. 1.2A) to emerge from the boot formed by the flag leaf sheath during the booting stage (Fig. 1.3; Acevedo et al., 2002).



Figure 1.1: Terminal spikelet initiation stage of wheat RIL 28

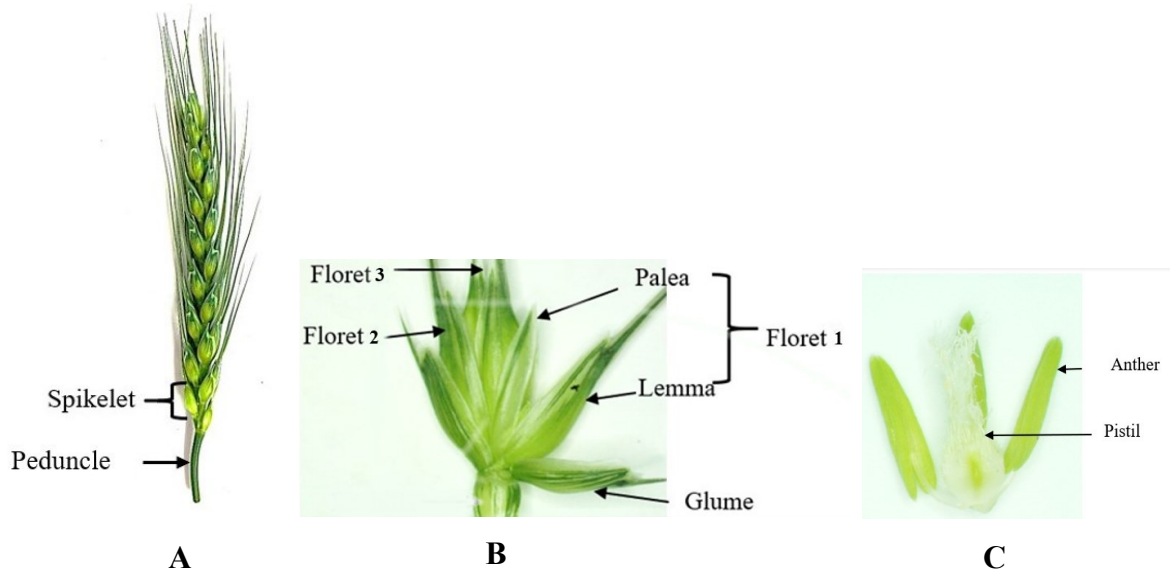


Figure 1.2: The structure wheat floral spike. (A), spikelet (B), floret with anthers and pistil (C)

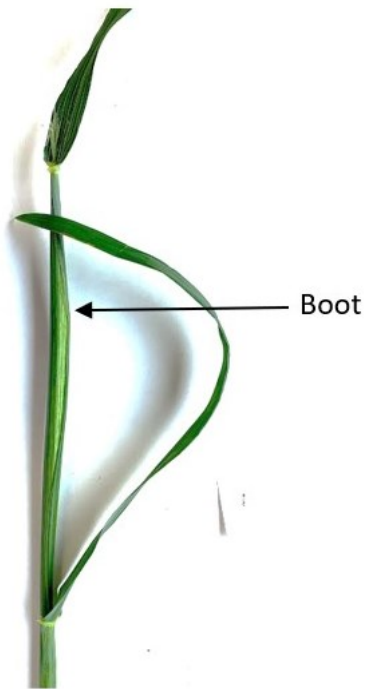


Figure 1.3: Late boot stage of wheat with swollen flag leaf sheath, BBCH 45.

The differentiation of stamens and carpels within the florets extends from the terminal spikelet stage to the anthesis stage when the florets become fully mature. The stamen first differentiates to form anther and filament. Anther development in wheat progresses through multiple stages (Browne et al., 2018). The early phase of the anther development involves differentiation of anther tissues and meiotic division of the pollen mother cells. In anther stage 1, stamen primordia develop from the floret meristem and differentiate into two distinct parts: anther and the filament. At this stage, the anther is a round and oval shape, and the inner tissue is comprised of primordial cells with little or no differentiation (Fig. 1.4, stage 1). In stage 2, archesporial cells form connective tissue to separate theca of the anther (Fig. 1.4, stage 2). Four independent lobes of the anther and vascular tissues begin to form in anther stage 3 and become clearly visible at anther stage 4 (Fig. 1.4, stage 3). At anther stage 4, each lobe consists of endothecium and the middle layer and sporogenous cells and four lobes are connected at the center where the vascular bundles are present (Fig. 1.4, stage 4). At this stage, the anther is short in length and appears white in colour (Bowden et al., 2008; Browne et al., 2018). The inner cell layer of the locule called the tapetum begins to form around each locule adjacent to the sporogenous cells in stage 5 (Fig. 1.4, stage 5). The four lobes of the anthers are surrounded by three distinct layers at this stage: endothecium, middle layer, and epidermis. The tapetal cells continue to grow from stage 5 and form a uniform complete layer around the locule at stage 6 (Fig. 1.4, stage 5 and 6). Sporogenous cells also develop into microspore mother cells and become surrounded by a callose wall at stage 6, which undergo meiotic cell division in stage 7 to form microspores (Fig. 1.4, stage 6 and 7). During this stage, anthers are bright green in colour with a short filament (usually 1 mm in length) and the spike is about to emerge from the boot (Kirby, 2002; Bowden et al., 2008; Browne et al., 2018). After meiosis, microspores move toward the wall of the tapetum forming a hollow region in the center of the locule (Fig. 1.4, stage 7). Subsequently, the haploid microspores encased within a callose wall separate from each other to form tetrads in stage 8 (Fig. 1.4, stage 8). In stage 9, the young microspores separate as the callose wall surrounding the tetrads degrades and continues to grow by forming a large central vacuole. The tapetum reaches its maximum size at this stage. The middle layer starts to degenerate following meiosis and it is barely seen in stage 9 (Fig. 1.4, stage 9). At stage 10, the vacuolated microspore is pressed into the tapetal wall and the exine layer is formed around the microspores. The tapetal degeneration also starts at this stage (Fig. 1.4, stage 10). Microspores

continue to grow and accumulate sugar and nutrients at stage 11 and become large and spherical with two nuclei (Figs. 1.4 and 1.5). The tapetal degeneration is at the maximum point and tapetal cell layer becomes thinner and uneven around the locule. Eventually, microspores become round and starch-filled pollen grains and differentiate into mature pollen grain with gametes inside at stage 12. The tapetum is very minimal or completely gone at this point (Browne et al., 2018; Fig. 1.4, stage 12). The anther is fully matured at this stage and changes its colour from green to yellow (Kirby, 2002; Bowden et al., 2008). At stage 13, the anther becomes bilocular due to the degradation of septum between upper and lower locules. Finally, at stage 14, endothecium enlarges and lignifies, and anther dehisce by rupturing the epidermal cells in the stomium (Fig. 1.4, stage 14).

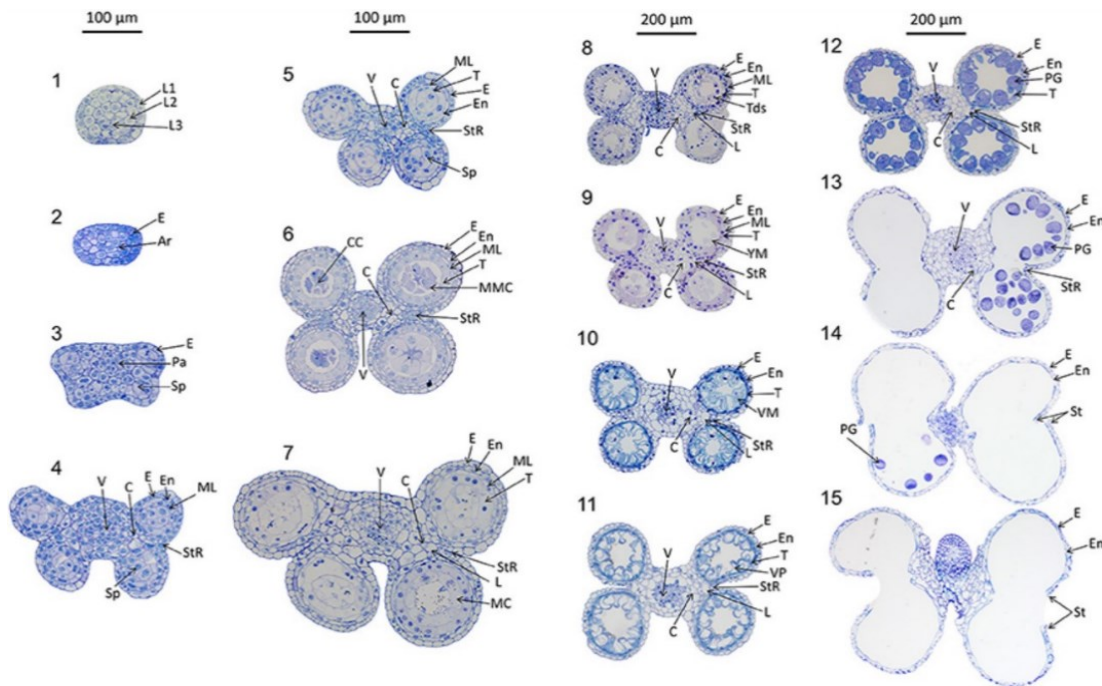


Figure 1.4: Transverse sections of anthers from wheat cultivars Halberd and Cranbrook over development (stages 1-15). Connective Tissue, C; Central Callose, CC; Epidermis, E; Endothecium, En; Lacunae, L; Meiotic cells, MC; Middle Layer, ML; Microspore Mother Cells, MMC; Parietal Tissue, Pa; Pollen Grains, PG; Sporogenous Tissue, Sp; Stomium Region, StR; Tapetum, T; Tetrads, Tds; Vacuolate Microspores, VM; Vascular Region, V; Vacuolated Pollen grains, VP; Young Microspores YM. Image from Browne et al., 2018, with permission.

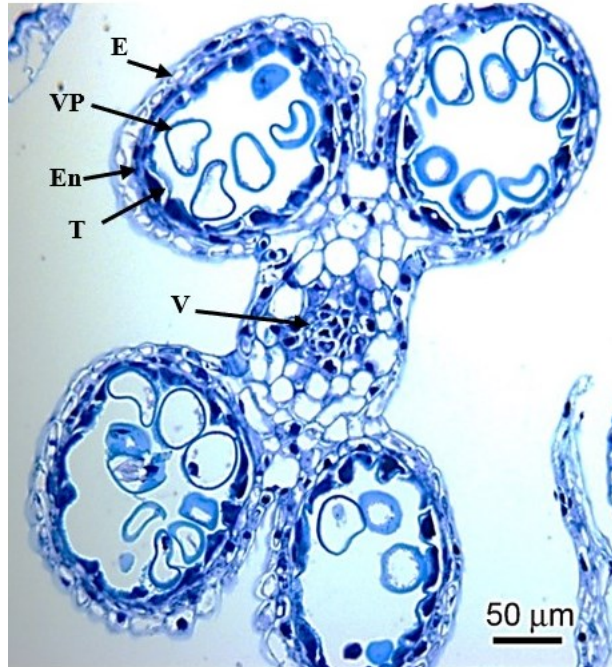


Figure 1.5: Developing wheat anther at stage 11 (vacuolated pollen stage) of ‘Attila’. Magnification, 20X. Epidermis, E; Endothecium, En; Tapetum, T; Vascular region, V; Vacuolated Pollen grains, VP.

The differentiation of the carpel begins after stamen initiation. The basal part of the carpel consists of an ovary with a single sessile anatropous (micropyle of the ovule directed towards the placenta due to their curvature) ovule which is surrounded by inner and outer integuments which further differentiate to form the seed coat during seed development (Aziz, 1972; Endress et al., 2011). The integuments arise from the region of the ovule which is known as the chalaza (Rudall, 1997). The micropyle is a narrow opening that is located opposite to the chalaza where the pollen tube enters the ovule for fertilization (Endress et al., 2011). The ovule contains the female gametophyte or embryo sac that is surrounded by the nucellus. The archesporial cells within the ovule differentiate to form a megaspore mother cell which undergoes meiosis to produce four haploid megaspores. Out of four megaspores, three megaspores will abort, and the remaining one megaspore will mitotically divide to form an 8-nucleate embryo sac. The meiotic division of the megaspore mother cells in the ovule and microspore mother cells in the anther occur at the same time. The carpel continues to grow by

forming a pistil with a two-lobed stigma with feathery branches and one style (Benett et al., 1973; Kirby, 2002).

The duration of anthesis for a wheat floral spike is normally 3 to 10 days depending on the environment (De Vries, 1971). It first occurs in florets in the center of the spike and then progresses to basal and distal regions of the spike after the ear fully emerges from the flag leaf sheath. During this time, the lodicules become swollen, first pushing the lemma and palea apart to open the floret (De Vries, 1971). Rapid elongation of the anther filaments causes anthers to extrude and hang down from the floret. The two stigma lobes move apart by spreading out receptive feathery branches to provide a wide area for pollen grain deposition (De Vries, 1971). In the meantime, the anthers dehisce releasing the pollen grains contained in the locules (Fig. 1.4, stage 15). Usually, 96% of the wheat florets are self-pollinated (Bowden et al., 2008). After anther dehiscence, pollen grains are first deposited on the stigma of the pistil of the same floret. The pollen grains will then germinate and produce pollen tubes that will grow down the style to reach the micropylar region of the ovule. One pollen-derived regenerative nucleus will fuse with the egg nucleus and develop into the embryo, and the other regenerative nucleus from the pollen tube will fuse with the two polar nuclei forming the endosperm. This process is called double fertilization (Kirby, 2002).

1.3 Role of plant hormones during reproductive development

Plant hormones including auxins, gibberellins (GAs), abscisic acid (ABA), and jasmonic acid (JA) play vital roles in coordinating the development of the male and female organs in flowering plants for successful reproduction. Many studies related to plant hormone function during reproductive development have been carried out using the model plant *Arabidopsis thaliana*. Auxins play an important role in floral initiation and floral primordia formation. Defects in auxin biosynthesis, polar auxin transport, and auxin signaling can cause aberrant flower development (Cheng and Zhao, 2007). Indole-3-acetic acid (IAA) is the ubiquitous naturally occurring auxin in all higher plants and it is synthesized by plants through either the tryptophan (Trp)-dependent or Trp-independent pathways (Zhao, 2012). Trp-dependent auxin biosynthesis is predominant in flower development. During the Trp-dependent auxin biosynthesis, first, Trp is converted into indole-3-pyruvate (IPA) by Trp aminotransferases (TAA), which is then converted into IAA by a family of YUCCA (YUC) flavin monooxygenases

(Won et al., 2011; Zhao, 2012). Cheng et al. (2006) showed that mutations in *Arabidopsis YUC* genes can result in the production of infertile flowers by affecting the formation of all four types of floral organs. The *YUC* double mutants (*yuc2yuc6* and *yuc1yuc4*) formed flowers with short stamens or stamens-like structures, delayed anther maturation, and the anthers rarely produce any pollen grains. Moreover, the *Arabidopsis* quadruple *YUC* mutant (*yuc1yuc2yuc4yuc6*) exhibited even stronger defects in flower development by forming inflorescences without any flower buds. In addition, the quadruple *YUC* mutant (*yuc1yuc2yuc4yuc6*) showed reduce flower size compared to the double mutants (*yuc2yuc6* and *yuc1yuc4*) and triple *YUC* mutants (*yuc1yuc2yuc4* and *yuc1yuc4yuc6*); Cheng et al., 2006). The polar auxin transport mutant (*pin 1*) in *Arabidopsis* showed similar patterns of abnormal flower development as mentioned for the *YUC* mutants (Okada et al., 1991).

Auxins also play an important role in later stages of stamen development such as anther dehiscence, pollen maturation and anther filament elongation. According to the study carried out by Cecchetti et al. (2008) with *Arabidopsis* containing the auxin-sensitive reporter marker gene (*DR5::GUS*), accumulation of auxin in surrounding sporophytic anther tissues, microspores and anther filament begins at the end of meiosis and declines when the microspores separate at anther stage 11. The DR5-signal was only observed in the remnants of the tapetum and middle layer, immature pollen grains and the anther filament at the end of stage 11, and it was no longer detected at stage 12 when the septum degenerated, and anthers became bilocular (Cecchetti et al., 2008). Expression patterns of auxin biosynthesis genes (*YUC2* and *YUC6*) in anther tissues similar to that of the DR5 auxin-sensitive reporter gene are consistent with tissue-specific localization of auxin during the late stamen development (Cecchetti et al., 2008). Additionally, polar auxin transport in the anther filament after floral organ differentiation is essential for anther filament elongation, pollen mitosis and normal pollen development. Blocking auxin flow in the anther filament by expressing the indoleacetic acid-lysine synthetase gene (*iaaL*, codes for an enzyme that catalyzes the inactivation of free IAA through its conjugation to the amino acid L-lysine) could result in abnormal pollen grains, which were defective in the first round of pollen mitosis (Feng et al., 2006). Further studies with transgenic tobacco plants (*Nicotiana tabacum* L. cv. Xanthi) transformed with the *iaaL* gene showed that the lack of auxin within the anther filament led to short filament length as a result of reduced elongation of the epidermal cells (Feng et al., 2006).

Normal pollen maturation and anther dehiscence occur via a sequential process. Cecchetti et al. (2008) showed that mutations in auxin receptor genes (*tir1* and *afb* multiple mutants) that are transcribed in the later stages of stamen development, accelerated the timing of pollen maturation and anther dehiscence. Premature anther dehiscence in the auxin receptor mutants (*tir1afb2afb3* and *tir1afb1afb2afb3*) was due to the early thickening of endothecium that induces the simultaneous breakage of stomium and septum. The auxin receptor mutants accelerated the time taken for two mitotic divisions of pollen during microsporogenesis, resulting in the early maturation of pollen grains. These findings suggest that auxin coordinates the correct timing of pollen maturation and anther dehiscence during anther development (Cecchetti et al., 2008). Auxin response factors (ARFs) bind to auxin response elements in the promoters of auxin response genes, promoting auxin response (Wang and Estelle, 2014). The auxin response factor 17 (ARF 17) regulates the primexine deposition within the tetrad in *Arabidopsis*. The primexine deposition between the callose layer and microspore membrane is crucial for pollen wall patterning during pollen maturation. Transmission electron microscopy analysis showed that the *Arabidopsis arf17* mutant inhibits primexine deposition, leading to subsequent aborted pollen wall pattern and pollen degradation (Yang et al., 2013). Also, the reduction of IAA in pollen grains can lead to abnormal pollen tube development resulting in lower seed production (Salinas-Grenet et al., 2018). Aloni et al. (2006) showed that free-IAA is present in higher levels in the mature pollen grain, which may help to promote the pollen germination on stigma and pollen tube growth.

In addition to auxin, GAs also regulates stamen development. GA deficiency or insensitivity in flowers can affect anther development, leading to male sterility. Rice GA deficiency mutants containing mutations in GA biosynthesis genes were found to have enlarged tapetal cells that have defects in programmed cell death during anther development (Aya et al., 2009). Furthermore, these rice GA deficiency mutants were observed to have impaired pollen exine formation due to the abnormalities associated with Ubisch body formation in tapetal cells (Aya et al., 2009). Ubisch bodies are important to supply sporopollenin to microspores for exine formation (Wang et al., 2003). Cheng et al. (2004) showed that the *Arabidopsis* GA-deficient mutant *gal-3* arrested microspore and tapetal cell development prior to mitosis. Moreover, the flowers of this GA-deficient mutant form relatively short stamen filaments due to arrest in filament cell elongation.

Mutant approaches have also shown that JA plays a vital role in anther filament elongation, viable pollen grains formation, and anther dehiscence (Stintzi and Browse, 2000; Ishiguro et al., 2001; Nagpal et al., 2005). Mutations in *Arabidopsis* auxin response transcription factors (*arf6 arf8* double mutants) can reduce JA biosynthesis and this results in anther dehiscence and pollen viability defects, and application of JA can restore the normal phenotype (Nagpal et al., 2005). Ishiguro et al. (2001) also found that JA application could rescue the defects in anther dehiscence, pollen maturation and flower opening that occurred in the *Arabidopsis dad 1* mutant.

In addition to male reproductive development, auxin also plays a vital role in female reproductive development. In *Arabidopsis*, expression of the auxin response marker DR5-GFP was observed in the micropylar pole of the embryo sac after the first mitotic division up to the 8-nucleate embryo sac stage (Pagnussat et al., 2009). Auxin was also shown to accumulate in the inner integument, and influence integument initiation or outgrowth (Benkova et al., 2003; Ceccato et al., 2013). Polar auxin transport in *Arabidopsis* is dependent on the PIN family proteins and mutation in *PIN* genes can lead to pin-shaped inflorescence meristems devoid of flowers. In addition to that, mutations in *PIN* genes (*pin1-5*) can also form flowers with abnormal pistils, few ovules and defective embryo sacs. This suggests the role of auxin during the early phase of ovule development (Ceccato et al., 2013).

1.4 Effect of heat stress on plant reproductive development

Recently, with signs of global warming, temperature fluctuation is becoming more prominent in every part of the world (Lindsey and Dahlman, 2021). High-temperature stress can affect wheat plant growth and development, and yield. Previous studies have shown that even a 1 °C increase in temperature during reproductive development can decrease world wheat production by 6% (Lesk et al., 2016). The degree of damage caused by high-temperature stress to wheat production depends on intensity, duration of stress, stage of crop development, and differential tolerance capacity of each variety (Wahid et al., 2007; Tomas et al., 2020).

1.4.1 Impact of heat stress on anther and pollen development

Male sterility caused by high-temperature stress is often accompanied by defects in anther development leading to the reduction in seed set and grain yield. All stages of anther development are affected by high-temperature stress. However, the sensitivity to heat stress can vary throughout anther/pollen development. The early stages of anther development (microsporogenesis) are more susceptible to heat stress than the later stages (pollen maturation to anther dehiscence; Raja et al., 2019). During microsporogenesis in the anther, the pollen mother cells undergo two rounds of mitosis (pollen mitosis I and II). Two different types of abnormal anthers/pollen grains were observed in wheat after subjecting the plant to a short period of moderate heat stress at pollen mother cell meiosis. One set of anthers showed complete sterility, due to the failure in mitosis I and premature degradation of the tapetal wall. In the second set of anthers, all the microspores completed mitosis I, but some microspores failed to complete mitosis II, resulting in a mixture of fertile and sterile pollen grains within the anther (Saini et al., 1982). Similar results were observed when two-row barley plants (*Hordeum vulgare* L.) were exposed to moderate heat stress at the 4 leaf or 6 leaf stage (Sakata et al., 2000).

The anther cell wall is composed of four distinct cell layers; epidermis, endothecium, middle layer and tapetum (Figs. 1.4 and 1.5), and these cell layers are important for anther dehiscence and are considered to provide nutrients for the developing microspores. The sequential degradation of these cell layers by programmed cell death is critical for pollen maturation and anther dehiscence (Varnier et al., 2005). The tapetum is the innermost layer of the anther wall that provides nutrients to the developing microspores during their development. Callase enzymes secreted from the tapetum help to release the microspores from the tetrad by degrading the surrounding callose wall (Lohani et al., 2020). The degradation of the tapetum begins after the microspores are released from the tetrad, and the timely degradation of tapetum is vital to the formation of the outer wall (exine) around the pollen grains during their maturation (Kurusu and Kuchitsu, 2017). Heat stress can induce the premature degradation of anther cell walls, particularly the tapetum, which leads to pollen abortion. A short period of moderate heat stress (30 °C for 3 days) imposed on wheat at meiosis can cause tapetum degradation in the early stages of anther development (Saini et al., 1982). Similarly, high temperature can induce the premature degeneration of the tapetum and the lack of endothelial cell development which leads to male sterility in cowpea (Ahmed et al., 1992). Tapetum cells are highly metabolically active

under normal growth temperatures. As a result of high metabolic activity in tapetum cells reactive oxygen species (ROS) are accumulated inside the cell. The programmed cell death of the tapetum is controlled by the action of ROS in the anther (Hu et al., 2011). Under optimum growth conditions, cells maintain proper balance between ROS production and scavenging in anthers (Hu et al., 2011). But heat stress induces excessive accumulation of ROS inside the tapetal cells which might result in premature degradation of the tapetum (De Storme and Geelen, 2014). In addition, subcellular alternations such as increasing number of vacuoles, excessive development of chloroplasts and irregularities in the rough-ER can also contribute to tapetum dysfunction and premature degradation under heat stress (Suzuki et al., 2001; Oshino et al., 2011).

Heat stress can shorten the period of anthesis and this can result in fewer fertile spikelets per spike eventually leading to a reduction in total grain number (Saini and Aspinall, 1982; Porter and Gawith, 1999). Successful fertilization depends on the amount of viable pollen grains that land on the stigma, followed by pollen germination, pollen tube growth and fusion of sperm cells with the egg nucleus. Heat stress can negatively affect all these steps which finally leads to reduced seed set and yield (Raja et al., 2019). Endo et al. (2009) observed that when rice plants were exposed to heat stress at the microspore stage, normal round-shaped pollen grains were produced, but heat stress impaired the number of pollen grains that adhered to the stigma, and their germination. The number of viable pollen grains and the capacity of the pollen grains to germinate on the stigma are among important factors that determining final seed yield. Begcy et al. (2019) showed that a short period of transient heat stress during the tetrad anther development stage can impair *in vitro* and *in vivo* pollen germination in maize. Starch is a major reserve in the mature pollen grain, and a net decrease in the photosynthetic rate under high temperature can decrease starch accumulation in the pollen grains. The reduction of the pollen germination capacity of maize under short periods of heat stress could be associated with reduced starch accumulation in the pollen grains (Begcy et al., 2019).

1.4.2 Impact of heat stress on hormonal regulation of anther and pollen development

Hormonal regulation of reproductive development is sensitive to abiotic/heat stress events (Ozga et al., 2017). Several studies have shown that heat stress-induced defects in anther/pollen development is associated with changes in the level of several plant hormones in the anther. Sakata et al. (2010) observed that expression of the *YUC* auxin biosynthesis genes (*YUC2* and *YUC6*) was repressed by high temperature in *Arabidopsis* and barley stamens. Under normal conditions endogenous auxin accumulates in the parietal, epidermal cells, sporogenous cells, and in the rachis cells around the vascular bundles of developing anthers in barley (*Horedum vulgare* L.; Sakata et al., 2010). Heat stress reduced the level of endogenous auxin in developing anthers of barley which might lead to loss of pollen viability, pollen germination or male sterility (Cecchetti et al., 2008; Sakata and Higashitani, 2008; Sakata et al., 2010; Higashitani, 2013). *Arabidopsis* lines expressing the DR5-GUS auxin response marker gene showed significant reduction in expression when exposed to moderate heat stress (31 or 33 °C) for 1 or 7 days. High temperature produced anthers with short filaments and fewer pollen grains due to the premature abortion of microsporogenesis (Sakata et al., 2010). Application of auxin (IAA, 1-naphthaleneacetic acid, or 2,4-dichlorophenoxyacetic acid) prior to heat stress reduced the negative effects of heat stress on anther length and the percentage of viable pollen grains in barley anthers (Sakata et al., 2010). These data indicate that high temperature affects auxin biosynthesis and signalling pathways, ultimately lead to abnormal pollen and anther development.

GAs are involved in anther filament elongation, microspore development and programmed cell death of the tapetum during normal stamen development (Plackett et al., 2012). The abnormalities in stamen development under heat stress can prevent mature pollen grain formation and male sterility. A decrease in GA levels in the anthers of heat-sensitive and heat-tolerant rice cultivars at the flowering stage was observed under high temperature (39 °C for 4 hours; Tang et al., 2008). In contrast, ABA accumulated in high concentration in rice florets when exposed to heat stress (Tang et al., 2008). ABA reduced pollen sterility caused by heat stress through increasing levels of soluble sugars, starch and non-structural carbohydrates (Rezaul et al., 2019).

1.4.3 Impact of heat stress on female reproductive development and early grain set

Female reproductive development is generally considered less sensitive to the negative effects of heat stress than male reproductive development. However, Saini et al. (1983) observed a number of aberrant changes in the nucellus or embryo sac in the ovaries of wheat plants exposed to a short period of moderate heat stress (3 days at 30 °C; control at 20 °C). Although the ovary wall appeared to develop normally, two major effects of heat stress on ovule anatomy were observed by Saini et al. (1983). One effect observed was the reduced development and degeneration of the nucellus leading to a proliferation of the integument cells to occupy this space. The other effect was on the embryo sac. Some heat-stressed ovaries did not develop an embryo sac, while others had a small embryo sac, in some cases without any recognizable cells or embryo sacs with incomplete cellular organization. In some cases, the nucellus tissue had proliferated into the empty embryo sac cavity (Saini et al., 1983).

Heat stress reduced the auxin levels in the pistil of heat susceptible genotypes of rice leading to spikelet sterility (Zhang et al., 2018). Moderate heat stress during early flowering/fruit set in pea can lead to seed/ovule abortion, reduced ovary length and a lower number of seeds at maturity. Early seed set and pericarp growth are mediated by the coordinated action of the network of plant hormone signalling molecules (Kaur et al., 2021). Moderate heat stress increased ethylene production and reduced bioactive GA levels in developing pea seeds which can promote ovary and seed senescence processes. However, heat stress also increased auxin and ABA levels in the developing pea seeds tissue, which can increase seed sink strength and growth. Kaur et al. (2021) hypothesized that seeds with higher auxin and ABA levels (have higher sink strength) continue to seed set under high-temperature conditions, while seeds with lower auxin, ABA and GA are more sensitive to the effects of ethylene and heat stress-induced ovule abortion.

1.4.4 Wheat grain growth and development

Wheat grain development begins after double fertilization in wheat florets and can be divided into three major stages: grain enlargement, grain filling and physiological maturity. The grain enlargement stage usually continues up to about 10 to 14 days after fertilization of florets. After flowering, grain size markedly increases due to the proliferation and expansion of the cells enclosing the embryo sac and water is rapidly accumulated in the grain. The grain enlargement stage continues until the grain reaches the watery-ripe period (BBCH 71; Lancashire et al., 1991). At this point, the grain mostly contains water, and it is ready to start filling. Then, the grain further progresses through its development by accumulating starch and proteins at a constant rate. This stage is known as grain filling and during this period grain weight increases linearly (Bowden et al., 2008). At the beginning of the grain filling stage, the endosperm only consists of a milky fluid and this stage is called the milk stage (BBCH 73-75). During this time, the grain reaches one-tenth of its final weight. At the end of the milk stage, half of the grain growth is completed (BBCH 77, Fig. 1.6 A). After this point, grain filling continues by the accumulation of carbohydrates and proteins. This is known as the soft dough stage (BBCH 85, 21 days after flowering, Fig. 1.6 B). After the soft dough stage, the grain changes its color from green to yellow. Grain filling continues until the grain reaches ~40% moisture content (Agriculture and Horticulture Development Board, 2018). The grain has a maximum weight at this point and no longer accumulates carbohydrates and proteins. This is called the hard dough stage (BBCH 87, Fig. 1.6 C) and at the end of this stage, the grain appears golden in color. Finally, when the grain has reached its physiological maturity, a waxy substance blocks the vascular system that provides nutrients and water to the grain. As a result, the water content of the grain is 30-40% of grain weight at the time of physiological maturity. Consequently, grain growth stops, and the grain turns brown in color (BBCH 92-93). The green color peduncle changes into a brown color. At this point, grain acquires 95% of its total dry weight. The moisture content of the grain further decreases to approximately 12% of grain weight when it is ripe to harvest (Fig. 1.6 D; Bowden et al., 2008).



Figure 1.6: Grain development using the BBCH scale A) late milk (BBCH 77), B) soft dough (BBCH 85), C) hard dough (BBCH 87), and D) ripe for harvest (BBCH 93). Pictures from Alberta Wheat Commission with permission.

1.4.5 Effect of heat stress on grain growth and development

High-temperature stress can impair grain development leading to reduced grain yield and grain quality. Grain yield is primarily determined by the total number of grains per spike, number of spikes per plant, grain weight, and grain size (Hutsch et al., 2018). Grain weight is mostly determined during the grain filling period and it is dependent on the genotype, length of grain filling period, and the post-anthesis assimilate supply (Porter & Gawith, 1999; Farooq et al., 2011). The optimum temperature for wheat grain filling ranges between 12-22 °C (Tewolde et al., 2006). Under normal temperature conditions, grain filling can take about 15 to 35 days to complete (Bowden et al., 2008). Elevated temperature can increase the rate of grain filling but shortens the duration of grain filling (Dias and Lidon, 2009; Talukder et al., 2014). A previous study reported that a 1 °C increase in temperature above the optimum growing temperature can decrease the grain filling duration by 2.8 days in the early grain filling stage (Streck, 2005). Yin et al. (2009) also recorded an increase in the grain filling rate and a decrease in the filling duration by 12 days after increasing temperature to 25 °C/20 °C (day/night) from 20 °C /15 °C (day/night). However, there is considerable variation in the effect of heat stress on grain filling duration among different varieties of wheat (Stone and Nicolas, 1995). Under mild heat-stress conditions (21 °C/16 °C (day/night)), it is possible that the increased rate of grain filling can be compensated by the weight loss caused by the shorter grain filling period. However, under higher temperatures (above 30 °C) the decrease in the grain filling rate is not balanced by the increase in the rate of grain filling (Wardlaw et al., 1980), leading to lower grain weight. The loss of grain

weight under heat-stress conditions during anthesis and grain filling stages increased with temperature and the duration of the stress (Liu et al., 2020).

The grain yield of the plant is also dependent on the availability of the photo-assimilate supply and the ability of the sink to utilize the available assimilates (Yin et al., 2009; Alonso et al., 2018). During grain filling, assimilates are provided by two sources, the products of current photosynthesis and stem reserves (Palta et al., 1994; Blum, 1998). The relative contribution of the two sources to grain filling is partially dependent on environmental factors. Under favourable environmental conditions, a relatively large proportion of assimilates are provided by the products derived from the current photosynthesis processes of the plant. The flag leaf is a major contributor of the photosynthetic products during the grain filling, but photosynthesis in the penultimate leaf, head and other leaves also contribute a significant amount of assimilates in determining final grain yield (Bowden et al., 2008). High temperature reduces the photosynthetic capacity of the plant by altering the Rubisco enzyme involved in the photosynthesis process, damaging the photosynthetic machinery, reducing flag leaf chlorophyll content, and increasing the rate of leaf senescence which can result in reduction in the photosynthetic source of assimilate supply to grain filling (Feng et al., 2014; Shirdelmoghanloo et al., 2016). To mitigate the assimilate limitation caused by the heat stress, the plant will tend to use stem reserves (water-soluble carbohydrates) as an alternative source for grain filling (Blum, 1998; Bowden et al., 2008). Talukder et al. (2013) reported that a single day high-temperature stress during anthesis and early grain setting can reduce the accumulation and movement of stem reserves (water-soluble carbohydrates). Moreover, the contribution of stem reserves for grain filling can significantly vary among different genotypes depending on their photosynthesis performance under heat stress (Yang et al., 2002).

The dry weight of mature wheat grains is mostly composed of starch and proteins. Starch is the major constituent of the wheat grain and it occupies 65-75% of the total dry weight of the grain (Kumar et al., 2018). When compared to proteins, starch content is much more sensitive to changes due to high-temperature stress (Farooq et al., 2011). Reduction of starch accumulation under heat stress is attributed to heat stress-induced negative changes in the enzymes involved in the starch biosynthesis pathway (Jenner, 1994). Even a short period of high temperature (>30 °C) can cause a reduction in the rate of starch accumulation (Jenner, 1994). Wang et al. (2012) also

recorded the reduction in the starch content in mature wheat grains after post-anthesis heat stress. Previous studies have shown that high temperature-induced reduction in starch accumulation is mainly attributed to the alterations in the conversion of sucrose to starch rather than the decline in the assimilate supply (Wardlaw et al., 1980; Bhullar and Jenner, 1986). Several enzymes involved in starch synthesis including sucrose synthase, soluble starch synthase, UDP-glucose pyrophosphorylase, and ADP-glucose pyrophosphorylase were assessed in developing wheat grains under heat stress conditions during the grain-filling stage (Hawker and Jenner, 1993). Both sucrose synthase and soluble starch synthase activities were reduced by heat stress in the developing wheat grains, contributing to lower starch accumulation in the grains. Hurkman et al. (2003) also found that high temperatures (37/17 °C Day/night) applied to wheat plants during anthesis to maturity can cause a significant reduction in the activity of soluble starch synthase enzyme.

Starch is present as semi-crystalline granules in the amyloplasts of wheat grain (Parker, 1985; Bechtel et al., 1990). It is mainly composed of two glucose polymers with different structural arrangements: linear helical amylose and the branched amylopectin. The relatively large proportion (75%) of wheat grain starch content is composed of amylopectin while amylose only contributes a small percentage (25%) to grain starch content (Wang et al., 2012). Starch granules with different sizes and shapes are formed at the different time points of grain filling (Parker, 1985; Zhang et al., 2010). In general, two or three different types of starch granules can be found in the endosperm of wheat grains. Type A granules are much larger and are formed after 4-5 DAA (days after anthesis), small B type granules are formed 12-16 DAA, and very small C type granules are formed at the end of grain filling (Parker, 1985; Zhang et al., 2010). The early stages of grain filling (6 to 8 DAA) were more susceptible to heat stress-induced reduction of starch concentration than the later stages of grain filling (36 to 38 DAA; Liu et al., 2011). Liu et al. (2011) observed that when wheat plants exposed to temperatures above 30 °C at the early stages (6 to 8 DAA) or middle stages (25 to 27 DAA) of grain filling could form small ellipsoid-shaped starch granules (cv. Yangmai 9) or damaged and compressed starch grains with fissures (cv. Yangmai 12) depending on the heat-tolerance capacity of the variety. Furthermore, high-temperature stress is reported to have varying effects on the size and frequency of different starch granule types (Hurkman et al., 2003; Liu et al., 2011; Li et al., 2018). The changes in the granule composition under heat stress could lead to alterations in the amylose and amylopectin

composition of starch and can lead to changes in the gelatinization, viscosity, pasting and gelation properties of starch (Zeng et al., 1997; Hurkman et al., 2003; Li et al., 2018). The differences observed in relative distribution and the size of the starch granules in Hurkman et al. (2003) and Li et al. (2018) studies could be due to the different thermotolerance capacities of the cultivars or the differences in duration of the heat stress treatment.

Grain quality is mainly determined by the chemical composition and the size of the grain. The final size of the grain is primarily determined during the early stages of grain development (Farooq et al., 2011). High-temperature can cause grain shrinkage through changes in the aleurone layer and endosperm cells (Dias et al., 2008). Heat stress can make endosperm cells thicker, denser, packed with starch granules (Dias et al., 2008). Grain protein content was increased under high temperature stress (Spiertz et al., 2006). The increase of grain protein content under heat stress is mostly because of the reduction of starch content rather than changes in N content (Castro et al., 2007). The influence of heat stress on grain protein content is also dependent on genotype (Spiertz et al., 2006).

1.5 Breeding for heat tolerance in wheat

Plants can achieve heat tolerance through interaction with various biochemical, morphological, and physiological mechanisms (Hasanuzzaman et al., 2013). Plant breeding is mainly focused on identifying and selecting plants with desirable traits that perform best under high temperature stress and in combining those traits to produce plants with improved quality through conventional or molecular breeding. The plant response to the heat stress is complex as it is controlled by interaction with various physiological, morphological, and biochemical traits (Pandey et al., 2019). Therefore, selection for heat tolerance based on morphological and biochemical traits is inefficient due to the low number traits identified for heat tolerance, the complexity of heat stress tolerance, and the high genotype x environment interaction. Marker-assisted selection (MAS) is a promising approach for plant breeders to study the genetic basis of heat tolerance in plants as it allows breeders to indirectly select the trait of interest linked to a marker (morphological, biochemical, or molecular; Maestri et al., 2002; Pandey et al., 2019). To increase the efficiency of selection, it is necessary to screen for traits which have high genetic correlation with grain yield, high heritability, and low environment and genetic interaction (Pandey et al., 2019). Identification of the genetic markers associated with quantitative trait loci

(QTL) is vital in marker-assisted selection. Several QTLs that are attributed to heat tolerance in wheat have been identified during plant reproductive development. However, the large genome size of the wheat and presence of repetitive DNA sequences in the genome limit the usefulness of QTL analysis (Vinh and Paterson, 2005). Several studies have identified QTLs related to traits such as the ‘stay green’ character (3 QTLs) (Kumar et al., 2010), senescence (Vijayalakshmi et al., 2010), and canopy temperature (QTL on chromosome 4A; Pinto et al., 2010) in wheat.

Heat shock proteins (HSPs) play an important role by acting as molecular chaperons to prevent protein denaturation and aggregation and thereby facilitating the function of proteins and membranes under heat stress (Wang et al., 2004). Proteomic studies carried out in a heat-tolerant wheat genotype showed that a diverse range of HSPs accumulated in the plants of this genotype under heat stress compared to a heat-sensitive genotype. Depending on the duration and level of heat stress, different types of HSPs can be produced in heat-tolerant genotypes of wheat (Skylas et al., 2002; Rampino et al., 2009; Sharma-Natu et al., 2010). An HSP (*HSP16.9*)-derived SNP marker has been identified in wheat which is attributed to grain weight under terminal heat stress (Garg et al., 2012). Identification of genetic variability related to HSPs in heat tolerant and heat susceptible genotypes will likely be important in breeding for thermotolerance.

1.6 Recombinant inbred lines (RIL)

In the RIL design process the parents with significant phenotypic divergence in the trait of interest will be crossed followed by repeated selfing to develop recombinants (Pollar, 2012). The recombinant inbred line population used in this study consists of 171 RILs and it was developed by crossing ‘Attila’ and ‘CDC Go’. The original population consisted of 171 RILs which were advanced to F6 using single seed descent. The RILs and two parents were planted in double head rows to multiply seed for experimental use as F6 derived F7 (Asif et al., 2015). This population was originally tested in organic and conventional systems to map quantitative trait loci (QTL) affecting various agronomic and quality traits. ‘Attila’ is a spring wheat cultivar that is early maturing, medium yielding, awned, and semi-dwarf, that is widely grown in Southeast Asia (Rosewarne et al., 2008; Zou et al., 2017). ‘CDC Go’ is a Western Canadian Red Spring wheat that is medium height, comparatively early maturing and high yielding with awned spikes and hollow stems (Asif et al., 2015). Generally, the parents produced higher grain yield, tall plants, higher kernel weight and took longer to mature under conventional systems. In organically

managed systems ‘Attila’ produced grains with higher protein content than ‘CDC Go’. The two parents showed differences in plant height, grain volume weight, kernel weight, days to flowering, early season vigor in organic systems, and grain protein content, early season vigor, days to flowering in organically managed systems. The RILs developed from two parents differed for all traits between two management systems except for days to flowering (Asif et al., 2015).

Within the ‘Attila’ × ‘CDC Go’ RIL population, D. Abeysingha found that heat stress at initial flowering decreased seed number and/or seed weight in many of the RIL lines. However, specific RIL lines were identified that did not exhibit reduced seed number and/or seed weight when exposed to the heat stress treatment. The RILs that produced at least 80% of the grain number and weight in the main spike under heat stress conditions as observed under non-stress conditions were considered as heat-resistant RILs and the RILs that produced 40% or less grain number and weight in the main spike under heat stress conditions compared to that under non-stress conditions were considered as heat-sensitive RILs.

1.7 *Rht* alleles

Semi-dwarfing genes have been incorporated into plants in breeding programs to obtain higher yielding varieties during the green revolution (Hedden, 2003). In hexaploid wheat, reduced height is often achieved by incorporating the *Reduced height-1 (Rht-1)* genes and different combinations of *Rht-1* genes can be introduced to obtain plants with a broad range of plant height that confer optimal yield (Filntham et al, 1997; Hedden, 2003). Most of the commercial wheat lines are composed of mutant alleles of *Rht-B1* and *Rht-D1* genes, located on chromosome 4. These *Rht* dwarfing mutant alleles achieve reduce height via producing mutated forms of DELLA GA-signaling proteins that lead it to function as a constitutive (GA-insensitive) growth repressor (Peng et al., 1999). This GA insensitivity of the *Rht* mutants not only reduces stem elongation but also can reduce cell elongation resulting in a reduction in coleoptile length and early vigor (Rebetzke et al., 2001). Reduction in stem stature facilitates greater fertile floret survival at anthesis and during grain set by increasing the photoassimilate supply to the spike (Youssefian et al., 1992).

1.8 Thesis hypothesis

The overall hypothesis tested in this thesis research was that heat-stress tolerance with respect to loss in grain yield in the RIL population of ‘CDC Go’ X ‘Attila’ is related to the ability of specific RILs to maintain normal anther/pollen and ovule development when exposed to moderate heat stress conditions at flowering.

Specific Thesis Objectives

1. To assess the effect of heat stress imposed at flowering on reproductive organ morphology (auricle distance, spike length, spikelet length, anther length, ovule length, ovule area), pollen viability, and grain yield of the wheat RIL parental lines ‘CDC Go’ and ‘Attila’, and selected heat-sensitive and heat-resistant RILs.
2. Using histological techniques, determine if heat stress at flowering alters the development of anther/pollen development in the selected heat-sensitive and heat-resistant RILs
3. To relate modifications in auxin level and GA response to heat stress tolerance by determining, a) if the presence of the reduced height gene *Rht-B* mutation (*Rht-B1b*), which reduce GA response, affects the plants response to heat stress in the wheat RIL parental lines ‘CDC Go’ and ‘Attila’ and selected RILs, and b) if the application of the auxin 4-Cl-IAA prior to heat stress affects the plants response to heat stress in selected RILs.

2. MATERIALS AND METHODS

2.1 Morphological characterization of the effect of heat stress on reproductive development

2.1.1 Plant material

The RILs for the present study were selected from the RIL population (consists of 171 RILs) developed from a cross between two spring wheat cultivars ‘Attila’ (CM85836-50Y-0M-0Y-3M-0Y) and ‘CDC Go’. ‘Attila’ is a spring wheat cultivar that is early maturing, medium yielding, awned, and semi-dwarf, which is widely grown in Southeast Asia (Rosewarne et al., 2008; Zou et al., 2107). ‘CDC Go’ is a Western Canadian Red Spring wheat that is medium height, comparatively early maturing and high yielding with awned spikes and hollow stems (Asif et al., 2015). The heat-resistant RILs (28, 148, 164, 123, 174, 36, 143, and 137), and heat-sensitive RILs (13, 26, 140, 153, 52, 116, 145, 40, 46, 131, and 80) were selected from this RIL population using grain yield data from heat stress studies carried out in the same manner as in this study by D. N Abeysingha, a graduate student in the Ozga lab. RILs with similar average days to anthesis were grouped together (Table 2.1).

Table 2.1 Average days to anthesis of selected heat-resistant and heat-sensitive RILs and parents grown in a growth chamber at 20 °C/17 °C (light /dark), 16 h photoperiod (personal communication, D. N. Abeysingha).

RIL Group	Average days to anthesis
Group 1 Heat-sensitive: 40, 46, 131 Heat-resistant: 36, 143	54-56
Group 2 Heat-sensitive: 52, 116, 145 Heat-resistant: 123, 174	57-59
Group 3 Heat-sensitive: 13, 26, 140, 153, Heat-resistant: 28, 148, 164	59-63
‘Attila’	69
‘CDC Go’	59

2.1.2 Plant growth conditions, heat stress treatment, and morphological trait sample collection

For phenotype assessment, the RIL population parents, and 19 RILs (7 heat-resistant and 10 heat-sensitive RILs) were seeded sequentially in groups of 2 to 3 lines per timing (with approximately 1.5 weeks between seedings) in a growth chamber. The general sequencing of planting was group 1 RILs, followed by group 2 RILs, then groups 3 RILs and the parents (Table 2.1), so that lines with similar days to anthesis were grown together. The growth chamber conditions were 20 °C/17 °C (light/dark), with a light intensity of 373 $\mu\text{mol m}^{-2} \text{s}^{-1}$ (Philips Silhouette High output fluorescent bulbs F54T5/835 Holland, Alto Collection), and a 16 h photoperiod. One to two seeds of each RIL or the parental lines ‘Attila’ and ‘CDC Go’ were planted in square pots (8.6 cm x 8.4 cm) filled with growth medium [1:4 Sunshine #4 potting mix [Sun Gro Horticulture, Canada) and sand]. After about 2 weeks, pots with two seedlings were thinned to one seedling per pot. The plant potting medium was maintained moist in all treatments throughout the experiment and the pots were rotated within the growth chamber weekly. Liquid fertilizer at 100 ppm was applied twice a week until the plants started to dry down (10:52:10, N:P: K early in the week and 12:2:14, N:P: K later in the week). The first three tillers were allowed to develop, and subsequent tillers were removed. For each plant line, 28 plants were grown under control temperature conditions until they approximately reached the developmental stage BBCH 37, when the flag leaf is just visible (still rolled) on the main tiller (the flag leaf usually emerges when at least three nodes on the main tiller are above the soil surface, see developmental assessment below). When plants reached BBCH 37, they were either transferred to a heat stress chamber maintained at 35 °C for 6 h per day for 8 days (a total of 14 plants per line) or they remained in a control chamber (a total of 14 plants per line).

In the heat stress growth chamber, the light cycle (using high fluorescent bulbs as described above) began at 7:00 h at a 24 °C air temperature. At 11:00 h the air temperature ramped up to 35 °C and was maintained for 6 h (until 17:30 h). The remainder of the light cycle was maintained at 24 °C air temperature. At 23:00 h the dark cycle began and was maintained at 20 °C. After 8 days (cycles) of the heat stress treatment, the plants were returned to the control temperature growth chamber and maintained under control conditions until the morphological measurements were taken at anthesis (ranging from approximately 1 to 2 weeks after removal from the heat stress treatment). The non-heat stress control plants remained in the control

temperature growth chamber for the entire length of the experiment (until anthesis for the morphological experiments).

To confirm the growth stage of the main tiller at the time of heat stress exposure, the main tillers of the RIL population parents, ‘CDC Go’ and ‘Attila’, were dissected and the developmental stage was assessed. For this assessment, seeds (two seeds per pot, 5 pots per line) were planted, thinned to 1 plant per pot after about 2 weeks, and maintained under control temperature conditions as described above until the flag leaf was just visible (still rolled) on the main tiller. The main tiller was then dissected and the number of nodes and length between each node were measured (see Appendix A; Fig. A.1 and Table A.1). The stage at the time of exposure to heat stress was confirmed to be BBCH 37 in ‘CDC Go’ and ‘Attila’.

For each line (28 plants total), 16 plants (8 plants exposed to the heat stress treatment and 8 plants from the control temperature treatment) were randomly selected for assessing auricle distance, spike length, spikelet length, pollen viability, anther length and ovule size at the anthesis stage (anthesis defined as the stage when a few spikelets had extruded anthers along the length of the spike, see Fig. A.2). The remaining 12 pots (6 plants exposed to the heat stress treatment and 6 plants from the control temperature treatment) were maintained in the control temperature growth chamber until maturity to measure grain yield. Pollen bags were placed on the spike of each plant at anthesis to prevent cross pollination. For all the measurements, the main tiller of each plant was utilized. For assessing spikelet length, pollen viability, anther length, and ovule size, the floral spike of the main tiller was sectioned into the basal (bottom 1/3 of the spike), the central (middle 1/3 of the spike) and the distal (top 1/3 of the spike) regions (see Appendix A; Fig. A.2). Three spikelets were randomly collected from each spike region (3 spikelets per region x 3 regions per spike=9 spikelets per spike) that had florets with extruded anthers which were not dehisced for assessment.

2.1.3 Assessment of auricle distance, spike length and spikelet length

The auricle distance (AD), and spike and spikelet lengths from the main tiller at anthesis were measured using a ruler in mm. The auricle distance (AD) is the distance between the auricle of the flag leaf and that of the penultimate leaf. Spike length was measured from the attachment of the lowest spikelet to the pedicel/rachis to the most distal spikelet, excluding the awns. The spikelet length was measured starting from the base (where the spikelet is attached to the rachis)

to the tip of the most distal floret, excluding any awns (see Appendix A; Fig. A.3 for depictions of measurements).

2.1.4 Pollen viability and anther length

Extruded anthers (non-dehisced) from the two most mature (basal) florets of the spikelet were collected separately from the basal, the central, and the distal regions of the main tiller spike at anthesis into microfuge tubes containing 1 mL of Carnoy's fixative solution (6:3:1, ethanol (100%): chloroform: acetic acid), and they were fixed and stained as described by Peterson et al. (2010). Specifically, after a minimum of 1 week of fixation at 4 °C in the Carnoy's solution, 3-4 anthers were placed onto a glass microscope slide (25 x 75 x 1 mm, Precleaned frosted end FisherBrand, Fisher Scientific, USA), and the fixative solution was thoroughly dried from the plant material with absorbent paper. Anthers were dissected to release the pollen grains and the remaining anther tissue was carefully removed from the slide using tweezers. Modified Alexander's staining solution [10 mL 95% alcohol, 1 mL malachite green solution (1% (w/v) in 95% alcohol), 50 mL distilled water, 25 mL glycerol, 5 mL acid fuchsin solution (1% (w/v) in distilled water), 0.5 mL orange G solution (1% (w/v) in distilled water), 4 mL glacial acetic acid, and 4.5 mL distilled water to a total of 100 mL] was added (2-4 drops) to the slide before the sample completely dried. The slide was slowly heated over an alcohol burner in a fume hood until the stain solution was near boiling (~30 seconds) by briefly moving the slide in and out of the flame (a more moderate rate of heating allows better penetration of the dye into the cellulose and protoplasm of the pollen grains). Extremely high temperatures resulting in smoking or bubbling of the stain can burn the dye and the sample. A coverslip (22 x 50 mm, cover glass No 1, Fisher Scientific, USA) was placed over the sample on the slide, a grid was adhered to the bottom of the slide to facilitate counting, and the pollen grains were examined under a light microscope (Wild Leitz, Canada) at 10X magnification. A total of 400 pollen grains were assessed for staining (red color = viable; green color = non-viable, see Appendix A; Fig. A4) per slide (100 pollen grains from four randomly selected locations on the slide). To measure anther lengths, three anthers were randomly chosen from each region of the spike from the mixture of previously collected anthers in Carnoy's fixing solution. Anthers were placed on a glass microscopic slide and few drops of water were added to prevent them from drying. Anther length was measured under a dissecting microscope (V8 discovery Stereo microscope, Carl Zeiss

Microscopy, Germany) using Zeiss Zen 2.3 lite (Blue edition) software (Carl Zeiss Microscopy, Germany).

2.1.5 Ovule measurements

The heat-resistant RIL 123 that exhibited a decrease in spikelet length with heat stress, and RIL 28 that did not, and the heat-sensitive RIL 131 that exhibited an increased in spikelet length with heat stress were chosen to determine if there is an association with ovule size and spikelet length changes due to heat stress.

Clearing of the pistils for ovule size measurements was performed as described by Wilkinson and Tucker (2017). Pistils were harvested from the same spikelets that were used to determine pollen viability and anther length in these RILs. The pistils were harvested from the florets with extruded anthers that have not dehisced. The extruded anthers had not dehisced when observed along the length of the spike; therefore, the pistils would likely not be fertilized at the time of collection. The pistils from the three spike regions (basal, central, and distal) were placed separately in microfuge tubes containing 1 mL of ice-cold FAA fixative [formaldehyde (10 mL), 100% EtOH (50 mL), glacial acetic acid (5 mL), distilled water (35 mL) per 100 mL]. After about 1 week of fixation, pistils were dehydrated through an aqueous ethanol series (70%, 80%, 90%, 100%, EtOH: water; v/v) for 20 min each at room temperature. Samples were kept in the final 100% ethanol wash overnight and then carefully transfer using a fine-tipped glass pipette into a microfuge tube containing 1 mL of Hoyer's solution [chloral hydrate (45 mL; 125 g of chloral hydrate in 50 mL of distilled water), distilled water (12 mL), glycerol (3 mL) for a total of 60 mL solution]. Samples were kept immersed in Hoyer's solution at room temperature for approximately 1 week. For measurements, pistils were transferred to a glass microscope slide by holding the pistil by the stigma to avoid damaging the ovary using fine-point tweezers. The pistil was placed with either the dorsal or ventral-side down onto the slide, making sure the branched-stigma of each pistil was laying parallel to the slide surface. On each slide, two to three pistils were equidistantly arranged and covered with a coverslip (22 x 50 mm, cover glass No 1, Fisher Scientific, USA). It is necessary to keep the coverslip flat to avoid the damage caused to the microscope when it is observed under the higher magnification of the microscope. To keep the coverslip flat, approximately equal-sized small clay putty balls were placed in the four corners of the microscope slide before placing the coverslip. After application of the coverslip, Hoyer's

solution was carefully pipetted underneath the coverslip onto the slide until all air was evacuated. Slides were placed flat into a slide storage box that allowed limited ventilation for 4 days. Pistils were imaged using differential contrast microscopy (DIC) at 5X, 10X, and 20X magnification using a Zeiss Axiomager M2 microscope (Carl Zeiss Microscopy, Canada). A Nomarski filter was used at 20X magnification. The cross-sectional area of the ovule and the ovule length for each pistil was measured using the line and contour (spline) graphics tools of the Zeiss Zen 2011 (Blue) software package (Carl Zeiss Microscopy, Germany). The ovule cross-sectional area was measured by encircling the boundary between integument and nucellus under 5X magnification (Fig. 2.1). The ovule length was taken by measuring from the micropyle to the chalazal region of the integument layer (Fig. 2.1). Attempts were made to obtain the embryo sac cross-sectional area by tracing the outline of the structure within the ovule under 20X magnification. However, the embryo sac structure was not clearly delineated in many ovules of the cleared pistils; therefore, quantitation of the embryo sac size was not possible.

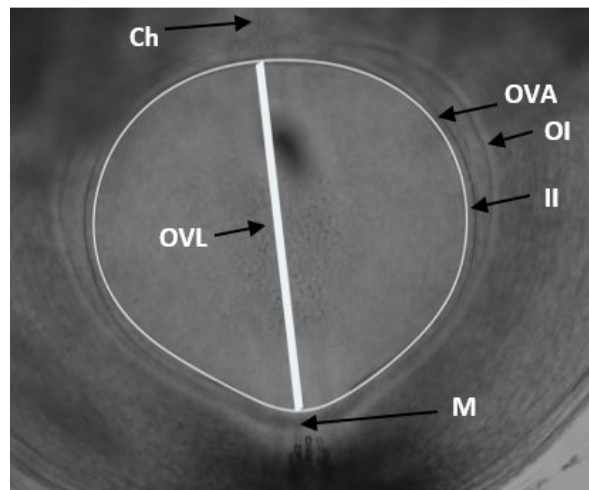


Figure 2.1: Wheat ovule at anthesis after pistil clearing. Imaged at 5X magnification. The image represents the ovule area (OVA) and ovule length (OVL) measurements. Chalazal region, Ch; Inner integument, II; Micropylar region, M; Outer integument, OI.

2.1.6 Grain yield parameters

The floral spike of the main tiller of each plant was harvested individually when the peduncles were dry and brown, and they were subsequently dried at 40 °C for two days to obtain a consistent grain moisture content. The total number of spikelets per spike were counted, and the grain weight and grain number of each spikelet were measured. The total grain weight and grain number per spike and the number of fertile spikelets per spike (defined as spikelets that had grains when harvested) were determined. The spike was divided into three equal sections (basal, central, and distal) based on the number of spikelets in each spike and the grain weight and grain number at each spike were calculated.

2.1.7 Histology

One heat-resistant (RIL 123, with high pollen viability under heat stress conditions) and one heat-sensitive (RIL 131, with reduced pollen viability under heat stress conditions) RIL was selected for this experiment. The experiment consisted of 2 RILs x 2 temperatures (heat stress and control temperature) x 10 reps (10 pots, 1 plant per pot) per treatment. Lines were seeded and grown as described above for the heat-stress and control temperature treatments.

The heat-stressed plants, four spikelets were removed from the central region of the main tiller spike of each plant one day after removing them from the heat treatment. The growth rate of the plants at control temperatures was slower compared to the plants exposed to the heat-stress treatment. Therefore, the plants from the control temperature treatment were kept under control conditions approximately 1.5 to 2 weeks longer than the plants exposed to heat stress, until they reached the equivalent developmental stage as the plants from the heat-stress treatment prior to harvesting the spikelets. The spike length and approximate BBCH stage of the heat stress treated plants 1 day after removal from heat stress were used as indicators to determine the approximate equivalent developmental stage for tissue collection from the control treatment plants within each RIL (RIL 123, BBCH stage 45-49 (flag leaf sheath opening to first awns visible); RIL 131 BBCH stage 45-53 (flag leaf sheath opening to 30% inflorescence emerge, see Appendix, Fig. A.5). Spike length and spikelet length of collected spikelets were measured, and the less mature inner florets were removed, leaving only the primary and secondary florets of each spikelet. The spikelets with lengths from 7 to 12 mm were selected for histological fixing and sectioning. Spikelets were fixed in an aqueous solution containing 0.2% glutaraldehyde (v/v), 3%

paraformaldehyde (v/v), 2 mM CaCl₂, 10 mM sucrose and 25 mM PIPES [piperazine-N, N'-bis (2-ethanesulfonic acid)] at pH 7. The samples were incubated in the fixing solution overnight under vacuum followed by two days at atmospheric pressure. The spikelets were then rinsed three times with 25 mM PIPES buffer, followed by tissue dehydration using a graded ethanol series of 30% and 50% EtOH in 25 mM PIPES buffer (pH 7; v/v), followed by 70% EtOH in water (v/v) for 15 min each. Spikelets were sequentially infiltrated with the following solutions using Leica tissue processor 1020 (Leica Biosystems, Germany) as follows: 1 hour in 70% aqueous ethanol (v/v), 1 hour in 90% aqueous ethanol (v/v), 1.5 hours in 100% ethanol, 1.25 hours in 1:1, ethanol: toluene mixture, 0.5 hours in toluene, 2 hours in paraplast tissue embedding medium (Fisher Scientific, USA), and finally a second immersion in new paraplast tissue embedding medium for 2 hours. Tissues were then embedded in proper orientation in paraffin blocks using a Tissue-TEK II Embedding centre (Tissue Tek, USA). Samples were sliced into 6 µm-thick sections using a Leica RM 2125 R25 microtome (Leica Biosystems, Germany), then placed into a 42-45 °C water bath (with approximately 0.05 g of gelatine added to 2 L of water to facilitate the adhesion of sections to the slide) and incubated until sections were flat (no wrinkles present). Sections were then affixed onto clean glass slides and incubated overnight at 37 °C. Removal of paraffin was performed on sections mounted on slides with two changes of toluene (5 min each), then sections were treated sequentially with 100% (two changes), 90%, 70%, and 50% aqueous EtOH (v/v), for 2 min each. Slides were then transferred to distilled water for 2 min before staining. Prepared sections were stained with a 0.025% aqueous toluidine blue (w/v) solution for 20 seconds at room temperature. Slides were then briefly rinsed three times with distilled water to remove excess stain. De-staining of tissue was carried out by briefly washing the slides by dipping in 95% aqueous EtOH (10 dips) followed by two changes in 100% EtOH (10 dips each). Slides were then immersed in toluene for 2 min, then they were transferred into a new toluene bath and kept another 2 min before coverslips were added. Coverslips were mounted on the slides using DPX mounting media (BDH Chemicals, USA). After drying slides overnight at 37 °C, they were observed under a Zeiss Axio Scope A1 light microscope (Zeiss, Germany).

2.2 Effect of 4-Cl-IAA application on grain yield

Two RILs (80 and 137) that showed a trend for increased grain yield with auxin (4-Cl-IAA) application in a previous experiment conducted by D. N. Abysingha in the Ozga lab were selected for this experiment. This experiment consisted of 2 plant lines (RIL 137 and 80) x 2 temperature (heat stress and control) x 2 treatment solutions (4-Cl-IAA in 0.25% Agral and 0.25% Agral only) x 14 replications (plants) per treatment. The RILs were grown under the same growth conditions as described in section 2.1.2. An aqueous solution of 4-Cl-IAA at 1 μ M in 0.25% Agral (v/v) or 0.25% Agral solution (control) was sprayed on the plants to run-off at the BBCH 37 stage. The plants for the heat-stress treatment were transferred into the heat-stress chamber 12 h after hormone application (temperature conditions were same as described in section 2.1.2) and returned to the control-temperature growth chamber after the heat treatment. The plants for the control temperature treatment were treated with the solutions and maintained under control temperature conditions (temperature conditions were the same as described in section 2.1.2) for the duration of the experiment. Eight plants per treatment were randomly selected during the anthesis stage of the plant to determine auricle distance, spike length, spikelet length, anther length, and pollen viability. The remaining 6 plants per treatment remained in the control temperature growth chamber until maturity for grain yield assessment (total grain number, total grain weight per spike, grain number and grain weight at each spike region, total number of spikelets and sterile spikelets per spike). All the measurements were taken from the floral spike of the main tiller of the plant. All the auxins and adjuvant solutions used for this experiment were prepared by Dr. D. M. Reinecke, University of Alberta, and stored in freezers in dark bottles until used.

2.3 *Rht* allele identification

2.3.1 Plant growth conditions and sample collection

The heat-resistant RILs 123 and 28 and the heat-sensitive RIL 131 were chosen as representative RILs from each of these classes, along with the RIL parental lines ('CDC Go' and 'Attila') for *Rht* allele identification. Two seeds were planted per pot (4 pots per line), and they were maintained under control-temperature conditions as described in section 2.1.2, except no seedlings were removed from the pots (8 plants total per line). A small piece of leaf tissue (~ 200 mg) was collected into a 2 mL microfuge tube for DNA extraction from each plant

approximately 2.5 weeks after planting. Samples were collected on dry ice and stored at -80 °C until required.

2.3.2 Genomic DNA extraction

The genomic DNA extraction was carried out by Dr. H. Kaur in Dr. Ozga's lab at the University of Alberta. Three glass beads (3 mm, Fisher Scientific, Germany) were added to each tube and the tissue was ground to a fine powder using a bead beater (Biospec Products) for 45 sec. To initiate genomic DNA extraction, 1mL of TRIzol (Invitrogen, USA) was added into each tube containing tissue samples and mixed thoroughly, and then samples were incubated at room temperature for 30 min. Subsequently, approximately 200 µL of chloroform was added to each tube and shake vigorously followed by incubation at room temperature for 5 min. After incubation at room temperature, the content was centrifuged at 14,800 rpm for 15 min at 4 °C. The upper aqueous layer was transferred into a new microfuge tube and the bottom organic layer containing DNA was collected into another new 1.5 mL microfuge tube for DNA extraction. Back Extraction Buffer (500 µL; 4 M Guanidine thiocyanate, 50 mM Sodium citrate, 1 M Tris base, MilliQ water) was added to each tube containing the organic layer with DNA, and the samples were mixed by inverting the tubes several times, followed by incubation at room temperature for 30 min. The samples were centrifuged at 13,000 g for 30 min at 4 °C, the upper aqueous layer was transferred into new tubes, and 400 µL of isopropanol was added and mixed by inverting tubes for 1 min. Samples were then placed on a shaker at 200 rpm at room temperature for 10 min. The temperature of the samples was brought down to 4 °C and then samples were centrifuged at 14,800 rpm for 15 min at 4 °C. After centrifugation, the supernatant was discarded, and the resulting pellet was washed with 100 µL of 70% ethanol by inverting the tube several times. The samples were then centrifuged at 14,800 rpm for 15 min at 4 °C, the supernatant was removed, and the pellet was air-dried and dissolved in 20 µL of nuclease free water. All the samples were stored at 4 °C. The concentration and the quality of the DNA were measured using a NanoDrop 1000 spectrophotometer (Thermo Fisher Scientific, USA). The DNA concentration of all the samples was adjusted to 100 ng/µL prior to PCR analyses.

2.3.3 Primers

The following primer sequences were used to amplify the target locus (Table 2.2). These primer sequences were originally designed by Wilhelm et al. (2013) and selected by Dr. Kaur for this analysis.

Table 2.2 List of primer sequences (Wilhelm et al., 2013).

Locus	Primer	Primer sequence	Size
<i>Rht-B1a</i>	Rht-B-F1	5'AGGCAAGCAAAAGCTTGAGA 3'	265 bp
	Rht-B1a-R1	5' CCATGGCCATCTCCAGATG 3'	
<i>Rht-B1b</i>	Rht-B-F1	5'AGGCAAGCAAAAGCTTGAGA 3'	237 bp
	Rht-B1b-R2	5' CCCATGGCCATCTCCAGATA 3'	

2.3.4. PCR amplification

The PCR reaction (25 µL) contained 2 µL of each of the forward and reverse primers (20 pmol/µL), 0.5 µL of 10 mM dNTPs, 0.5 µL of 5U of Taq polymerase, 2.5 µL of 10X PCR buffer (Mg²⁺ 5 µL), and 3 µL of template DNA. The PCR reaction was performed using a thermocycler (Applied Biosystems, Singapore), and with the following thermocycling program; initial activation of Taq polymerase for 5 min at 94 °C; 30 cycles at 94 °C for 30s, 60 °C 30 sec and 72 °C for 1 min; and a final extension at 72 °C for 4 min 30 sec. Then, the PCR product (with 2 µL 6X loading dye) was run on a 3% (w/v) agarose gel (140 V, 30 min) and stained with SyBR safe dye (1/100000 dilution). A ladder of 100 bp lengths was run in parallel to approximate the size of the amplified product.

2.4 Statistical analyses

Data on percent pollen viability, anther length, spikelet length, ovule area, ovule length, number of fertile spikelets per spike, grain weight, and grain number of the main tiller spike were analyzed as a two-factor factorial [2 temperatures (control and heat stress) x 3 spike regions (basal, central, and distal)] analysis of variance (ANOVA) within RIL (17 lines) and parents ('CDC Go' and 'Attila') using R studio software (RStudio Team, 2016 RStudio: Integrated Development for R. RStudio, Inc., USA). Auricle distance, spike length, total grain weight, total seed number,

number of spikelets per spike, and number of fertile spikelets per spike for the main tiller were analyzed as a two-factor factorial [2 temperatures (control and heat stress) x 19 lines (17 RILs and 2 parents)] ANOVA using the R studio software. Mean separation was determined using the Fisher's Least Significant Difference test (LSD) with significance declared at $P \leq 0.05$. The degrees of freedom, probabilities, and F values from the ANOVA analysis for temperature, RIL ID, spike region, temperature x RIL ID, temperature x spike region interactions were indicated in Tables A.2 to A.14.

To study the effect of 4-Cl-IAA application on grain yield, auricle distance, spike length, total grain weight, total seed number, number of spikelets per spike, and number of fertile spikelets per spike at maturity were analyzed as a two-factor factorial [2 temperatures (control and heat stress) x 2 solution treatments (4-Cl-IAA in Agral or Agral only control)] ANOVA for RIL 80 and RIL 137 using R studio software. Percent pollen viability, anther length, spikelet length, grain number and grain weight within each spike section of the main tiller were analyzed as a three-factor factorial [2 temperatures (control and heat stress) x 2 treatment solutions (4-Cl-IAA with 0.25% Agral and 0.25% Agral only) x 3 spike sections (basal, central, and distal)] ANOVA using R studio software. Mean separation was determined using the Fisher's Least Significant Difference test (LSD) with significance declared at $P \leq 0.05$. The degrees of freedom, probabilities, and F values from the ANOVA analysis for temperature, hormone treatment, spike region, temperature x hormone treatment, temperature x hormone, temperature x spike region, temperature x hormone treatment x spike region interactions were indicated in Tables A.15 to A.24.

3. RESULTS

3.1 Morphological characterization of the effect of heat stress on wheat reproductive development

The effect of moderate heat stress at flowering on reproductive development was assessed in specific heat-resistant and heat-sensitive RILs of wheat selected from the RIL population developed by crossing ‘CDC Go’ and ‘Attila’ that segregate for heat tolerance with respect to grain yield.

3.1.1 Effect of heat stress on auricle distance and spike length

Under control temperature conditions, the auricle distance at anthesis was greater for ‘Attila’ than ‘CDC Go’, and it varied from 284 to 146 mm in the heat-resistant RILs, and 218 to 179 mm in the heat-sensitive RILs (Table 3.1). The RILs tested differed in their auricle growth response to the moderate heat-stress treatment. Auricle distance decreased in both parental lines when they were exposed to heat stress at BBCH 37, ‘Attila’ by 18 % and ‘CDC Go’ by 11% (Table 3.1). A heat stress-induced reduction in auricle distance occurred in six of ten heat-sensitive RIL (52, 153, 145, 116, 131 and 40; reduced by 30, 22, 20, 18, 17 and 16%, respectively; Table 3.1). A reduction in auricle distance with the heat-stress treatment was observed in three of seven heat-resistant RILs (36, 28 and 164; reduced by 33, 26 and 16%, respectively; Table 3.1).

Under control temperature conditions, spike length at anthesis was similar for ‘Attila’ (91.3 mm) and ‘CDC Go’ (85.9 mm), and it varied from 76.6-105.4 mm in the heat-resistant RILs, and 77.3-97.4 mm in the heat-sensitive RILs. The RIL parents and most of the RILs tested showed no change in the spike length under the moderate heat stress conditions (Table 3.1). However, a heat stress-induced reduction in spike length (9%) was observed at anthesis in the heat-resistant RIL 36, and an increase in length in the heat-sensitive RIL 131 (16%; Table 3.1).

Table 3.1 Effect of heat stress on auricle distance and spike length of the main tiller of selected heat-resistant and heat-sensitive RILs and parents.

Line	Auricle Distance (mm)		Spike Length (mm)	
	Control ^w	HS ^x	Control	HS
Heat resistant				
RIL 28	283.5 a ^y	211.1 defg	95.5 cdefg	91.8 efghijk
RIL 148	252.6 b	245.8 b	95.9 cdef	92.5 efghi
RIL 164	244.3 bc	204.6 defghi	105.4 a	100.4 abc
RIL 123	222.8 cd	209.6 defg	104.3 ab	98.6 bcd
RIL 174	166.0 mnopq	159.0 opq	76.6 qrs	76.4 rs
RIL 143	149.9 pqr	130.8r	89.9 ghijklm	88.0 hijklmn
RIL 36	145.9qr	97.1 s	80.4 opqr	73.0 s
‘Attila’	216.4 de	177.8 klmno	91.3 fghijkl	91.3 fghijkl
Heat sensitive				
RIL 153	218.0 de	170.6 lmnop	91.3 fghijkl	88.5 hijklm
RIL 46	213.9 def	207.1 defgh	80.7 opqr	80.8 opqr
RIL 140	197.8 efghijk	203.6 defghij	97.4 cde	99.4 bc
RIL 116	192.5 fghijkl	158.3 opq	92.1 efghij	89.4 hijklm
RIL 145	187.3 hijklm	150.5 pqr	82.1 nopq	84.6 mno
RIL 52	185.8 hijklmn	130.3 r	88.0 hijklmn	86.0 klmno
RIL 26	185.0 ijklmn	182.1 jklmn	80.5 opqr	82.4 nop
RIL 131	183.5 ijklmn	153.1 pq	77.3 pqrs	89.6 hijklm
RIL 40	180.0 klmno	151.1 pqr	85.0 mno	87.3 ijklmn
RIL 13	179.1 klmno	163.8 nopq	93.6 defgh	93.6 defgh
‘CDC Go’	190.8 ghijkl	170.6 mnopq	85.9 lmno	86.6 jklmn
Temperature x line		S ^z		S

^wControl-temperature treatment; ^xHS = Heat-stress treatment.

^yData are means, n=7-8; Means followed by a different letter (auricle distance, a-r; Spike length, a-s) are significantly different among lines and temperature treatment within parameter by the LSD test, with the significance level at $P \leq 0.05$; ^zS, significantly different.

3.1.2 Effect of heat stress on spikelet length

Spikelets in the distal region of the spike were smaller in length than those in the basal and central spike regions for all the heat-sensitive lines and 3 of the 8 heat-resistant lines (see section main effect means; Tables 3.2 and 3.3). Heat stress decreased spikelet length in 4 of the 7 heat-resistant RILs but only in 1 of the 10 heat-sensitive RILs (see temperature main effect means; Tables 3.2 and 3.3). Reduction in spikelet length with heat stress varied with spike section across the RILs with the heat-resistant RIL 123 exhibiting a reduction in all 3 spike sections, resulting in the largest decrease in spikelet length per spike with heat stress (10%, compare temperature main effect mean; Table 3.2). In contrast, exposure to the heat stress treatment increased the spikelet length of the heat-sensitive RIL 131 (6.6%, compare temperature main effect mean; Table 3.3). The parents ‘Attila’ and ‘CDC Go’ did not exhibit a reduction in the spikelet length when exposed to the heat stress treatment (Tables 3.2 and 3.3).

Table 3.2 The effect of heat-stress on spikelet length from the basal, central, and distal regions of the main tiller of selected heat-resistant RILs and parent ‘Attila’.

Line	Spikelet length (mm)							
	Spike section						Temperature MEM ^w	
	Basal		Central		Distal		Control	HS
	Control ^x	HS ^y	Control	HS	Control	HS		
Heat resistant								
RIL 28	13.5 a ^z	13.2 a	13.7 a	13.5 a	13.2 a	13.0 a	13.4 m	13.2 m
RIL 148	14.2 a	13.6 a	14.0 a	13.8 a	13.6 a	13.5 a	13.9 m	13.6 n
RIL 164	13.8 a	13.5 a	14.1 a	13.6 a	13.7 a	12.8 b	13.9 m	13.3 n
RIL 123	13.8 a	12.1 c	13.4 ab	12.3 c	12.6 bc	11.3 d	13.2 m	11.9 n
RIL 174	12.7 ab	12.8 a	12.8 a	12.8 a	11.6 b	11.9 ab	12.4 m	12.5 m
RIL 143	11.4 a	11.0 a	11.8 a	11.8 a	11.1 a	11.3 a	11.4 m	11.4 m
RIL 36	12.7 a	12.0 b	12.8 a	11.9 b	11.3 bc	10.7 c	12.3 m	11.5 n
‘Attila’	13.1 a	12.4 a	12.7 a	12.5 a	12.5 a	12.3 a	12.7 m	12.4 m
Section MEM	Basal		Central		Distal			
RIL 28	13.3 f		13.6 f		13.1 f			
RIL 148	13.9 f		13.9 f		13.6 f			
RIL 164	13.6 fg		13.8 f		13.2 g			
RIL 123	12.9 f		12.8 f		11.9 g			
RIL 174	12.8 f		12.9 f		11.8 g			
RIL 143	11.2 f		11.8 f		11.2 f			
RIL 36	12.3 f		12.3 f		11.0 g			
‘Attila’	12.7 f		12.6 f		12.4 f			

^wMEM, main effect mean; ^xControl-temperature treatment; ^yHS = Heat-stress treatment.

^zData are means, n=8; Means followed by different letters are significantly different among temperature treatment and spike section (a-d), within lines and parameters; section main effect means (f-g); temperature main effect means (m, n) by the LSD test, with the significance level at $P \leq 0.05$; The temperature x spike region interaction was not significant for all lines assessed.

Table 3.3 The effect of heat-stress on spikelet length from the basal, central, and distal regions of the main tiller of selected heat-sensitive RILs and parent ‘CDC Go’.

Line	Spikelet length (mm)						Temperature MEM ^w	
	Spike section						Control	HS
	Basal		Central		Distal			
Control ^x	HS ^y	Control	HS	Control	HS			
Heat sensitive								
RIL 153	12.7 a ^z	12.5 a	12.4 a	12.3 a	11.3 b	11.1 b	12.1 m	12.0 m
RIL 46	11.8 a	11.8 a	11.8 a	11.5 a	10.2 b	10.3 b	11.2 m	11.2 m
RIL 140	13.4 ab	13.5 a	13.7 a	13.4 ab	12.6 bc	12.4 c	13.2 m	13.1 m
RIL 116	14.0 a	13.4 b	13.3 b	13.3 b	12.0 c	11.8 c	13.1 m	12.8 m
RIL 145	13.3 a	13.5 a	12.7 a	13.1 a	11.3 b	11.4 b	12.4 m	12.7 m
RIL 52	14.2 a	13.9 a	14.1 a	13.2 b	12.3 c	11.9 c	13.5 m	13.0 n
RIL 26	10.9 abc	11.1 ab	11.2 a	11.3 a	10.3 c	10.4 bc	10.8 m	10.9 m
RIL 131	12.4 bc	13.4 a	12.4 bc	13.1 ab	11.2 d	11.9 cd	12.0 n	12.8 m
RIL 40	13.4 a	13.3 a	13.7 a	13.6 a	12.2 b	12.1 b	13.1 m	13.0 m
RIL 13	14.1 a	13.8 a	13.8 a	13.4 a	12.3 b	12.2 b	13.4 m	13.1 m
‘CDC Go’	14.4 a	14.0 a	14.2 a	14.2 a	12.5 b	12.8 b	13.7 m	13.6 m
Section MEM	Basal		Central		Distal			
RIL 153	12.6 f		12.4 f		11.2 g			
RIL 46	11.8 f		11.6 f		10.3 g			
RIL 140	13.5 f		13.5 f		12.5 g			
RIL 116	13.7 f		13.3 g		11.9 h			
RIL 145	13.4 f		12.9 f		11.4 g			
RIL 52	14.0 f		13.6 f		12.1 g			
RIL 26	11.0 f		11.2 f		10.3 g			
RIL 131	12.9 f		12.7 f		11.6 g			
RIL 40	13.3 f		13.6 f		12.1 g			
RIL 13	14.0 f		13.6 f		12.2 g			
‘CDC Go’	14.2 f		14.2 f		12.7 g			

^wMEM, main effect mean; ^xControl-temperature treatment; ^yHS = Heat-stress treatment.

^zData are means, n=8; Means followed by different letters are significantly different among temperature treatment and spike section (a-d), within lines and parameters; section main effect means (f-h); temperature main effect means (m, n) by the LSD test, with the significance level at $P \leq 0.05$; The temperature x spike region interaction was not significant for all lines assessed.

3.1.3 Effect of heat-stress on pollen viability

The pollen viability in the all three spike sections was similar for 6 of 7 heat-resistant RILs and 8 of 10 heat-sensitive RILs (see section main effect mean, Tables 3.4 and 3.5). Heat stress decreased the percentage of viable pollen in 2 of the 7 heat-resistant RILs and 4 of the 10 heat-sensitive RILs (see the temperature main effect means, Tables 3.4 and 3.5). The reduction in pollen viability with heat stress varied with spike section across the RILs. The heat resistant RIL 28 and 174 exhibited a small heat stress-induced reduction in pollen viability of 2% (temperature main effect mean), focused in two regions of the spike (in the basal and central spike regions of RIL 28 and the central and distal spike regions of RIL 174; Table 3.4). Among the heat-sensitive RILs, RIL 131 exhibited the largest pollen viability decrease with heat stress (22%, temperature main effect means), with a reduction in all three spike sections (Table 3.5). In contrast, exposure to the heat-stress treatment resulted in a small increase in the pollen viability of the heat-resistant RIL 164 (3% increase, temperature main effect means), with increased pollen viability observed in the distal region of the spike (Table 3.4). Pollen viability was not affected by the heat stress treatment in the parental lines ‘Attila’ and ‘CDC Go’ (Tables 3.4 and 3.5). High temperature treatment did not affect the pollen viability of the main spike of RIL 143, 46 and 40, but reduction of pollen viability at the basal spike section was observed (see temperature main effect means, Tables 3.4 and 3.5).

Table 3.4 The effect of heat stress on percentage pollen viability in the basal, central, and distal regions of the main spike of selected heat-resistant RILs, and parent ‘Attila’.

Line	Pollen viability (%)								Spike section X Temp.
	Spike sections								
	Basal		Central		Distal		Temperature MEM ^u		
	Control ^v	HS ^w	Control	HS	Control	HS	Control	HS	
Heat Resistant									
RIL 28	96.6 ab ^x	94.1 c	97.5 a	94.8 bc	95.4 bc	95.2 bc	96.5 m	94.7 n	NS ^y
RIL 148	96.2 a	94.3 a	96.2 a	97.6 a	95.3 a	94.0 a	95.9 m	95.3 m	NS
RIL 164	96.7 a	97.4 a	95.4 a	96.9 a	91.8 b	97.2 a	94.6 n	97.1 m	NS
RIL 123	95.2 a	94.6 a	94.5 a	96.0 a	93.0 a	95.0 a	94.3 m	95.2 m	NS
RIL 174	94.7 abc	94.0 abc	96.3 a	93.0 bc	95.3 ab	92.3 c	95.4 m	93.1 n	NS
RIL 143	92.9 a	87.0 b	92.9 a	92.5 a	92.4 ab	93.0 a	92.7 m	90.8 m	NS
RIL 36	90.0 a	92.3 a	89.6 a	91.0 a	87.9 a	90.6 a	89.2 m	91.3 m	NS
‘Attila’	97.7 a	97.7 a	98.9 a	96.8 a	97.2 a	97.6 a	97.9 m	97.4 m	NS
Section MEM	Basal		Central		Distal				
RIL 28	95.4 f		96.2 f		95.3 f				
RIL 148	95.2 f		96.9 f		94.6 f				
RIL 164	97.0 f		96.2 fg		94.6 g				
RIL 123	94.9 f		95.2 f		94.1 f				
RIL 174	94.3 f		94.6 f		93.8 f				
RIL 143	89.7 f		92.7 f		92.7 f				
RIL 36	91.2 f		90.3 f		89.2 f				
‘Attila’	97.7 f		97.8 f		97.4 f				

^uMEM, main effect mean; ^vControl-temperature treatment; ^wHS = Heat-stress treatment.

^xData are means, n=8; Means followed by different letters are significantly different among temperature treatment and spike sections (a-c), within lines; section main effect means (f-g); temperature main effect means (m, n) by the LSD test, with the significance level at $P \leq 0.05$;

^yNS, not significantly different.

Table 3.5 The effect of heat stress on percentage pollen viability in the basal, central, and distal regions of the main spike of selected heat-sensitive RILs, and parent ‘CDC Go’.

Line	Pollen viability (%)						Temperature MEM ^u		Spike section X Temp
	Spike sections								
	Basal		Central		Distal		Control	HS	
	Control ^v	HS ^w	Control	HS	Control	HS			
Heat Sensitive									
RIL 153	94.6 a ^x	95.0 a	92.7 ab	94.3 a	94.5 a	91.3 b	93.9 m	93.5 m	S ^y
RIL 46	89.6 a	81.8 b	87.5 ab	85.7 ab	84.8 ab	84.2 ab	87.3 m	83.9 m	NS ^z
RIL 140	94.0 ab	96.5 a	94.9 ab	96.2 a	91.8 b	93.5 ab	93.6 m	95.4 m	NS
RIL 116	95.0 a	93.3 ab	95.3 a	93.1 ab	93.3 ab	90.9 b	94.5 m	92.4 n	NS
RIL 145	96.0 a	94.1 ab	94.9 ab	94.3 ab	93.6 ab	92.3 b	94.8 m	93.6 m	NS
RIL 52	96.1 a	94.7 a	95.8 a	95.4 a	96.2 a	94.7 a	96.0 m	94.9 n	NS
RIL 26	95.5 a	93.3 a	95.9 a	94.8 a	95.3 a	89.4 a	95.6 m	92.5 n	NS
RIL 131	90.5 a	64.4 b	86.6 a	68.4 b	81.7 a	69.3 b	86.3 m	67.4 n	NS
RIL 40	95.7 a	91.3 b	94.6 a	93.4 ab	92.7 ab	93.9 ab	94.3 m	92.9 m	NS
RIL 13	93.8 a	95.0 a	92.9 a	93.4 a	94.9 a	92.3 a	93.9 m	93.6 m	NS
‘CDC Go’	97.5 a	96.6 a	96.9 a	95.6 a	94.5 a	94.6 a	96.3 m	95.6 m	NS
Section MEM	Basal		Central		Distal				
RIL 153	94.8 f		93.5 f		92.9 f				
RIL 46	85.7 f		86.6 f		84.5 f				
RIL 140	95.2 f		95.6 f		92.7 f				
RIL 116	94.1 fg		94.2 f		92.1 g				
RIL 145	95.0 f		94.6 fg		93.0 g				
RIL 52	95.4 f		95.6 f		95.4 f				
RIL 26	94.4 f		95.3 f		92.3 f				
RIL 131	77.4 f		77.5 f		75.5 f				
RIL 40	93.5 f		94.0 f		93.3 f				
RIL 13	94.4 f		93.2 f		93.6 f				
‘CDC Go’	97.0 f		96.3 f		94.6 f				

^uMEM, main effect mean; ^vControl-temperature treatment; ^wHS = Heat-stress treatment.

^xData are means, n=8; Means followed by different letters are significantly different among temperature treatment and spike sections (a,b), within lines; section main effect means (f-h); temperature main effect means (m, n) by the LSD test, with the significance level at $P \leq 0.05$; ^yS, significantly different; ^zNS, not significantly different.

3.1.4 Effect of heat stress on anther length

The anther lengths of the heat-resistant RILs were either similar in all three spike sections (RIL 36,143,174) or lower in the distal spike section (RIL 28, 164, 148 and 123, see section main effect means, Table 3.6). Heat-sensitive lines had lower anther lengths in the distal (RIL 153, 140, 145, 52, and 131) or both central and distal spike sections (RIL 46, 26, 40, and 13) compared to the basal section of the main spike (see section main effect mean, Table 3.7). The heat-sensitive line 116 showed similar anther length in all three spike sections (see section main effect mean, Table 3.7). Heat stress decreased the anther length at anthesis in 4 of 7 heat-resistant RILs (143, 28, 164, and 123; reduced by 11, 10, 7 and 7%, respectively) and 8 of 10 heat-sensitive RILs (52, 116, 13, 145, 131, 40, 153, 46; reduced by 20, 17, 15, 16, 14, 8, 5, and 5%; temperature main effect means; Tables 3.6 and 3.7). The reduction in the anther length with heat stress occurred in all three regions of the spike across most heat-resistant and heat-sensitive RILs (Tables 3.6 and 3.7). In contrast, exposure to heat stress increased the anther length in the heat-resistant RIL 148 (6%, temperature main effect means) and the heat-sensitive RIL 140 (5%, temperature main effect means, Tables 3.6 and 3.7). The parents ‘CDC Go’, and ‘Attila’ exhibited a decrease in anther length after the heat-stress treatment (see the temperature main effect mean, Tables 3.6 and 3.7), with reduction occurring in all three spike sections (Tables 3.6 and 3.7).

Table 3.6 The effect of heat stress on anther length in the basal, central, and distal regions of the main spike of selected heat-resistant RILs and parent ‘Attila’.

Line	Anther length (mm)						Temperature MEM ^u		Spike section X Temp.
	Spike section						Control	HS	
	Basal		Central		Distal				
Control ^v	HS ^w	Control	HS	Control	HS	Control	HS		
Heat Resistant									
RIL 28	0.152 a ^x	0.138 b	0.150 a	0.136 bc	0.143 ab	0.126 c	0.148 m	0.133 n	NS ^y
RIL 148	0.166 a	0.168 a	0.156 ab	0.168 a	0.149 b	0.163 ab	0.157 n	0.166 m	NS
RIL 164	0.167 a	0.153 b	0.164 a	0.151 b	0.153 b	0.146 b	0.161 m	0.150 n	NS
RIL 123	0.170 a	0.155 bc	0.165 a	0.155 bc	0.157 b	0.150 c	0.164 m	0.153 n	NS
RIL 174	0.148 a	0.145 a	0.147 a	0.144 a	0.135 a	0.136 a	0.143 m	0.141 m	NS
RIL 143	0.134 a	0.120 bc	0.132 a	0.117 c	0.129 ab	0.114 c	0.132 m	0.117 n	NS
RIL 36	0.162 a	0.145 a	0.152 a	0.153 a	0.151 a	0.145 a	0.155 m	0.147 m	NS
‘Attila’	0.143 a	0.124 b	0.138 a	0.125 b	0.136 a	0.124 b	0.139 m	0.124 n	NS
Section MEM	Basal		Central		Distal				
RIL 28	0.145 f		0.143 f		0.135 g				
RIL 148	0.167 f		0.162 fg		0.156 g				
RIL 164	0.160 f		0.157 f		0.149 g				
RIL 123	0.162 f		0.162 f		0.153 g				
RIL 174	0.146 f		0.146 f		0.135 f				
RIL 143	0.127 f		0.124 f		0.121 f				
RIL 36	0.153 f		0.152 f		0.148 f				
‘Attila’	0.133 f		0.131 f		0.130 f				

^uMEM, main effect mean; ^vControl-temperature treatment; ^wHS = heat-stress treatment.

^xData are means, n=8; Means followed by different letters are significantly different among temperature treatment and spike sections (a-c), within lines; section main effect means (f-g); temperature main effect means (m, n) by the LSD test, with the significance level at $P \leq 0.05$;

^yNS, not significantly different.

Table 3.7 The effect of heat stress on anther length in the basal, central, and distal regions of the main spike of selected heat-sensitive RILs and parent ‘CDC Go’.

Line	Anther length (mm)						Temperature MEM ^u		Spike section X Temp.
	Spike section						Control	HS	
	Basal		Central		Distal				
	Control ^v	HS ^w	Control	HS	Control	HS			
Heat Sensitive									
RIL 153	0.127 a ^x	0.123 a	0.121 ab	0.115 c	0.115 bc	0.107 d	0.121 m	0.115 n	NS ^y
RIL 46	0.160 a	0.151 ab	0.149 b	0.143 bc	0.144 bc	0.136 c	0.151 m	0.143 n	NS
RIL 140	0.135 abc	0.140 a	0.131 bc	0.137 ab	0.124 d	0.130 cd	0.130 n	0.136 m	NS
RIL 116	0.168 a	0.136 b	0.165 a	0.139 b	0.157 a	0.129 b	0.163 m	0.135 n	NS
RIL 145	0.144 a	0.116 c	0.138 b	0.116 c	0.121 c	0.106 d	0.134 m	0.112 n	S ^z
RIL 52	0.169 a	0.136 c	0.163 a	0.131 c	0.154 b	0.120 d	0.162 m	0.129 n	NS
RIL 26	0.125 a	0.122 ab	0.118 ab	0.126 a	0.111 b	0.119 ab	0.118 m	0.122 m	NS
RIL 131	0.167 a	0.146 b	0.161 a	0.133 c	0.147 b	0.130 c	0.159 m	0.137 n	NS
RIL 40	0.183 a	0.165 b	0.175 a	0.165 b	0.162 b	0.150 c	0.173 m	0.160 n	NS
RIL 13	0.139 a	0.119 bc	0.141 a	0.119 bc	0.127 ab	0.108 c	0.136 m	0.115 n	NS
‘CDC Go’	0.164 a	0.142 c	0.159 ab	0.142 c	0.146 bc	0.126 d	0.156 m	0.136 n	NS
Section MEM	Basal		Central		Distal				
RIL 153	0.125 f		0.118 g		0.111 h				
RIL 46	0.156 f		0.146 g		0.140 g				
RIL 140	0.137 f		0.134 f		0.127 g				
RIL 116	0.152 f		0.152 f		0.143 f				
RIL 145	0.130 f		0.127 g		0.113 h				
RIL 52	0.155 f		0.147 g		0.138 h				
RIL 26	0.123 f		0.121 fg		0.115 g				
RIL 131	0.157 f		0.147 g		0.139 h				
RIL 40	0.174 f		0.170 f		0.156 g				
RIL 13	0.129 f		0.130 f		0.117 g				
‘CDC Go’	0.153 f		0.150 f		0.136 g				

^uMEM, main effect mean; ^vControl-temperature treatment; ^wHS = heat-stress treatment.

^xData are means, n=8; Means followed by different letters are significantly different among temperature treatment and spike sections (a-d), within lines; section main effect means (f-h); temperature main effect means (m, n) by the LSD test, with the significance level at $P \leq 0.05$;

^yNS, not significantly different; ^zS, significantly different.

3.1.5 Effect of heat stress on pollen morphology

Cross-sections of anthers approximately at stage 11 were obtained from spikelets from the heat-sensitive RIL 131 that exhibited a large reduction in pollen viability with heat stress, and from the heat-resistant RIL 123, where heat stress did not affect the pollen viability. RILs under control and heat stress conditions. The anther morphology did not appear to be affected in these RILs by the heat-stress treatment, with intact tapetum, endothecium, and epidermal cell layers visible in the anther cross-sections from both heat-stress and control treatments (Fig. 3.1). Although the pollen morphology varied across anthers within and among the spikelets assessed, degradation of pollen grains under heat stress conditions was observed at a much greater frequency in the heat-sensitive RIL 131 when exposed to heat stress than observed for the heat-resistant RIL 123 (Fig. 3.1 B and D).

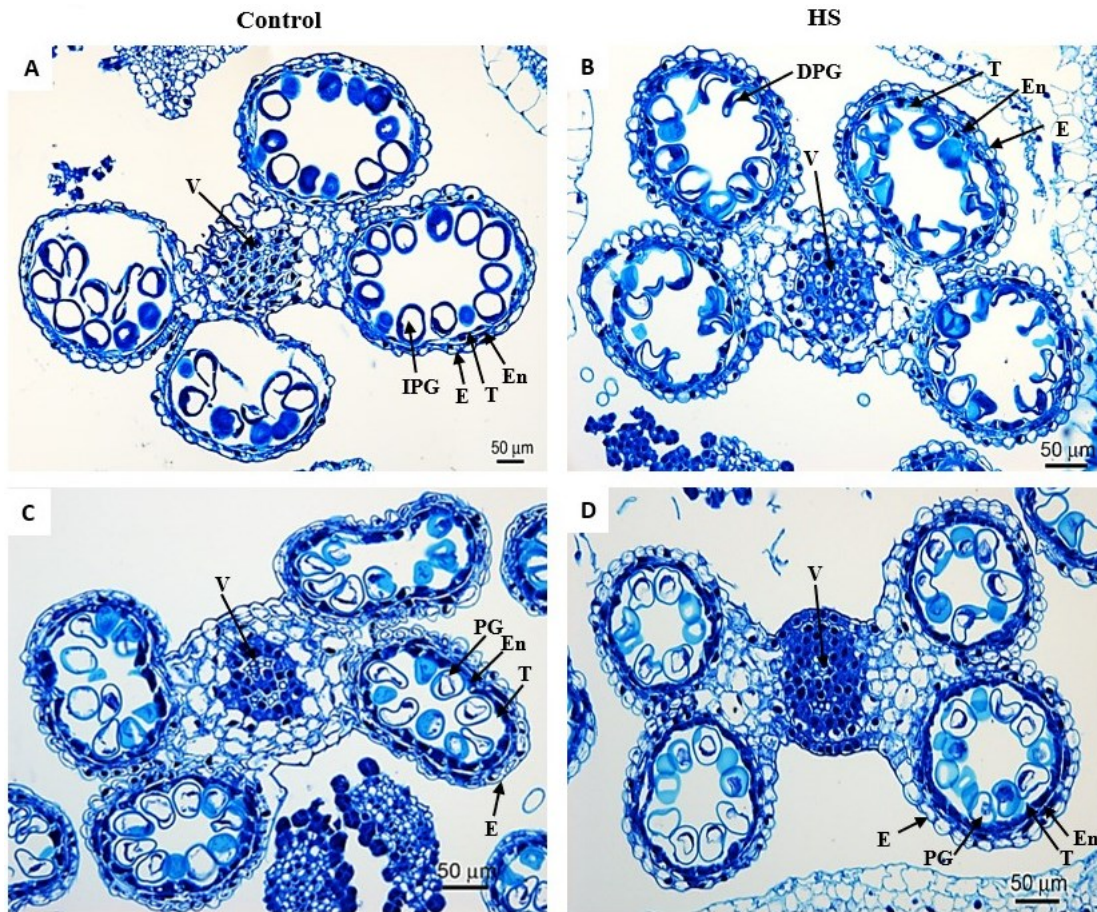


Figure 3.1: Representative micrographs of the cross sections of anthers at approximately stage 11 from heat-sensitive RIL 131 and heat-resistant RIL 123. Imaged at 20X magnification. Heat-sensitive RIL 131 (A, B) and heat-resistant RIL 123 (C, D) from control (A, C) and heat stress (B, D) treatments. Degraded Pollen Grain, DPG; Epidermis, E; Endothecium, En; Intact Pollen Grain, IPG; Tapetum, T; Vascular region, V.

3.1.6 Wheat carpel structure prior to fertilization

The wheat carpel consists of a stigma/style and an ovary with a single ovule (Fig. 3.2 A and B). The ovule is comprised of an embryo sac (female gametophyte) embedded in the nucellus tissue, and it is surrounded by the inner and outer integuments. A vascular bundle is present at the dorsal side of the ovary connecting the ovary to the base of the floret (Fig. 3.2).

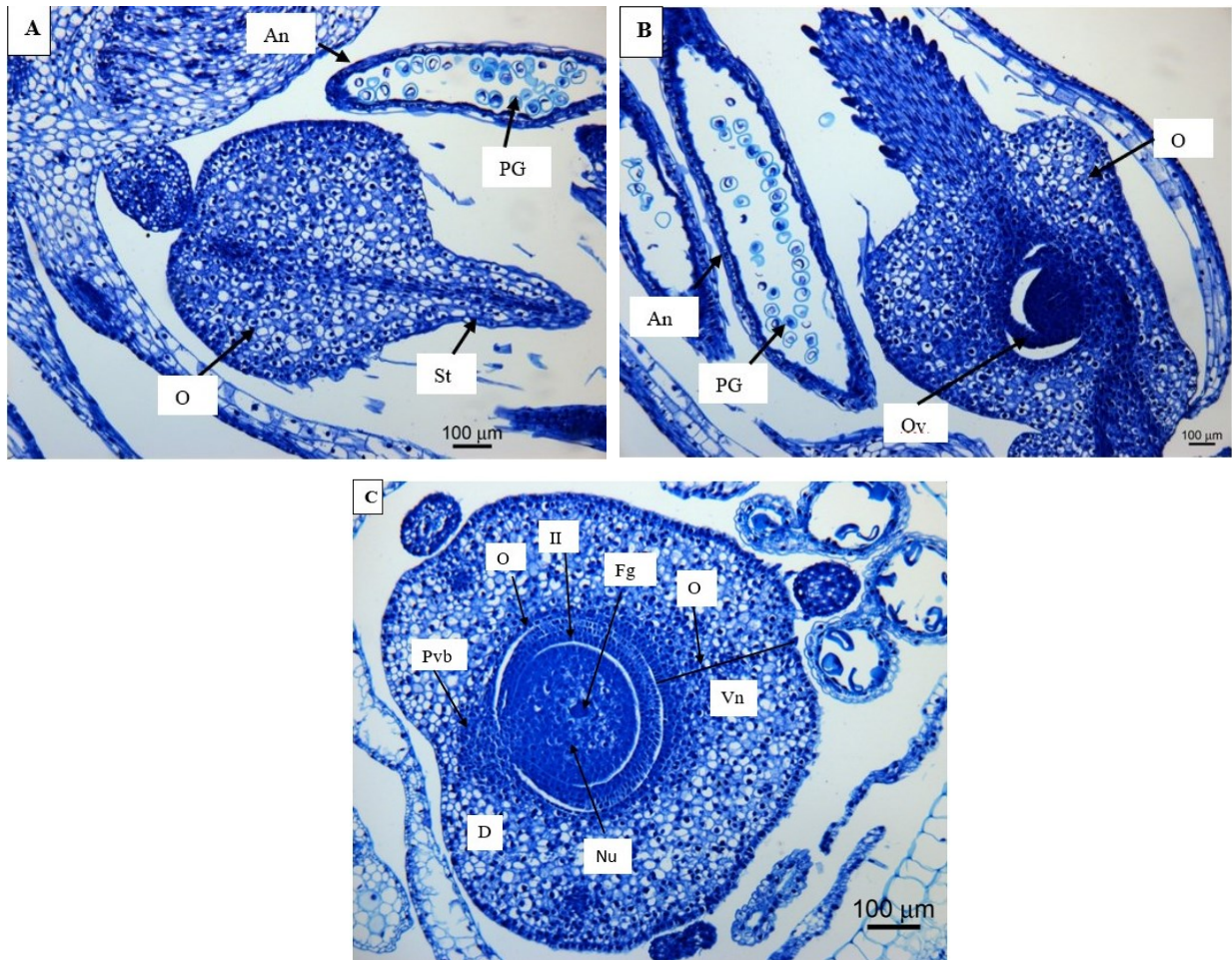


Figure 3.2: Wheat floret and carpel structure prior to anthesis. Longitudinal sections of developing wheat floret from ‘Attila’ at magnification 10X (A and B). Transverse section of carpel from floret is from ‘CDC Go’ at magnification 20X (C). Anther, An; Female gametophyte, Fg; Dorsal, D; Inner Integument, II; Ovary, O; Outer Integument, OI; Ovule, Ov; Nucellus, Nu; Pollen Grains, PG; Provascular bundle, Pvb; Ventral, Vn; Style/Stigma, St.

3.1.7 Effect of heat stress on ovule and embryo sac size

The effect of heat stress on ovule area and length was studied using the two heat-resistant RILs 28 and 123, and the heat-sensitive RIL 131. Under control temperature conditions, the ovule area and length were similar in the florets from all three spike sections within each RIL assessed (Table 3.8; Fig. 3.3). High temperature treatment did not affect the area and length of ovules from florets at the basal, the central, and the distal position of the spikes in the two heat-resistant RILs (28 and 123; Fig. 3.3; Table 3.8). However, an increase in ovule area (109%) and ovule length (50%) with heat stress was observed in heat-sensitive RIL 131 (see temperature main effect means; Table 3.8). The trend of heat stress-induced increase in ovule size was observed in all spike sections of heat-sensitive RIL 131, but it was only significant in the basal spike section (107% increase in ovule area and 55% increase ovule length (Table 3.8, Fig. 3.3). Selected images of the embryo sac area from all three RILs are shown in Fig. 3.4. An attempt was made to measure the embryo sac area of selected heat-resistant and heat-sensitive lines; however, most images were not clear enough to accurately measure the boundary of the embryo sac area.

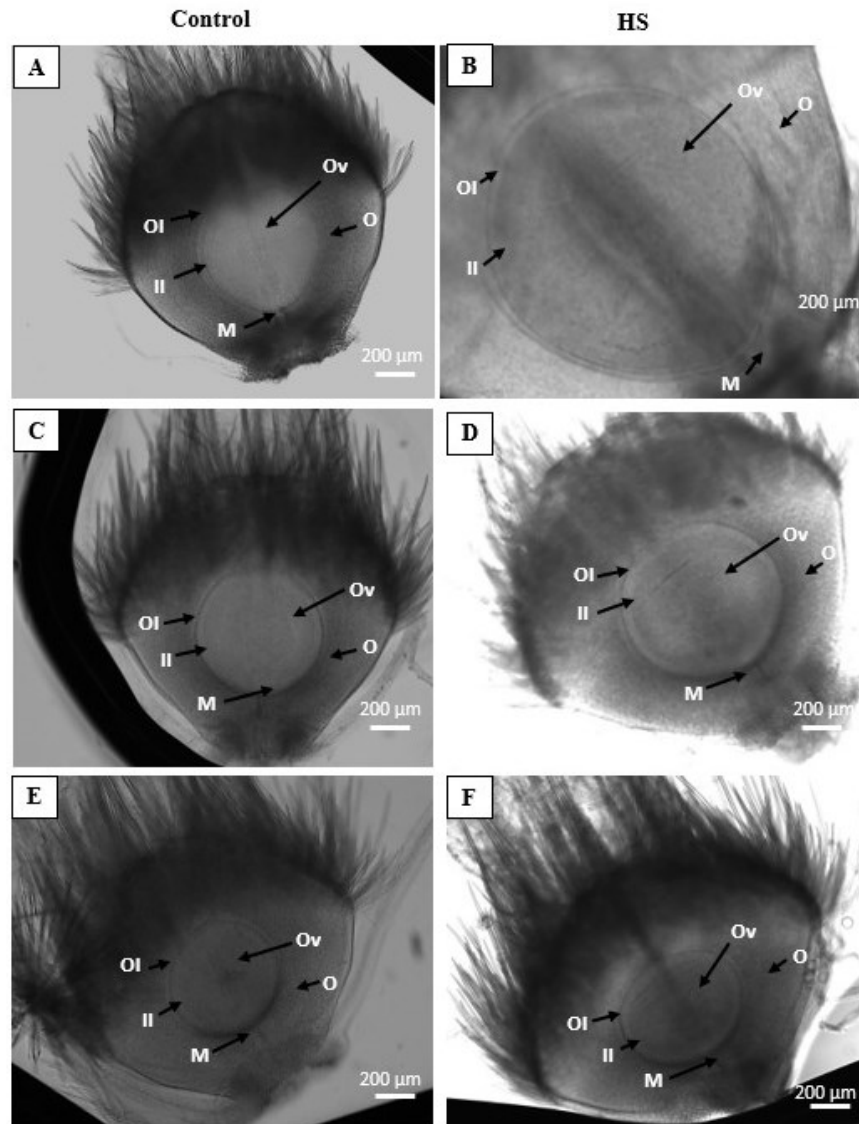


Figure 3.3: Representative micrographs of ovules within the carpels from heat-resistant and heat-sensitive RILs obtained from the central region of the spike grown under control or heat stress conditions. The ovules are from florets at anthesis just prior to anther dehiscence and imaged at 5X magnification. Heat-sensitive RIL 131 (A, B) and heat-resistant RILs 123 (C, D) and RIL 28 (E, F) from control (A, C, E) and heat stress (B, D, F) treatments. Inner integument, II; Micropylar region, M; Outer Integument, OI; Ovary, O; Ovule, Ov.

Table 3.8 The effect of heat stress on the area and length of ovules from florets at the basal, central, and distal positions of the main tiller spike of heat-resistant and heat-sensitive RILs, and parents.

Parameter	RIL ID	Spike section						Temperature MEM ^v	
		Basal		Central		Distal		Control	HS
		Control ^w	HS ^x	Control	HS	Control	HS		
Ovule area (µm ²)	28	231,821 a ^y	268,398 a	293,068 a	288,555 a	311,040 a	312,514 a	278,643 m	289,822 m
	123	318,523 a	360,245 a	392,944 a	354,953 a	370,721 a	410,532 a	360,729 m	375,244 m
	131	369,962 bc	767,220 a	362,027 bc	733,338 ab	296,501 c	644,866 abc	342,830 n	715,141 m
	Section MEM		Basal		Central		Distal		
	28		250,110 g		290,812 fg		311,777 f		
	123		339,384 f		373,949 f		390,627 f		
	131		568,591 f		547,683 f		470,684 f		
	Temperature x spike section	NS ^z							
Ovule Length (µm)	28	519 a	551 a	591 a	569 a	617 a	582 a	576 m	567 m
	123	619 a	663 a	667 a	655 a	668 a	688 a	651 m	669 m
	131	663 c	1029 a	672 bc	982 ab	610 c	903 abc	649 n	971 m
	Section MEM		Basal		Central		Distal		
	28		535 f		580 f		600 f		
	123		641 f		661 f		678 f		
	131		846 f		827 f		757 f		
	Temperature x spike section	NS							

^vMEM, main effect means; ^wControl-temperature treatment; ^xHS = Heat-stress treatment.

^yData are means, n=8; Means followed by different letters are significantly different among spike section and temperature treatment within line and parameter (Ovule area and length a-c); section main effect means (f, g); temperature main effect means (m, n) by the LSD test, with the significance level at $P \leq 0.05$; ^zNS, not significantly different.

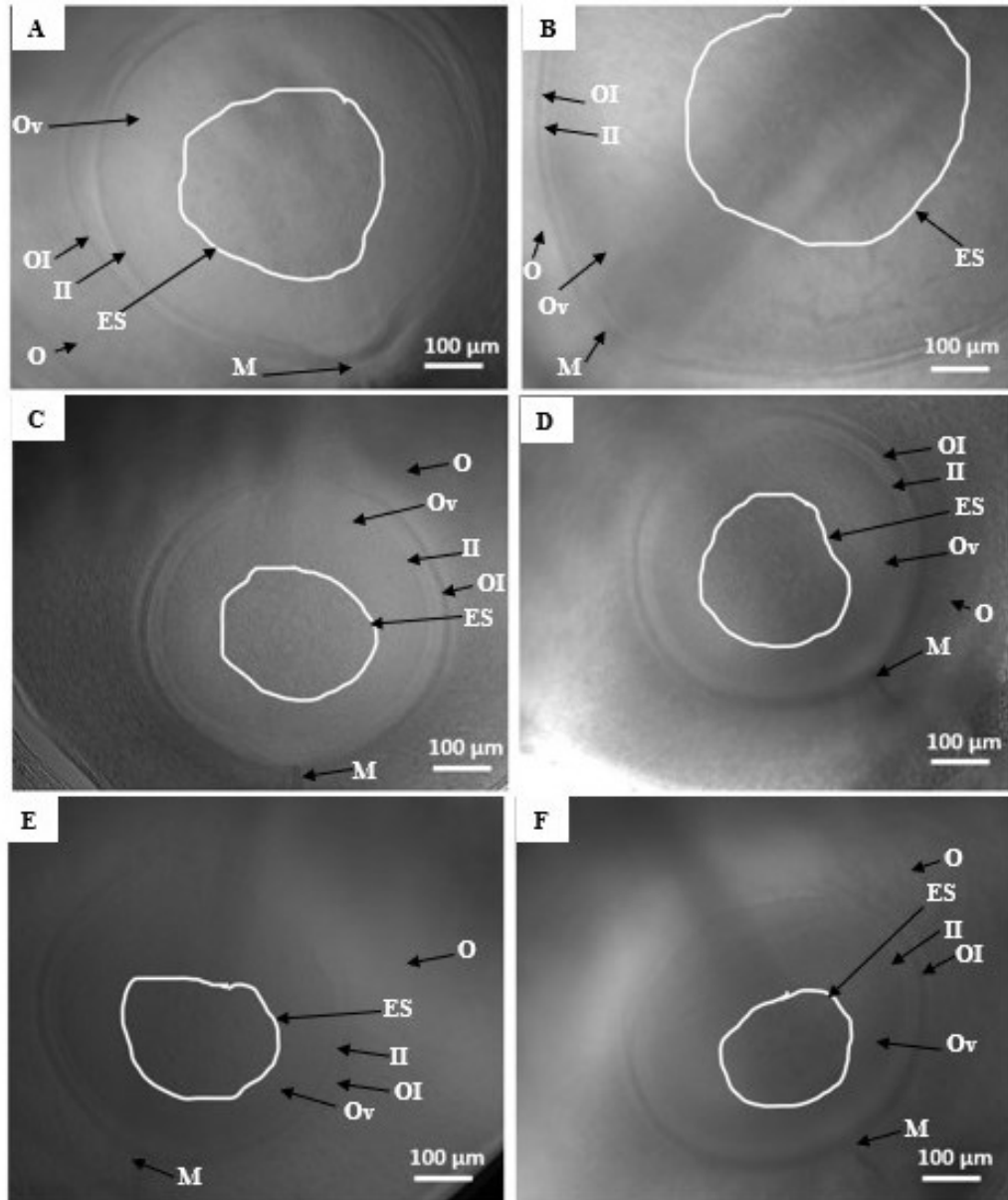


Figure 3.4: Representative micrographs of ovules from florets at anthesis just prior to anther dehiscence with the area of the embryo sac delineated from carpels (white outline) of heat-resistant and heat-sensitive RILs obtained under control and heat-stress conditions. Imaged at 10X magnification. Heat-sensitive RIL131 (A, D) and heat-resistant RILs 123 (B, E) and RIL 28 (C, F) from control (A, B, C) and heat stress (D, E, F) treatments. Embryo Sac, ES; Inner Integument, II; Micropylar region, M; Outer Integument, OI; Ovary, O; Ovule, Ov.

3.1.8 Effect of heat stress on grain yield

Under control temperature conditions, the number of spikelets on the main tiller was higher for ‘Attila’ (20) than ‘CDC Go’ (16), and they varied from 15 to 20 per spike in the heat-resistant and heat-sensitive RILs (Table 3.9). The number of fertile spikelets per spike (have a minimal of 1 mature seed) in ‘Attila’ and ‘CDC Go’ was similar, and they varied from 13 to 16 in the heat-resistant RILs and 9 to 15 in the heat-sensitive RILs (Table 3.9). The number of spikelets or fertile spikelets per spike was not reduced by the heat stress treatment in ‘Attila’ or ‘CDC Go’, or any of the RILs (Table 3.9). However, ‘Attila’ produced more fertile spikelets per spike (17) than ‘CDC Go’ (14) when exposed to heat stress (Table 3.10). Within the heat-resistant group, the RILs 28, 164, and 123 produced more fertile spikelets (17-18) than RILs 148, 174, 143, and 36 (13-14), and within the heat-sensitive group the RILs 153, 140, 26 and 131 produced the lowest number of fertile spikelets (10-13) when exposed to the heat stress treatment (Table 3.9). A greater number of fertile spikelets was observed in the central spike section or both central and distal spike sections of most heat-resistant lines, while variation in the number of fertile spikelets was observed among the spike sections of the heat-sensitive lines (section main effect mean, Tables 3.10 and 3.11). High temperature stress did not affect the number of fertile spikelets per spike in heat-resistant lines except for RIL 36 which showed an increase in number of fertile florets with heat stress in the basal spike section (Table 3.10). Within heat-sensitive lines, an increase in the number of fertile spikelets per spike was observed in the basal spike section of RIL 140 and distal spike section of RIL 116 and 145 (Table 3.11) under heat-stress conditions. In contrast, a decrease in number of fertile spikelets per spike was observed with the heat stress treatment in central spike section of RIL 26 (Table 3.11).

Under control temperature conditions, the total spike grain number and weight of ‘Attila’ and ‘CDC Go’ were similar (Table 3.12). The total grain weight varied from 1.0329 to 1.5335 g and 0.8270 to 1.5639 g in heat-resistant and heat-sensitive RILs, respectively (Table 3.12). The total grain number varied from 21-41 and 19-33 in heat-resistant and heat-sensitive RILs, respectively (Table 3.12). The heat-stress treatment did not affect the total grain weight and number of ‘Attila’ and ‘CDC Go’ (Table 3.12). However, ‘Attila’ produced more seeds (44.7) than ‘CDC Go’ (26.8) when exposed to the heat stress conditions. Within the heat-resistant group, RILs 28, 164, 123 and 148 produce more grains in the spike of main tiller (36.3-44.7) than RILs 174, 143 and 36 (21.7-32), within the heat-sensitive group RILs 153, 46, 52, 26 and

131 produce lowest number of grains (26 to 18.3) in the spike of main tiller when exposed to heat stress treatment (Table 3.12). An increase in both total grain number and weight was observed in the heat-sensitive RIL 116 with heat stress (Table 3.12) and this was the result of minimal grain set in the distal spike region under control treatment conditions (Tables 3.14 and 3.16). The heat sensitive RIL 145 also exhibited an increase in total grain number after exposure to heat stress (Table 3.12) with means trending higher in all three sections of the spike with the central region of the spike having significantly higher grain number in the heat stress treatment compared to the control (Table 3.14). In contrast, the heat-sensitive RIL 131 showed 38% reduction in the total grain weight of the spike after exposure to heat stress (Table 3.12), with means trending lower in all three section and significant reduction in grain weight observed in the basal and the central regions of the main spike (Table 3.16). Even though the heat-stress treatment did not affect the total grain weight of the spike in heat-resistant RILs 28, 174 and 36 when compared among lines (Table 3.12) changes in grain weight were observed within specific spike sections of the plant with the heat-stress treatment (Table 3.15). High temperature treatment did not affect the grain number of the heat-resistant RILs in all three spike sections (Table 3.13).

Table 3.9 The effect of heat stress on the number of spikelets and fertile spikelets on the main tiller spike of heat-resistant and heat-sensitive RIL and parental lines.

Line	No. of spikelets per spike		No. of fertile spikelets per spike	
	Control ^v	HS ^w	Control	HS
Heat Resistant				
RIL 28	20 abc ^x	21 a	14 cdefgh	17 abc
RIL 148	20 abcd	19 abcde	14 bcdefg	14 defgh
RIL 164	18 cdefgh	21 a	16 abcde	18 a
RIL 123	20 ab	19 abcde	16 abcd	17 abc
RIL 174	16 lm	15 m	13 efgh	13 fghi
RIL 143	18 defgh	18 efghi	14 bcdefg	14 defgh
RIL 36	15 lm	15 lm	12 ghij	13 fghi
‘Attila’	20 ab	21 a	15 abcde	17 ab
Heat Sensitive				
RIL 153	19 bcdef	18 efghij	13 fghi	10 ij
RIL 46	16 ijklm	17 fghijk	12 ghi	14 cdefgh
RIL 140	18 defgh	20 abcd	12 ghi	13 efghi
RIL 116	16 ijklm	17 hijklm	9 j	15 abcde
RIL 145	16 ijklm	17 fghijk	10 ij	14 cdefgh
RIL 52	15 lm	16 jklm	12 fghi	14 cdefgh
RIL 26	19 bcdefg	19 bcdefg	11 hij	12 ghi
RIL 131	16 ijklm	16 ijklm	14 cdefg	12 fghi
RIL 40	17 hijkl	18 efghi	14 defgh	15 bcdef
RIL 13	16 jklm	6 klm	13 defgh	14 cdefg
‘CDC Go’	16 ijklm	17 ghijkl	15 bcdef	14 cdefgh
Temperature x line		NS ^y		S ^z

^vControl-temperature treatment; ^wHS = Heat-stress treatment.

^xData are means, n=7-8; Means followed by a different letter (number of spikelets per spike, a-m; number of fertile spikelets per spike, a-j) are significantly different among lines within parameter by the LSD test, with the significance level at $P \leq 0.05$; ^yNS, not significantly different; ^zS, significantly different.

Table 3.10 The effect of heat stress on the number of fertile spikelets at the basal, central, and distal positions on the main tiller spike of heat-resistant RILs, and parent ‘Attila’

Line	Spike section						Temperature MEM ^u		Spike section X Temp.
	Basal		Central		Distal		Control	HS	
	Control ^v	HS ^w	Control	HS	Control	HS	Control	HS	
Heat Resistant									
RIL 28	5 bc ^x	6 ab	7 a	7 a	2 d	4 cd	5 m	6 m	NS ^y
RIL 148	6 ab	5 b	7 a	6 a	5 b	5 ab	6 m	5 m	NS
RIL 164	5 c	5 bc	6 ab	7 a	5 bc	6 ab	5 m	6 m	NS
RIL 123	5 cd	5 cd	7 a	7 ab	4 d	6 bc	5 m	6 m	NS
RIL 174	5 ab	4 ab	5 a	5.0 a	4 ab	4 b	5 m	4 m	NS
RIL 143	3 b	2 b	6 a	6 a	6 a	6 a	5 m	5 m	NS
RIL 36	3 c	4 ab	5 a	5 ab	4 ab	4 b	4 m	4 m	S ^z
‘Attila’	3 c	5 bc	7 a	7 a	6 ab	6 ab	5 m	6 m	NS
Section MEM	Basal	Central	Distal						
RIL 28	5 g	7 f	3 h						
RIL 148	5 g	6 f	5 g						
RIL 164	5 g	7 f	6 fg						
RIL 123	5 g	7 f	5 g						
RIL 174	4 fg	5 f	4 g						
RIL 143	2 g	6 f	6 f						
RIL 36	3 g	5 f	4 g						
‘Attila’	4 g	7 f	6 f						

^uMEM, main effects mean; ^vControl-temperature treatment; ^wHS =Heat-stress treatment.

^xData are means, n=8; Means followed by different letters are significantly different among temperature treatment and spike sections (a-d), within lines and parameters; section main effect means (f-h); temperature main effect means (m) by the LSD test, with the significance level at $P \leq 0.05$; ^yNS, not significantly different; ^zS, significantly different.

Table 3.11 The effect of heat stress on the number of fertile spikelets at the basal, central, and distal positions on the main tiller spike of heat-sensitive RILs, and parent ‘CDC Go’.

Line	Spike section								Spike section X Temp.
	Basal		Central		Distal		Temperature MEM ^u		
	Control ^v	HS ^w	Control	HS	Control	HS	Control	HS	
Heat Sensitive									
RIL 153	5 ab ^x	5 b	6 a	5 b	2 c	1 c	4 m	3 m	NS ^y
RIL 46	4 bc	4 b	6 a	6 a	3 c	4 bc	4 m	5 m	NS
RIL 140	3 b	5.0 a	6 a	7 a	3 bc	1 c	4 m	4 m	S ^z
RIL 116	4 b	5 ab	5 ab	6 a	0 c	5 ab	3 n	5 m	S
RIL 145	4 bc	5 ab	5 ab	6 a	1 d	3 c	3 n	5 m	NS
RIL 52	4 ab	4 ab	5 a	5 a	3 b	4 ab	4 m	5 m	NS
RIL 26	3 b	3 b	5 a	3 b	3 b	4 b	4 m	3 m	S
RIL 131	5 a	4 a	6 a	4 a	4 a	4 a	5 m	4 m	NS
RIL 40	5 bc	6 ab	6 ab	6 a	4 c	4 c	5 m	5 m	NS
RIL 13	4 bc	4 c	5 a	5 a	5 ab	5 a	5 m	5 m	NS
‘CDC Go’	5 ab	4 b	5 a	6 a	5 a	5 a	5 m	5 m	NS
Section MEM	Basal	Central	Distal						
RIL 153	5 f	5 f	2 g						
RIL 46	4 g	6 f	3 g						
RIL 140	4 g	6 f	2 h						
RIL 116	4 f	5 f	3 g						
RIL 145	4 g	6 f	2 h						
RIL 52	4 g	5 f	4 g						
RIL 26	3 f	4 f	3 f						
RIL 131	4 f	5 f	4 f						
RIL 40	5 f	6 f	4 g						
RIL 13	4 g	5 f	5 f						
‘CDC Go’	4 g	6 f	5 fg						

^uMEM, main effects mean; ^vControl-temperature treatment; ^wHS =Heat-stress treatment.

^xData are means, n=8; Means followed by different letters are significantly different among temperature treatment and spike sections (a-d), within lines and parameters; section main effect means (f-h); temperature main effect means (m, n) by the LSD test, with the significance level at $P \leq 0.05$; ^yNS, not significantly different; ^zS, significantly different.

Table 3.12 The effect of heat stress on total grain weight and number of the main tiller spike of heat-sensitive and heat-resistant RILs and parental lines.

Line	Total grain number		Total grain weight (g)	
	Control ^v	HS ^w	Control	HS
Heat resistant				
RIL 28	34.8 bcdef ^x	41.5 ab	1.2406 bcdefghij	1.4886 abcd
RIL 148	36.3 abcde	32.2 cdefghij	1.2564 bcdefghij	1.1406 efghijklm
RIL 164	37.0 abcd	37.7 abc	1.5075 abcd	1.3076 abcdefghi
RIL 123	34.2 bcdefg	36.7 abcde	1.5335 abc	1.5445 ab
RIL 174	27.5 fghijklm	23.2 klmn	1.1904 cdefghijkl	0.8464 lmn
RIL 143	32.0 cdefghijk	26.7 fghijklmn	1.1610 defghijklm	1.0628 fghijklmn
RIL 36	21.7 lmn	23.0 lmn	1.0329 ghijklmn	1.2386 bcdefghijk
‘Attila’	41.2 ab	44.7 a	1.3611 abcdefg	1.3078 abcdefghi
Heat sensitive				
RIL 153	26.7 fghijklmn	21.7 lmn	1.0002 hijklmn	0.8726 lmn
RIL 46	21.0 lmn	24.0 jklmn	0.8428 lmn	0.9194 jklmn
RIL 140	25.2 hijklmn	28.5 efghijkl	0.9557 jklmn	1.0575 fghijklmn
RIL 116	22.7 lmn	33.3 bcdefgh	1.0146 ghijklmn	1.3956 abcdef
RIL 145	19.3 mn	29.0 defghijkl	0.8270 mn	1.1648 defghijklm
RIL 52	24.5 ijklmn	26.0 ghijklmn	1.2494 bcdefghij	1.2562 bcdefghij
RIL 26	21.3 lmn	18.3 n	0.8912 klmn	0.7576 n
RIL 131	32.5 cdefghi	24.4 ijklmn	1.5639 ab	0.9677 ijklmn
RIL 40	28.7 defghijkl	32.2 cdefghij	1.4737 abcde	1.6162 a
RIL 13	32.0 cdefghijk	33.2 bcdefgh	1.3522 abcdefgh	1.3582 abcdefg
‘CDC Go’	33.3 bcdefgh	26.8 fghijklm	1.4758 abcde	1.1293 efghijklm
Temperature x line	NS ^y		S ^z	

^vControl-temperature treatment; ^wHS = Heat-stress treatment.

^xData are means, n=7-8; Means followed by a different letter (Total grain weight, a-n; Total grain number, a-n) are significantly different among lines within parameter by the LSD test, with the significance level at $P \leq 0.05$; ^yNS, not significantly different; ^zS, significantly different.

Table 3.13 The effect of heat stress on grain number at the basal, central, and distal regions of the main tiller spike of heat-resistant RILs, and parent ‘Attila’.

Line	Spike section						Temperature MEM ^u		Spike section X Temp.
	Basal		Central		Distal		Control	HS	
	Control ^v	HS ^w	Control	HS	Control	HS			
Heat Resistant									
RIL 28	13.5 b ^x	15.5 ab	17.8 a	18.8 a	3.5 c	7.2 c	11.6 m	13.8 m	NS ^y
RIL 148	12.5 ab	11.5 ab	13.2 ab	15.2 a	9.3 b	8.0 b	11.7 m	11.6 m	NS
RIL 164	10.7 b	10.0 b	17.0 a	16.7 a	9.3 b	11.0 b	12.3 m	12.6 m	NS
RIL 123	11.3 b	10.2 b	16.3 a	17.0 a	6.5 c	9.5 bc	11.4 m	12.2 m	NS
RIL 174	11.2 a	8.2 ab	11.0 a	10.0 a	5.3 b	5.0 b	9.2 m	7.7 m	NS
RIL 143	5.5 de	4.3 e	16.2 a	13.2 ab	10.3 bc	9.2 cd	10.7 m	8.9 m	NS
RIL 36	5.5 b	8.2 ab	10.2 a	9.3 a	6 b	5.5 b	7.2 m	7.7 m	NS
‘Attila’	9.8 b	12.2 b	20.0 a	21.5 a	11.3 b	11.0 b	13.7 m	14.9 m	NS
Section MEM									
	Basal		Central		Distal				
RIL 28	13.3 f		13.6 f		13.1 f				
RIL 148	12.0 fg		14.2 f		8.7 g				
RIL 164	10.3 g		16.8 f		10.2 g				
RIL 123	10.8 g		16.7 f		8.0 h				
RIL 174	9.7 f		10.5 f		5.2 g				
RIL 143	4.9 h		14.7 f		9.8 g				
RIL 36	6.8 g		9.8 f		5.8 g				
‘Attila’	11.0 g		20.8 f		11.2 g				

^uMEM, main effects mean; ^vControl-temperature treatment; ^wHS =Heat-stress treatment.

^xData are means, n=8; Means followed by different letters are significantly different among temperature treatment and spike sections (a-e), within lines and parameters; section main effect means (f-h); temperature main effect means (m) by the LSD test, with the significance level at $P \leq 0.05$; ^yNS, not significantly different.

Table 3.14 The effect of heat stress on grain number at the basal, central, and distal regions of the main tiller spike of heat-sensitive RILs, and parent ‘CDC Go’.

Line	Spike section						Temperature MEM ^u		Spike section X Temp.
	Basal		Central		Distal		Control	HS	
	Control ^v	HS ^w	Control	HS	Control	HS			
Heat sensitive									
RIL 153	11.3 a ^x	11.2 a	13.7 a	10.3 a	2.0 b	1.5 b	9.0 m	7.7 m	NS ^y
RIL 46	7.0 bc	8.5 ab	10.2 ab	10.5 a	3.8 c	5.0 c	7.0 m	8.0 m	NS
RIL 140	7.7 bc	11.3 ab	13.3 a	15.2 a	4.2 cd	2.0 d	8.4 m	9.5 m	NS
RIL 116	10.0 b	10.2 b	12.3 ab	14.7 a	0.3 c	8.5 b	7.6 n	11.1 m	S ^z
RIL 145	8.8 b	11.2 ab	9.2 b	13.3 a	1.3 c	4.5 c	6.4 n	9.7 m	NS
RIL 52	9.5 ab	8.3 bc	11.5 a	11.7 a	3.5 d	6.0 cd	8.2 m	8.7 m	NS
RIL 26	6.0 bc	4.8 c	11.8 a	9.5 ab	3.5 c	4.0 c	7.1 m	6.1 m	NS
RIL 131	11.5 ab	9.6 bc	15.2 a	9.2 bc	5.8 c	5.6 c	10.8 m	8.1 m	NS
RIL 40	11.0 b	12.8 ab	12.7 ab	13.8 a	5.0 c	5.5 c	9.6 m	10.7 m	NS
RIL 13	8.6 b	9.7 b	16.2 a	14.3 a	7.2 b	9.2 b	10.7 m	11.1 m	NS
‘CDC Go’	12.2 a	7.8 b	13.8 a	12.2 a	7.3 b	6.8 b	11.1 m	8.9 n	NS
Section MEM	Basal		Central		Distal				
RIL 153	11.3 f		12.0 f		1.8 g				
RIL 46	7.8 g		10.3 f		4.4 h				
RIL 140	9.5 g		14.3 f		3.1 h				
RIL 116	10.1 g		13.5 f		4.4 h				
RIL 145	10.0 f		11.3 f		2.9 g				
RIL 52	8.9 g		11.6 f		4.8 h				
RIL 26	5.4 g		10.7 f		3.8 g				
RIL 131	10.6 f		12.5 f		5.7 g				
RIL 40	11.9 f		13.3 f		5.3 g				
RIL 13	9.2 f		15.2 f		8.3 g				
‘CDC Go’	10.0 g		13.0 f		7.1 h				

^uMEM, main effects mean; ^vControl-temperature treatment; ^wHS =Heat-stress treatment.

^xData are means, n=8; Means followed by different letters are significantly different among temperature treatment and spike sections (a-d), within lines and parameters; section main effect means (f-h); temperature main effect means (m, n) by the LSD test, with the significance level at $P \leq 0.05$; ^yNS, not significantly different; ^zS, significantly different.

Table 3.15 The effect of heat stress on grain weight at basal, central, and distal regions of the main tiller spike of heat-resistant RILs and parent ‘Attila’.

Line	Spike section						Temperature MEM ^u		Spike Sec. X Temp.
	Basal		Central		Distal		Control	HS	
	Control ^v	HS ^w	Control	HS	Control	HS			
Heat Resistant									
RIL 28	0.4776 b ^x	0.5607 ab	0.6602 a	0.6788 a	0.1028 d	0.2492 c	0.4135 n	0.4962 m	NS ^y
RIL 148	0.4307 abc	0.4037 abc	0.4657 ab	0.5528 a	0.2916 bc	0.2710 c	0.3960 m	0.4092 m	NS
RIL 164	0.4658 ab	0.3294 b	0.7107 a	0.5625 ab	0.3310 b	0.4156 b	0.5025 m	0.4358 m	NS
RIL 123	0.5418 b	0.4552 bc	0.7800 a	0.7737 a	0.2116 d	0.3155 cd	0.5112 m	0.5148 m	NS
RIL 174	0.4922 a	0.3051 bc	0.4917 a	0.3909 ab	0.2065 cd	0.1504 d	0.3968 m	0.2821 n	NS
RIL 143	0.2164 c	0.2755 c	0.6303 a	0.5048 ab	0.3142 bc	0.2826 c	0.3870 m	0.3543 m	NS
RIL 36	0.2273 c	0.5095 a	0.4883 ab	0.5148 a	0.3150 bc	0.2143 c	0.3435 m	0.4129 m	S ^z
‘Attila’	0.3591 b	0.3489 b	0.6986 a	0.6267 a	0.3034 b	0.3322 b	0.4537 m	0.4359 m	NS
Section MEM	Basal		Central		Distal				
RIL 28	0.5191 g		0.6695 f		0.1760 h				
RIL 148	0.4172 f		0.5093 f		0.2813 g				
RIL 164	0.3976 g		0.6366 f		0.3733 g				
RIL 123	0.4985 g		0.7769 f		0.2636 h				
RIL 174	0.3987 f		0.4413 f		0.1784 g				
RIL 143	0.2459 g		0.5676 f		0.2984 g				
RIL 36	0.3684 fg		0.5016 f		0.2647 g				
‘Attila’	0.3540 g		0.6626 f		0.3178 g				

^uMEM, main effect means; ^vControl-temperature treatment; ^wHS = Heat-stress treatment.

^xData are means, n=8; Means followed by different letters are significantly different among temperature treatment and spike section (a-d), within lines and parameters; section main effect means (f-h); temperature main effect means (m, n) by the LSD test, with the significance level at $P \leq 0.05$; ^yNS, not significantly different; ^zS, significantly different.

Table 3.16 The effect of heat stress on grain weight at basal, central, and distal regions of the main tiller spike of heat-sensitive RILs and parent ‘CDC Go’.

Line	Spike section						Temperature MEM ^a		Spike Sec. X Temp.
	Basal		Central		Distal		Control	HS	
	Control ^v	HS ^w	Control	HS	Control	HS			
Heat Sensitive									
RIL 153	0.4351 a ^x	0.4475 a	0.4880 a	0.3610 a	0.0771 b	0.0641 b	0.3334 m	0.2909 m	NS ^y
RIL 46	0.2918 b	0.3294 ab	0.4330 a	0.4421 a	0.1180 c	0.1480 c	0.2809 m	0.3065 m	NS
RIL 140	0.3023 cd	0.4144 bc	0.5081 ab	0.5773 a	0.1454 de	0.0657 e	0.3186 m	0.3525 m	NS
RIL 116	0.4543 bc	0.4560 bc	0.5474 ab	0.6494 a	0.0129 d	0.2902 c	0.3382 n	0.4652 m	NS
RIL 145	0.3790 b	0.4670 ab	0.4033 b	0.5568 a	0.0448 c	0.1411 c	0.2757 n	0.3883 m	NS
RIL 52	0.5001 ab	0.4345 b	0.6040 a	0.5804 ab	0.1453 c	0.2414 c	0.4165 m	0.4187 m	NS
RIL 26	0.2573 bc	0.1993 c	0.5118 a	0.4108 ab	0.1220 c	0.1476 c	0.2971 m	0.2525 m	NS
RIL 131	0.6488 a	0.4254 b	0.6866 a	0.3797 bc	0.2286 bc	0.1626 c	0.5213 m	0.3226 n	NS
RIL 40	0.5680 b	0.6533 ab	0.6886 ab	0.7305 a	0.2171 c	0.2324 c	0.4912 m	0.5387 m	NS
RIL 13	0.2164 c	0.2755 c	0.6303 a	0.5048 ab	0.3142 bc	0.2826 c	0.4507 m	0.4527 m	NS
‘CDC Go’	0.5275 a	0.3344 b	0.6385 a	0.5374 a	0.3098 b	0.2576 b	0.4919 m	0.3764 n	NS
Section MEM	Basal		Central		Distal				
RIL 153	0.4413 f		0.4245 f		0.0706 g				
RIL 46	0.3106 g		0.4375 f		0.1330 h				
RIL 140	0.3583 g		0.5427 f		0.1055 h				
RIL 116	0.4551 g		0.5984 f		0.1515 h				
RIL 145	0.4230 f		0.4800 f		0.0929 g				
RIL 52	0.4673 g		0.5922 f		0.1934 h				
RIL 26	0.2283 g		0.4613 f		0.1348 h				
RIL 131	0.5472 f		0.5471 f		0.1986 g				
RIL 40	0.6106 g		0.7096 f		0.2247 h				
RIL 13	0.4116 g		0.6656 f		0.2781 h				
‘CDC Go’	0.4309 g		0.5879 f		0.2837 h				

^uMEM, main effect means; ^vControl-temperature treatment; ^wHS = Heat-stress treatment.

^xData are means, n=8; Means followed by different letters are significantly different among temperature treatment and spike section (a-e), within lines and parameters; section main effect means (f-h); temperature main effect means (m, n) by the LSD test, with the significance level at $P \leq 0.05$; ^yNS, not significantly different.

3.2 Effect of 4-Cl-IAA application on grain yield

For RIL 80, the heat-stress treatment decreased the auricle distance (11%), spike length (11%), number of spikelets (15%) and fertile spikelets per spike (47%), and total grain number (51%) and weight (43%) of the main tiller (see the temperature main effect means, Table 3.17). The heat-stress treatment also reduced pollen viability (5%), grain number (50%) and weight of the main tiller (31%) (see the temperature main effect means, Table 3.18). Furthermore, the high temperature treatment decreased the anther length and spikelet length in all three spike sections in RIL 80 (reduced anther length by 21,16 and 15%, and spikelet length by 17,16, and 16%, in the basal, central, and distal spike sections respectively, Table 3.18).

Application of 4-Cl-IAA decreased the anther length in the basal and distal spike sections of RIL 80 when plants were grown under control conditions (Table 3.18). Under heat stress conditions, 4-Cl-IAA increased the spike length (Table 3.17) and spikelet length in the central spike section, while decreasing the pollen viability in the distal spike section in RIL 80 (Table 3.18). Grain weight and number were not affected by 4-Cl-IAA application under control or heat stress conditions in RIL 80 (Table 3.18).

For RIL 137, the heat-stress treatment decreased the auricle distance (10%), spike length (7%), number of fertile spikelets per spike (22%), and total grain number (37%) and weight (26%) of the main tiller but did not affect the number of spikelets per spike (see the temperature main effect means, Table 3.17). The heat stress treatment also reduced pollen viability (4%), anther length (15%), spikelet length (10%), grain weight (26%) of the main tiller (see the temperature main effect means, Table 3.19). Furthermore, high temperature treatment decreased the grain number in the basal and central spike sections (reduced by 63 and 38% in basal and central spike sections respectively, Table 3.19).

Application of 4-Cl-IAA to RIL 137 decreased the auricle distance when plants were grown under control conditions while increasing grain number in the central spike section (Table 3.17). Under heat stress conditions, 4-Cl-IAA increased the total grain weight of the spike by increasing the grain weight in the basal and central spike sections (Table 3.19).

Table 3.17 The effect of 4-Cl-IAA application and heat stress on auricle distance, spike length, total grain weight and number, and number of spikelets and fertile spikelets per spike at the basal, central, and distal regions of the main tiller spike of RILs 80 and 137.

RIL	4-Cl-IAA Conc. ^y	Heat trt. ^w	Auricle Distance (mm)	Spike length (mm)	Total grain number	Total grain weight (g)	No. of spikelets per spike	No. of fertile spikelets per spike	
80	1 µM	+	137.6 a ^x	80.4 a	16 b	0.5702 c	16 b	8 b	
	1 µM	-	154.3 a	85.8 a	41 a	1.1898 a	19 a	17 a	
	0	+	137.1 a	73.3 b	23 b	0.7783 bc	17 b	11 b	
	0	-	154.4 a	86.0 a	42 a	1.1685 ab	20 a	18 a	
	Temperature MEM ^y	+	137.4 n	76.8 n	20 n	0.6743 n	17 n	9 n	
		-	154.3 m	85.9 m	41 m	1.1792 m	20 m	17 m	
	Auxin MEM	1 µM	145.9 q	83.1 q	29 q	0.8800 q	18 q	12 q	
		0	145.8 q	79.6 q	32 q	0.9734 q	18 q	14 q	
	Temperature x auxin			NS ^z	NS	NS	NS	NS	NS
	137	1 µM	+	149.1 b	85.5 b	38 b	1.3333 a	19 a	15 ab
1 µM		-	155.3 b	90.0 ab	52 a	1.5890 a	20 a	19 a	
0		+	160.8 b	84.8 b	28 b	0.8591 b	19 a	13 b	
0		-	187.3 a	92.6 a	51 a	1.3898 a	19 a	18 a	
Temperature MEM		+	154.9 n	85.1 n	33 n	1.0962 n	19 m	14 n	
		-	171.3 m	91.3 m	52 m	1.4894 m	19 m	18 m	
Auxin MEM		1 µM	152.2 r	87.8 q	45 q	1.4611 q	19 q	17 q	
		0	174.0 q	88.7 q	39 q	1.1244 r	19 q	16 q	
Temperature x auxin			NS	NS	NS	NS	NS	NS	

^yAqueous solutions of 4-Cl-IAA (1 µM) in 0.25% Agral or control (0) 0.25% Agral adjuvant.

^wHeat-stress treatment, (+); Control treatment, (-).

^xData are means, n=8 for pollen viability, anther length and spikelet length; n=4-6 for grain weight and number; Means followed by different letters are significantly different among temperature and auxin treatments (a-c), within lines and parameters; auxin main effect means (q, r); temperature main effect means (m, n) by the LSD test, with the significance level at $P \leq 0.05$.

^yMEM, main effect mean; ^zNS, not significantly different.

Table 3.18 The effect of 4-Cl-IAA application and heat stress on pollen viability, anther length, spikelet length, and grain weight and number at the basal, central, and distal regions of the main tiller spike of RIL 80.

RIL	Spike section ^t	4-Cl-IAA Conc. ^u	Heat trt ^v	% Pollen viability	Anther length (mm)	Spikelet length (mm)	Grain weight (g)	Grain number	
80	Basal	1 μ M	+	90.5 de ^w	0.136 de	11.6 d	0.2294 de	5 ef	
	Basal	1 μ M	-	95.4 abc	0.153 bc	13.2 a	0.4421 abc	15 ab	
	Basal	0	+	93.3 bcd	0.131 ef	11.3 de	0.2409 de	6 def	
	Basal	0	-	97.7 a	0.165 a	13.6 a	0.4030 bcd	14 b	
	Central	1 μ M	+	92.4 cde	0.132 ef	12.2 bc	0.3755 cd	10 bed	
	Central	1 μ M	-	97.2 a	0.148 bc	13.0 a	0.5601 ab	19 a	
	Central	0	+	92.1 cde	0.131 ef	11.2 de	0.4439 abc	13 bc	
	Central	0	-	97.2 a	0.156 ab	13.4 a	0.5810 a	20 a	
	Distal	1 μ M	+	89.3 e	0.124 f	10.8 ef	0.0794 e	2 f	
	Distal	1 μ M	-	96.4 ab	0.129 ef	12.0 bc	0.1877 e	8 de	
	Distal	0	+	93.0 bcd	0.123 f	10.3 f	0.1605 e	4 ef	
	Distal	0	-	96.1 ab	0.144 cd	12.2 b	0.1845 e	8 cede	
	Temperature MEM ^x			+	91.7 n	0.129 n	11.2 n	0.2719 n	7 n
				-	96.7 m	0.149 m	12.9 m	0.3931 m	14 m
Auxin MEM			1 μ M	93.6 r	0.137 r	12.1 q	0.3321 q	10 q	
			0	95.0 q	0.142 q	12.0 q	0.3436 q	11 q	
Spike section MEM			Basal	94.2 g	0.146 g	12.4 g	0.3425 h	10 h	
			Central	94.9 g	0.142 g	12.4 g	0.4901 g	15 g	
			Distal	93.8 g	0.130 h	11.3 h	0.1597 i	5 i	
Temperature x spike section				NS ^y	NS	NS	NS	NS	
Temperature x auxin				NS	S ^z	S	NS	NS	
Temperature x auxin x spike section				NS	NS	NS	NS	NS	

^uAqueous solutions of 4-Cl-IAA (1 μ M) in 0.25% Agral or control (0) 0.25% Agral adjuvant.

^vHeat-stress treatment, (+); Control treatment, (-).

^wData are means, n=8 for pollen viability, anther length and spikelet length; n=4-6 for grain weight and number; Means followed by different letters are significantly different among temperatures auxin treatments and spike regions (a-f), within parameters; section main effect means (g-i); auxin main effect means (q, r); temperature main effect means (m, n) by the LSD test, with the significance level at $P \leq 0.05$; ^xMEM, main effect mean; ^yNS, not significantly different; ^zS, significantly different.

Table 3.19 The effect of 4-Cl-IAA application and heat stress on pollen viability, anther length, spikelet length, and grain weight and number at the basal, central, and distal regions of the main tiller spike of RIL 137.

RIL	Spike section	4-Cl-IAA Conc. ^u	Heat trt ^v	% Pollen viability	Anther length (mm)	Spikelet length (mm)	Grain weight (g)	Grain number
137	Basal	1 µM	+	93.3 cde ^w	0.135 cde	12.4 ef	0.3905 defg	10 def
	Basal	1 µM	-	98.3 a	0.159 a	14.2 a	0.5203 bcd	18 bc
	Basal	0	+	93.5 cde	0.142 cd	13.1 cde	0.1988 h	7 f
	Basal	0	-	97.6 ab	0.161 a	14.3 a	0.4972 bcde	19 ab
	Central	1 µM	+	92.4 de	0.129 ef	12.6 def	0.6514 ab	17 bc
	Central	1 µM	-	96.5 abc	0.154 a	14.0 ab	0.7268 a	23 a
	Central	0	+	92.6 de	0.132 def	12.7 def	0.4625 cdef	13 cd
	Central	0	-	94.1 bcde	0.156 a	13.9 abc	0.6150 bc	21 ab
	Distal	1 µM	+	91.8 e	0.125 ef	11.4 g	0.2914fgh	10 def
	Distal	1 µM	-	94.0 bcde	0.144 bc	13.3 bcd	0.3419 efgh	12 de
	Distal	0	+	91.6 e	0.124 f	12.1 fg	0.1978 h	8 ef
	Distal	0	-	95.9 abcd	0.151 ab	13.3 bcd	0.2776 gh	11 def
Temperature MEM ^x			+	92.5 n	0.131 n	12.4 n	0.3654 n	11 n
			-	96.0 m	0.154 m	13.8 m	0.4965 m	17 m
Auxin MEM			1 µM	94.4 q	0.141 q	13.0 q	0.4870 q	15 q
			0	94.1 q	0.144 q	13.2 q	0.3748 r	13 q
Spike section MEM			Basal	95.6 i	0.149 i	13.5 i	0.4017 j	13 j
			Central	93.9 ij	0.143 j	13.3 i	0.6139 i	19 i
			Distal	93.3 j	0.136 k	12.5 j	0.2772 k	10 k
Temperature x spike section				NS ^y	NS	NS	NS	S ^z
Temperature x auxin				NS	NS	NS	NS	NS
Temperature x auxin x spike section				NS	NS	NS	NS	NS

^uAqueous solutions of 4-Cl-IAA (1 µM) in 0.25% Agral or control (0) 0.25% Agral adjuvant.

^vHeat-stress treatment, (+); Control treatment, (-).

^wData are means, n=8 for pollen viability, anther length and spikelet length; n=4-6 for grain weight and grain number; Means followed by different letters are significantly different among temperature treatment, auxin treatments and spike regions (a-h), within parameters; section main effect means (i-k); auxin main effect means (q, r); temperature main effect means (m, n) by the LSD test, with the significance level at $P \leq 0.05$; ^xMEM, main effect means; ^yNS, significantly not different; ^zS, significantly different.

3.3 *Rht-B1* allele determination

Strong amplicon band intensity for the *Rht-B1b* allele was generally consistent across the replicates of the parent ‘CDC Go’ and heat-sensitive RIL 131, denoting its presence in these lines (Fig. 3.5B). Weak or absent band intensity in ‘Attila’ and RILs 123 and 28 denotes its absence in these lines (Fig. 3.5B). Amplicon band intensity for *Rht-B1a* (wild-type) was weak or absent across the selected RILs and parents (Fig. 3.5A).

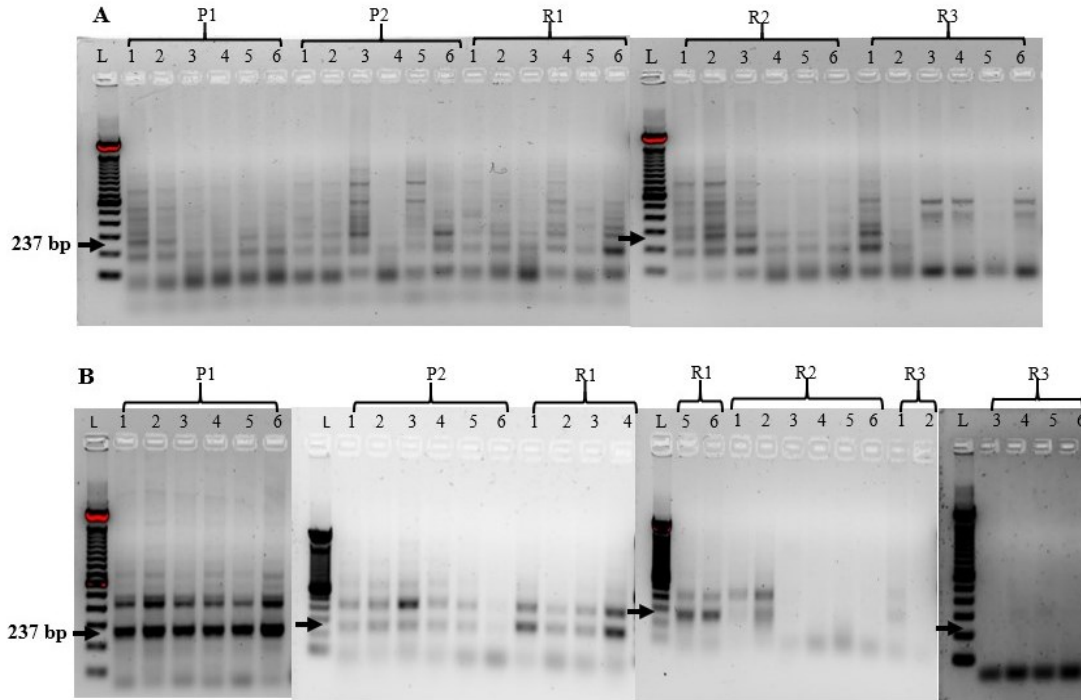


Figure 3.5: Amplification profiles for *Rht-B1a* and *Rht-B1b* dwarfing alleles present in selected heat-resistant and heat-sensitive RILs and parental lines. (A) *Rht-B1a* (wild-type allele); (B) *Rht-B1b* (semi-dwarf mutant allele). The presence of *Rht-B1b* allele was previously confirmed in ‘CDC Go’ and its absence was confirmed in ‘Attila’ by Asif et al. (2015). L=DNA ladder; P1=‘CDC Go’; P2=‘Attila’; R1=RIL131; R2=RIL123; R3=RIL28. 1-6: replicate

4. DISCUSSION

4.1 Reduction of auricle distance is a general response to heat stress in wheat

Auricle distance often increased with the progression of anther development in wheat, is highly variable between cultivars, and is commonly used in studies to rapidly determine the anther developmental stage for the application of abiotic stress (Browne et al., 2018; Erena et al., 2021). Auricle distance usually decreases after application of heat stress at the early flowering stage (Erena et al., 2021). A similar response in auricle distance to heat stress was observed in the wheat lines tested in this study (Table 3.1). High temperature treatment imposed at the flag leaf-emerging stage decreased the auricle distance at anthesis in both parents, ‘Attila’ and ‘CDC Go’, regardless of their heat tolerance capacity with respect to grain yield (‘Attila’ is heat-resistant parent and ‘CDC Go’ is heat-sensitive parent; Table 3.1). High temperature stress caused either a decrease or no change in auricle distance at anthesis in heat-resistant and heat-sensitive RILs (Table 3.1). Browne et al. (2018) observed that tall wheat plants had higher auricle distance when compared to the shorter plants at each of the corresponding anther development stages of the plant. This indicates that spikes of the taller plants had to develop further to reach the target auricle distance (corresponding anther development stage) of the shorter plants. It was suggested that plants with shorter auricle distance have a potential to complete their sensitive development stages at the time of reaching the target auricle distance for heat stress and thereby potentially reduce the negative effects of heat stress. Therefore, Erena et al. (2021) hypothesized that shortening the auricle distance under heat stress allows the sensitive stages of reproductive development to complete with reduced exposure to the negative effects of heat stress. Also, can facilitate adequate supply of photoassimilate to developing grains. The data from this study are consistent with the reduction of auricle distance with heat stress as potential mechanism used by the plant to escape the negative effects of heat stress on reproductive development.

4.2 Spikelet length, a potential indicator of developing grains within the spikelet grown under heat stress conditions

The spikelet is the basic floral unit of the spike and the number and the position of the spikelets, along with the number of florets per spikelet that produced grains, will determine the final grain yield of the spike (Guo et al., 2018). Spikelet differentiation usually begins at the double ridge stage of the plant and is complete after forming the terminal spikelet (this occurs before flag leaf emerging from the plant; Acevedo et al., 2002). The effect of heat stress on spike and spikelet development is dependent on the timing of heat stress. The moderately high temperature imposed at the flag leaf-emerging stage of the plant did not affect the number of spikelets per spike, since spikelet differentiation was completed before the heat-stress treatment was imposed (Table 3.9). The spike starts to grow after the terminal spikelet stage and it usually continues 10 days past anthesis (Acevedo et al., 2002), the period of heat-stress exposure for the main spike tiller in this study. Generally, high temperature treatment did not affect the spike length of the RILs and parents tested (Table 3.1). However, an increase in spike length was observed in heat-sensitive RIL 131 while decrease in spike length occurred in heat-resistant RIL 36 (Tables 3.1). Erena et al. (2021) observed increased in spike length when heat stress was imposed at the mid-booting stage of wheat lines. Since the increase in spike length in response to high temperature treatment was solely due to the increase in rachis internode length (Erena et al., 2021), it is likely that this was also the case in RIL 131, as the number of the spikelets per spike remain unchanged after heat stress (Table 3.9). Heat stress reduced spikelet length in more than half of the heat-resistant RILs tested (4 of 7), but only in 10 % of the heat sensitive RILs tested (1 of 10; Tables 3.2 and 3.3, see temperature MEM). The reduction in the spikelet length varied with the spike section among the RILs (Tables 3.2 and 3.3). Of note, spikelet length was reduced by heat stress in the heat-resistant RIL 123 (by 10%, MEM), and increased (by 7%, MEM) in the heat-sensitive RIL 131 (Tables 3.2 and 3.3). High temperature decreases the photosynthetic capacity of wheat plants, which results in modification of photoassimilate partitioning among different tissues (Feng et al., 2014; Shirdelmoghanloo et al., 2016). Modification of spikelet length under heat stress could be attributed to increased competition for photoassimilate between the developing grain and surrounding floral structures (glume, palea and florets). The decrease in spikelet length in RIL 123 may be the result of more photoassimilate available for grain growth than for growth of the surrounding floral tissues. The

increase in spikelet length in RIL 131 could be the result of more photoassimilate available for the growth of the surrounding floral tissues due to the lack of grain development (grain weight reduced by heat stress; Table 3.16).

4.3 Reduction in anther length, a general response to heat stress in wheat lines

Anther length is positively correlated with the anther developmental stage in wheat and is less variable between cultivars during the early stages of development (anther stage 4-10) than the later stages (anther stage 11-15; Browne et., 2018). High temperature stress (starting from flag-leaf emerging stage for 8 days) decreased the anther length at anthesis in the RIL parents, ‘Attila’ (heat resistant) and ‘CDC Go’ (heat sensitive) regardless of their heat tolerance capacity with respect to grain yield (Tables 3.6 and 3.7). Heat stress-induced reduction in anther length was observed in over 50% of the heat-resistant RILs and 80% of the heat-sensitive RILs at anthesis (Tables 3.6 and 3.7). High temperature treatment decreased the anther length in most heat-resistant and heat-sensitive RILs regardless of spikelet position (Tables 3.6 and 3.7). It can be hypothesized that reduction in anther length under heat stress is a potential mechanism used to shorten the duration of heat-stress exposure during the temperature-sensitive anther development stages.

4.4 Pollen viability decreased with heat stress

The heat-stress treatment imposed during the early flowering stage did not affect the pollen viability of heat-resistant parent ‘Attila’ or heat-sensitive parent ‘CDC Go’ at anthesis (Tables 3.4 and 3.5). However, heat stress decreased pollen viability in 3 of 7 (43%) heat-resistant, and 4 of 10 (40%) heat-sensitive RILs, in at least one section of the spike (Tables 3.4 and 3.5). A large reduction (22%) in pollen viability was observed in heat-sensitive RIL 131 at anthesis (in all three spike sections) after expose to the heat-stress treatment (Table 3.5). Heat stress-induced reduction in pollen viability is commonly observed in wheat when the heat stress treatment is imposed early reproductive development (Begcy et al., 2018).

The histological analysis of anther cross-sections in this study indicated that the decrease in the pollen viability under heat stress in heat-sensitive RIL 131 was due to the degraded pollen grains and not because of degradation of the anther cell layers (tapetum, endothecium, and

epidermal cell layers were intact in anther cross sections from heat-stress and control treatments; Fig. 3.1). Degradation of pollen grains under heat stress could be due developmental abnormalities in the tapetal cells and/or timing of tapetal degradation during early stages of pollen development since these cells are responsible for nutrient translocation to the developing pollen grain (Browne et al., 2021). A slight increase in pollen viability under heat stress was observed in the spikelets at the distal spike position in heat-resistant RIL 164 (Table 3.4). This experiment should be repeated for RIL 164 to determine if this effect is reproducible over time, given that is not the general trend observed in the lines tested.

4.5 Enlargement in ovule tissue with heat-stress was observed in heat-sensitive RIL 131

Wheat ovary size is determined to a large part by the genes that regulate cell division and therefore, it is often correlated with cell number (Reale et al., 2017). Ovule area and length were similar among the heat-resistant and heat-sensitive RILs tested when grown under control temperature conditions (Table 3.8). The heat-stress treatment did not affect ovary size in the heat-resistant RILs (28 and 123; Fig. 3.3; Table 3.8). In contrast, the heat-sensitive RIL 131 exhibited enlargement of ovary tissue under heat stress conditions (Fig. 3.3; Table 3.8). The increase in ovule size in RIL 131 due to heat stress could be due to the abnormal proliferation of nuclear tissues in the absence of normal embryo sac development as observed by Saini et al. (1983) in the wheat ovules under heat stress.

4.6 Heat-resistant RIL 123 maintained normal pollen viability and ovule size, and reduced spikelet growth facilitating normal grain yield under heat stress, and the heat-sensitive RIL 131 did not.

The grain yield per spike is initially determined by the number of spikelets formed during spikelet differentiation. Subsequently, grain yield is dependent on the number of florets per spikelet that produce mature grains. The number of fertile florets per spike are usually determined during the stem elongation phase when florets compete with rapidly developing stem for assimilates (Guo et al., 2018). Under stress conditions, the number of fertile florets can be lower and developing florets can abort prematurely when competing for assimilates. In this study, the number of fertile spikelets per spike was not affected by heat stress in any of the heat-sensitive and heat-resistant RIL and parents tested (Table 3.9). Therefore, when decreases in

grain number were observed, they were due to fewer florets per spikelet producing grains. For the RIL parental lines, no morphological trait assessed at anthesis in this study was specific to the heat-sensitive parent ‘CDC Go’ when compared to the heat-resistant parent ‘Attila’ (Fig. 4.1). Comparison of the heat-resistant RIL (123) with the most heat-sensitive RIL (131) assessed in this study (with respect to grain yield) helps define the traits most affected by heat stress in this RIL population (Fig. 4.2). The most heat-sensitive RIL assessed (RIL 131) exhibited reduced pollen viability and an increase in ovule size under heat stress conditions at anthesis indicating abnormal reproductive development (Fig. 4.2). Increased spike length in heat-sensitive RIL 131 may indicate the partitioning of more assimilate into the spike rachis growth, and increased spikelet length may indicate more assimilate flow into floral structures such as the palea and lemma, than for grain development under heat stress (Fig. 4.2). In contrast, heat-resistant RIL 123 maintained grain yield under the heat-stress conditions by maintaining normal pollen viability and ovule size and reducing spikelet length (Fig. 4.2). Reduced spikelet length when under heat stress, may indicate that partitioning of assimilate for grain development will be favored over that for surrounding floral tissues (Fig. 4.2).

4.7 The application of 4-Cl-IAA increased the grain weight in RIL 137 without affecting other morphological parameters tested

Preliminary studies carried out in our lab (personal communication with D. N. Abeysingha) identified RILs 80 and 137 as potentially responsive to a one-time foliar application of 4-Cl-IAA with respect to maintaining grain yield under heat stress conditions. High temperature decreased all the morphological parameters tested in RIL 80 and 137, with the exception of the number of spikelets per spike in RIL 137 (Tables 3.17, 3.18 and 3.19). 4-Cl-IAA application prior to heat stress increased grain weight in RIL 137 but did not affect the other parameters assessed (Table 3.19). This may indicate that auxin application promoted photoassimilate partitioning into the spike (particularly into the central and basal spikelets) improving grain set and yield as suggested by Bangerth et al. (1985) and Darussalam et al. (1998). Bangerth et al. (1985) observed that the differences in the dry matter accumulation in spikelets in different regions within the ear were positively correlated with the differences in the IAA levels. Darussalam et al. (1998) found that exogenous IAA induced photoassimilate accumulation within the developing wheat grain and

suggested that IAA may regulate the plasma membrane transport processes that control photoassimilate influx and efflux into endosperm cavity.

4.8 The presence of *Rht* mutant allele in ‘CDC Go’ and RIL 131 did not confer higher grain yield under heat stress

The presence of the *Rht-B1b* mutant allele in the heat-sensitive RIL 131 and parent ‘CDC Go’ may enhance the photoassimilate supply to developing florets under control conditions by reducing stem elongation (Hedden et al., 2003; Fig. 3.5), but this alone did not improve grain yield under heat stress in these lines.

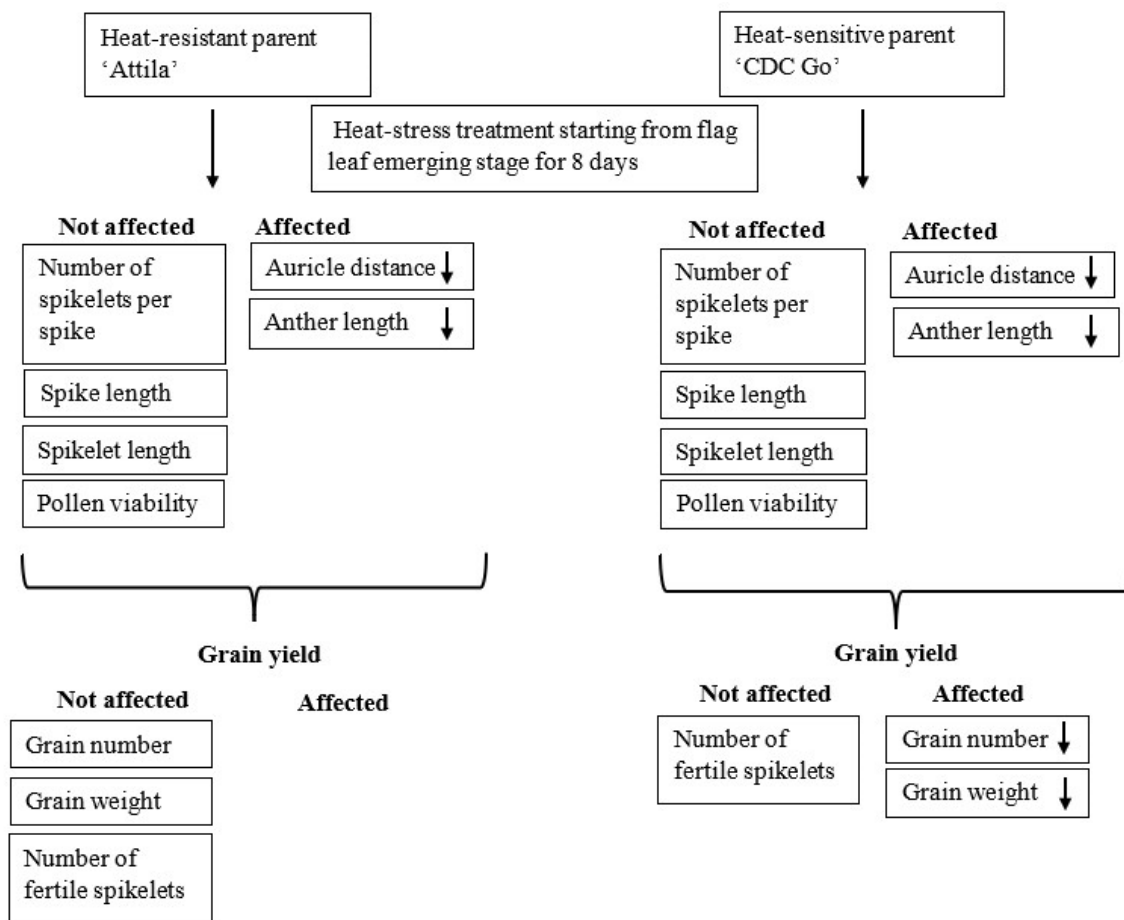


Figure 4.1: Schematic overview of the comparison of the effect of heat stress on morphological and yield parameters of heat-resistant parent ‘Attila’ and heat-sensitive parent ‘CDC Go’

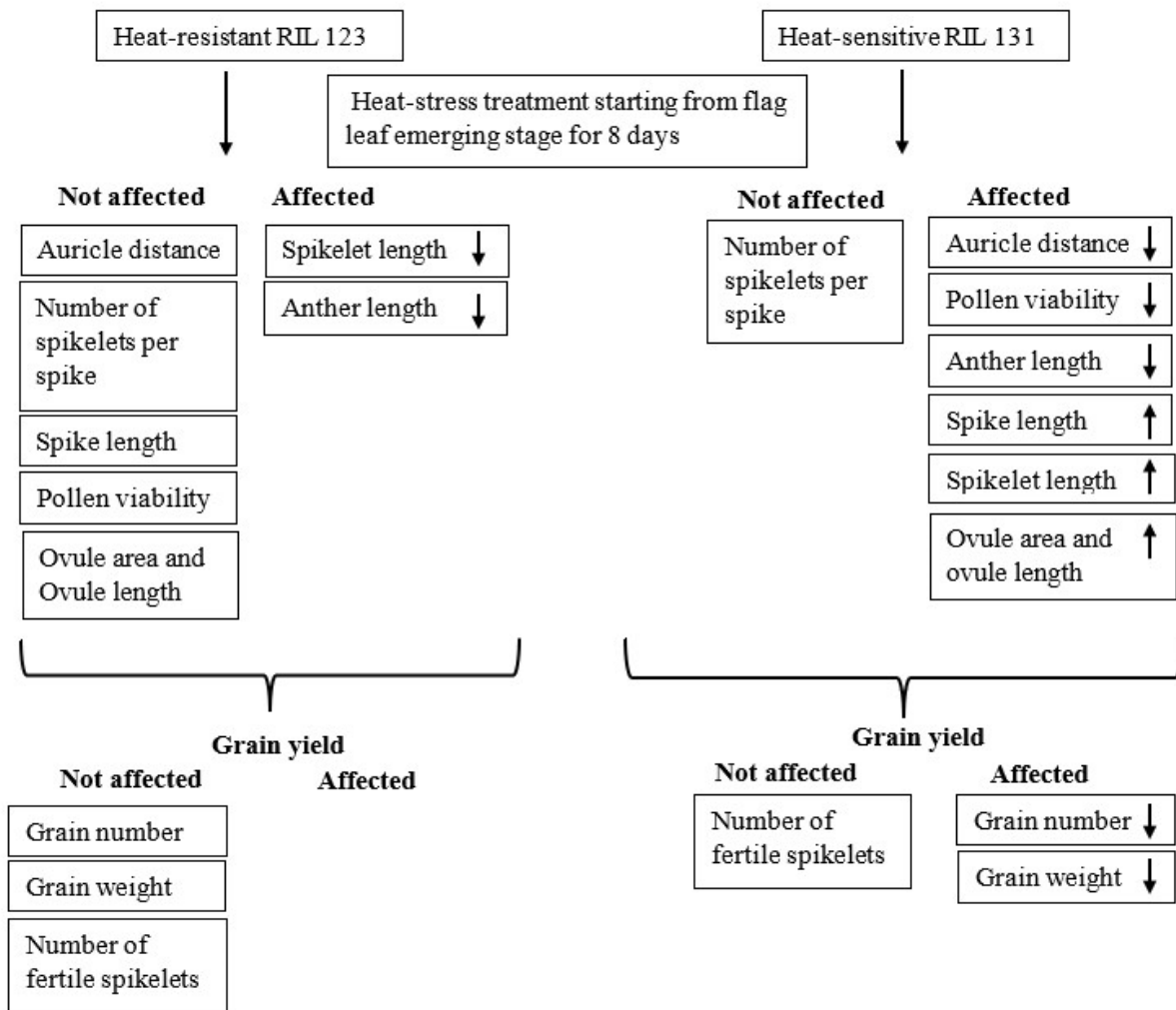


Figure 4.2: Schematic overview of the comparison of the effect of heat stress on morphological and yield parameters of heat-resistant RIL 123 and heat-sensitive RIL 131

4.9 Summary

A general response to heat stress across the RILs and parental lines was to reduce the growth of the tiller (reduced auricle distance) and anthers, potentially allowing the sensitive stages of reproductive development to complete with reduced exposure to the negative effects of heat stress. Reduction of auricle distance under heat stress could also facilitate an adequate supply of photoassimilate to developing grains. Heat-resistant RILs maintained grain yield under heat stress by maintaining pollen viability and ovule size indicative of normal reproductive development. Heat stress also decreased spikelet length in 57% of the heat-resistant RILs, but only in 10% of the heat-sensitive RILs assessed. Therefore, reduced spikelet length appears to be a common trait in heat-resistant lines, indicative of more favorable partitioning of assimilates to the developing grain than the surrounding floral structures.

The most heat-sensitive RIL assessed (RIL 131) exhibited reduced pollen viability and an increase in ovule size under heat stress conditions at anthesis indicating abnormal reproductive development. The spike and spikelet length at anthesis were also greater in RIL 131 under heat stress conditions suggesting a more favorable partitioning of assimilates to the tissues that will surround the developing grain which may negatively affect grain development.

The application of 4-Cl-IAA prior to heat stress in RIL 137 increased grain yield under heat stress conditions but did not affect any morphological parameters assessed. These data suggest that in this RIL auxin may have facilitated photoassimilate partition to the developing grains thereby maintaining grain yield under heat stress conditions.

Heat tolerance is a complex process controlled by the interactive effects of number of morphological, physiological and growth changes. The ability of some RILs to maintain better grain yield under heat stress could not be explained by just one single trait assessed. To improve heat tolerance, it is necessary to further identify the effect of heat stress on wheat plant reproductive development and the underlying mechanisms that leading to variation in grain yield. The heat-resistant RIL 123 and heat-sensitive RIL 131 identified in this study would be useful to compare in future studies to this end.

5. CONCLUSIONS

The atmospheric temperature is steadily rising, and it is projected to continue with climate change. The increase in temperature can cause severe damage to the growth and productivity of wheat plants. Particularly, the reproductive phase of the wheat growth cycle is highly sensitive to high temperature, and damage to reproductive organs can cause substantial yield losses (Talukder et al., 2014). In wheat plants exposed to high temperatures, structural and functional abnormalities reduce pollen and ovule viability and cause growth abnormalities in the endosperm (Ahmed et al., 1992; Sakata et al., 2010). The limited supply of photoassimilate under heat stress is another crucial factor contributing to a reduction in final grain yield (Charles-Edwards 1984; Rijven 1986). The plant response to high temperature varies depending on their tolerance capacity. Therefore, understanding how high temperature during early reproductive development affects reproductive organ development in wheat varieties with different tolerance capacities is vital to advance our current knowledge on heat stress susceptibility in wheat.

5.1 Heat stress reduces tiller and anther length in wheat

Plants being sessile organisms, are more exposed to stress conditions such as high temperatures. Therefore, plants have adapted different tolerance and escape mechanisms to avoid the adverse effects of heat stress (Bueckert and Clarke, 2013). This study demonstrates that reduction in tiller length and anther length is one such mechanism that all heat-resistant and heat-sensitive wheat lines use to limit the heat exposure of sensitive developmental stages of the reproductive organs to heat stress (Tables 3.1, 3.6 and 3.7). Furthermore, reducing tiller length (auricle distance) facilitates more assimilate supply for grain development (Guo et al., 2016). However, those responses alone would not be sufficient to curtail all the negative effects of heat stress on seed development. Several other morphological and physiological mechanisms appear to play a role in maintaining the grain yield of the wheat plants exposed to heat stress (Kumar et al., 2013).

5.2 The negative effects of heat stress on pollen viability, and ovule size could lead to a reduction in grain yield in lines highly sensitive to heat stress

Heat stress has been shown to affect female and male reproductive development leading to defects in fertilization and grain development in wheat (Saini et al., 1983; Narayan, 2018). Thus, the correct development of female and male reproductive organs is an important determinant of floral fertility and yield in wheat under high-temperature conditions.

The pollen viability is an indication of the ability of pollen grains to deliver their sperm cells to embryo sacs following pollination (Ahmed et al., 1992). The occurrence of heat stress during male reproductive development can reduce pollen viability leading to decreased seed set (De Storme and Geelen, 2014; Muller and Rieu, 2016). Our study demonstrated a reduction in pollen viability in both heat-resistant and heat-sensitive wheat lines if heat stress is imposed during the early stages of reproductive development; however, the level of impact varied between heat-resistant and heat-sensitive lines (Tables 3.4 and 3.5). The most heat-sensitive line RIL 131 experienced a substantial reduction in pollen viability, which appears to be associated with the degradation of pollen grains (Table 3.5, Fig. 3.1). The heat-resistant lines, on the other hand, showed only a slight reduction in pollen viability in the specific region of the spike (Table 3.4).

Female reproductive development is equally important as male reproductive development in determining final grain yield. A previous study has reported that the negative impact of heat stress on ovule development can also cause yield losses (Saini et al., 1983). In our study, we observed an abnormal enlargement of ovules in heat-sensitive RIL 131 when exposed to heat stress, while heat-resistant RIL 123 maintained a normal ovule size (Table 3.8). The pistil clearance method described in this thesis only provides quantitative morphological information about the developing ovule under heat stress. Therefore, it is recommended to dissect the ovule to further understand the underlying changes that occur in ovule anatomy. Altogether, internal changes in the ovules that caused an increased ovule size, and the reduced pollen viability under heat stress appear to be responsible for reduced grain yield in heat sensitive line.

5.3 Increased growth of spikelets could decrease photoassimilate partitioning to developing grains

A balanced distribution and allocation of photoassimilates to reproductive organs is crucial for plant growth and development (Aluko et al., 2021). Under high-temperature stress, wheat yield is controlled by the balance between photoassimilate amount available for grain development and the efficient use of these assimilates for reproductive organ growth and seed development (Girousse et al., 2018; Hutsch et al., 2018). Any disruption of this sink-source balance could adversely affect the final grain yield of the plant. Under limited assimilate supply during the heat stress, some heat-resistant lines decreased the growth of spikelet and surrounding floral tissues to potentially facilitate the partitioning of more assimilates towards the grain development to ensure economic grain yield (Tables 3.2 and 3.12). In contrast, increase growth of spikelet and surrounding floral tissues in heat-sensitive lines under heat stress limit the assimilate available for grain development and this can lead to reduction in grain yield (Tables 3.3 and 3.12).

5.4 Auxin application increases the grain yield of RIL 137

Auxins are plant hormones that play a vital role in plant growth and development. It has been reported that one-time foliar application of auxin partially ameliorates the negative effects of heat stress (Bangerth et al., 1985). Furthermore, high temperature-induced reduction of auxin level can lead to a reduction in pollen viability (Sakata et al., 2010). However, our observations indicate that auxin application does not improve the negative impacts of heat stress on pollen viability or the spike and spikelet length in RIL 137. Instead, the application of auxin may improve grain yield by facilitating the assimilate partitioning to developing grains.

5.5 Future perspectives

The findings from this project have provided a better understanding of the effects of heat stress on the reproductive development of wheat and could be used in future genetic studies and breeding programs focusing on heat tolerance. A few suggestions have been made in this section that will help to further extend this research in the future. This research was carried out under controlled environment conditions to isolate the effect of high temperature stress from the other environmental stresses. But under field conditions plants will experience both drought and heat

stresses simultaneously. Relatively limited work has been carried out to identify the effect of both stresses on wheat yield. Therefore, understanding the confounding effect of heat and drought stress on reproductive organ development in future studies would help plant breeders to further improve abiotic stress tolerance in wheat.

The ability of the plant to maintain pollen viability would only provide a likelihood estimation of successful seed production under heat stress. The stigma functionality and fertility and anther dehiscence are equally important for successful fertilization. Previous studies have shown that high-temperature induced the failure in anther dehiscence and reduce the capacity of pollen grains to germinate on the stigmatic surface (Shivanna, 2003; Prasad and Djanaguiraman, 2014). Therefore, it would be informative to investigate the structural changes associated with the stigma receptivity and anther dehiscence in heat-resistant and heat-sensitive lines under heat stress.

In addition, to develop heat-tolerant lines it is important to understand the biochemical and molecular basis of thermo-tolerance in combination with genetic approaches like identification and mapping of heat-tolerant QTL. This would allow conventional plant breeders to develop effective heat-tolerant cultivars and help molecular biologists to characterize genes associated with heat tolerance, which can be used in developing genetically modified heat-tolerant plants in future.

References

- Acevedo E, Silva P, Silva H** (2002) Wheat growth and physiology. *In* Curtis BC, Rajaram S, Macpherson HG, eds, Bread wheat. FAO of the UN, Rome, pp 3
- Agriculture and Horticulture Development Board of United Kingdom** (2018) Wheat growth guide Available at <https://ahdb.org.uk/knowledge-library/wheat-growth-guide> Access date 5th March, 2021
- AGRI-FACTS practical information for Alberta's agriculture industry (2011)** Irrigation scheduling for spring wheat in southern Alberta Available at [https://www1.agric.gov.ab.ca/\\$department/deptdocs.nsf/all/agdex13568/\\$file/112_561-2.pdf?OpenElement](https://www1.agric.gov.ab.ca/$department/deptdocs.nsf/all/agdex13568/$file/112_561-2.pdf?OpenElement) Access date 20th January, 2021
- Ahmed FE, Hall AE, DeMason DA** (1992) Heat injury during floral development in cowpea (*Vigna unguiculata*, Fabaceae). *Am J Bot* **79**: 784-791
- Aloni R, Aloni E, Langhans M, Ullrich CI** (2006) Role of auxin in regulating *Arabidopsis* flower development. *Planta* **223**: 315-328
- Alonso MP, Abbate PE, Mirabella NE, Merlos FA, Panelo JS** (2018) Analysis of sink/source relations in bread wheat recombinant inbred lines and commercial cultivars under a high yield potential environment. *Eur J Agron* **93**: 82-87
- Aluko OO, Li C, Wang Q, Liu H** (2021) Sucrose utilization for improved crop yields: A review article. *Int J Mol Sci* **22**: 1-29
- Asif M, Yang RC, Navabi A, Iqbal M, Kamran A, Lara EP, Randhawa H, Pozniak C, Spaner D** (2015) Mapping QTL, Selection differentials, and the effect of *Rht-B1* under organic and conventionally managed systems in the Attila× CDC Go spring wheat mapping population. *Crop Sci* **55**: 1129-1142
- Aya K, Tanaka MU, Kondo M, Hamada K, Yano K, Nishimura M, Matsuoka M** (2009) Gibberellin modulates anther development in rice via the transcriptional regulation of GAMYB. *Plant cell* **21**: 1453-1472
- Aziz P** (1972) Histogenesis of the carpel in *Triticum aestivum* L. *Bot Gaz* **133**: 376-386

Bangerth F, Aufhammer W, Baum O (1985) IAA level and dry matter accumulation at different positions within a wheat ear. *Physiol Plant* **63**: 121-125

Bechtel DB, Zayas I, Kaleikau L, Pomeranz Y (1990) Size-distribution of wheat starch granules during endosperm development. *Cereal Chem* **67**: 59-63

Begcy K, Nosenko T, Zhou LZ, Fragner L, Weckwerth W, Dresselhaus T (2019) Male sterility in maize after transient heat stress during the tetrad stage of pollen development. *Plant Physiol* **181**: 683-700

Begcy K, Weigert A, Egesa AO, Dresselhaus T (2018) Compared to Australian cultivars, European summer wheat (*Triticum aestivum*) overreacts when moderate heat stress is applied at the pollen development stage. *Agronomy* **99**: 1-16

Benkova E, Michniewicz M, Sauer M, Teichmann T, Seifertova D, Jurgens G, Friml J (2003) Local, efflux-dependent auxin gradients as a common module for plant organ formation. *Cell* **115**:591-602

Bennett MD, Rao MK, Smith JB, Bayliss MW (1973) Cell development in the anther, the ovule, and the young seed of *Triticum aestivum* L. var. chinese spring. *Phil Trans Royal Soc Lond* **66**: 39-81

Bhullar SS, Jenner CF (1986) Effects of temperature on the conversion of sucrose to starch in the developing wheat endosperm. *Aust J Plant Physiol* **13**: 605-615

Blum A (1998) Improving wheat grain filling under stress by stem reserve mobilization. *Euphytica* **100**: 77-83

Bowden P, Edwards J, Ferguson N, McNee T, Manning B, Roberts K, Schipp A, Schulze K, Wilkins J (2008) Wheat growth and development. *In* Edwards J, Roberts K, eds, Reproductive development. New South Wales Department of Primary industries, pp 51-58

Browne RG, Iacuone S, Li SF, Dolferus R, Parish RW (2018) Anther morphological development and stage determination in *Triticum aestivum*. *Front Plant Sci* **9**: 1-13

Browne RG, Li SF, Lacone S, Dolferus R, Parosh RW (2021) Differential responses of anthers of stress tolerant and sensitive wheat cultivars to high temperature stress. *Planta* **254**: 1-20

Bueckert RA, Clarke JM (2013) Review: Annual crop adaptation to abiotic stress on the Canadian prairies: Six cases. *Can J Plant Sci* **93**: 375-385

Bushuk W, Rasper (1994) *Wheat production properties and quality*. Springer Science and Business Media, Dordrecht

Byrne P (2020) Case Study: Wheat Domestication and Breeding. Department of Soil and Crop Sciences, Colorado State University Available at <https://colostate.pressbooks.pub/cropwildrelatives/chapter/wheat-breeding-with-crop-wild-relatives/> Access date 3rd February, 2021

Canada Statistics (2021) Production of principal field crops Available at <https://www150.statcan.gc.ca/n1/daily-quotidien/210830/dq210830b-eng.htm> Access date 14th September, 2021

Castro M, Peterson CJ, Rizza MD, Dellavalle PD, Vazquez D, Vazquez D, Ibanez V, Ross A (2007) Influence of heat stress on wheat grain characteristics and protein molecular weight distribution. *In* Buck HT, Nisi JE, Salomon N, eds, *Wheat Production in Stressed Environment*, Springer, Netherlands, pp 365–371

Ceccato L, Masiero S, Roy DS, Bencivenga S, Roig-Villanova I, Ditengou FA, Palme K, Simon R, Colombo L (2013) Maternal control of PIN1 is required for female gametophyte development in *Arabidopsis*. *PLoS One* **8**: 2-8

Cecchetti V, Altamura MM, Falasca G, Costantino P, Cardarelli M (2008) Auxin regulates *Arabidopsis* anther dehiscence, pollen maturation, and filament elongation. *Plant Cell* **20**: 1760-1774

Charles-Edwards DA (1984) On the ordered development of plants: An hypothesis. *Ann Bot* **53**: 699-707

- Cheng H, Qin L, Lee S, Fu X, Richards DE, Cao D, Luo D, Harberd NP, Peng J (2004)** Gibberellin regulates *Arabidopsis* floral development via suppression of DELLA protein function. *Development* **131**: 1055–1064
- Cheng Y, Dai X, Zhao Y (2006)** Auxin biosynthesis by the YUCCA flavin monooxygenases controls the formation of floral organs and vascular tissues in *Arabidopsis*. *Genes Dev* **20**: 1790-1799
- Cheng Y, Zhao Y (2007)** A role for auxin in flower development. *J Integr Plant Biol* **49**: 99-104
- Darussalam M, Cole MA, Patrick JW (1998)** Auxin control of photoassimilate transport to and within developing grains of wheat. *Aust J Plant Physiol* **25**: 69-78
- De Storme N, Geelen D (2014)** The impact of environmental stress on male reproductive development in plants: biological processes and molecular mechanisms. *Plant Cell Environ* **37**: 1-18
- De Vries Ap (1971)** Flowering biology of wheat, particularly in view of hybrid seed production- A review. *Euphytica* **20**: 152-170
- Dias AS, Bagulho AS, Lidon FC (2008)** Ultrastructure and biochemical traits of bread and durum wheat grains under heat stress. *Brazilian J Plant Physiol* **20**: 323-333
- Dias AS, Lidon FC (2009)** Evaluation of grain filling rate and duration in bread and durum wheat, under heat stress after anthesis. *J Agron Crop Sci.* **195**: 137–147
- Erena MF, Lohraseb I, Munoz-Santa I, Taylor JD, Emebiri LC, Collins NC (2021)** The *WtmsDW* locus on wheat chromosome 2B controls major natural variation for floret sterility responses to heat stress at booting stage. *Front Plant Sci* **12**: 1-11
- Endo M, Tsuchiya T, Hamada K, Kawamura S, Yano K, Ohshima M, Higashitani A, Watanabe M, Kawagishi-Kobayashi M (2009)** High temperatures cause male sterility in rice plants with transcriptional alterations during pollen development. *Plant Cell Physiol* **50**: 1911-1922
- Endres PK (2011)** Angiosperm ovules: diversity, development, evolution. *Ann Bot* **107**: 1465-1489

FAOSTAT (2019) Crops Available at <http://www.fao.org/faostat/en/#data/QC> Access date 20th January, 2020

FAO (2002) Bread wheat improvement and production Available at <http://www.fao.org/3/y4011e00.htm#Contents>. Access date 20th January, 2020

Farooq M, Bramley H, Palta JA, Siddique KHM (2011) Heat stress in wheat during reproductive and grain-filling phases. *Crit Rev Plant Sci* **30**: 491-507

Feng B, Liu P, Li G, Dong ST, Wang FH, Kong LA, Zhang JW (2014) Effects of heat stress on the photosynthetic characteristics in flag leaves at the grain-filling stage of different heat-resistant winter wheat varieties. *J Agro Crop* **200**: 143-155

Feng N, Song G, Guan J, Chen K, Jia M, Huang D, Wu J, Zhang L, Kong X, Geng S, et al (2017) Transcriptome profiling of wheat inflorescence development from spikelet initiation to floral patterning identified stage-specific regulatory genes. *Plant Physiol* **174**: 1779-1794

Feng XL, Ni WM, Elge S, Mueller-Roeber B, Xu ZH, Xue HW (2006) Auxin flow in anther filaments is critical for pollen grain development through regulating pollen mitosis. *Plant Mol Biol* **61**: 215-226

Flintham JE, Borner A, Worland AJ, Gale MD (1997) Optimizing wheat grain yield: effects of *Rht* (gibberellin-insensitive) dwarfing genes. *J Agric Sci* **128**: 11–25

Garg D, Sareen S, Dalal S, Tiwari R, Singh R (2012) Heat shock protein based SNP marker for terminal heat stress in wheat (*Triticum aestivum* L). *Aust J Crop Sci* **6**: 1516-1521

Girousse C, Roche J, Guerin C, Le Gouis J, Balzegue S, Mouzeyar S, Bouzidi MF (2018) Coexpression network and phenotypic analysis identify metabolic pathways associated with the effect of warming on grain yield components in wheat. *PLoS ONE* **13**: 1-22

Gol L, Tome F, Von Korff M (2017) Floral transitions in wheat and barley: Interactions between photoperiod, abiotic stresses, and nutrient status. *J Exp Bot* **68**: 1399-1410

Gonzalez FG, Slafer GA, Miralles DJ (2005) Floret development and survival in wheat plants exposed to contrasting photoperiod and radiation environments during stem elongation. *Funct Plant Biol* **32**: 189-197

- Guo Z, Chen D, Schnurbusch T** (2018) Stages during the stem elongation phase in wheat. *Front Plant Sci* **9**: 1-13
- Guo Z, Slafer GA, Schnurbusch T** (2016) Genotypic variation in spike fertility traits and ovary size as determinants of floret and grain survival rate in wheat. *J Exp Bot* **67**: 4221–4230
- Hasanuzzaman M, Kamrun N, Alam MM, Roychowdhury R, Fujita M** (2013) Physiological, biochemical, and molecular mechanisms of heat stress tolerance in plants. *Int J Mol Sci* **12**: 9643-9684
- Hawker JS, Jenner CF** (1993) High temperature affects the activity of enzymes in the committed pathway of starch synthesis in developing wheat endosperm. *Aust J Plant Physiol* **20**: 197-209
- Hedden P** (2003) The genes of the Green Revolution. *Trends Genet* **19**: 5-9
- Higashitani A** (2013) High temperature injury and auxin biosynthesis in microsporogenesis. *Front Plant Sci* **4**: 1-3
- Hu L, Liang W, Yin C, Cui X, Zong J, Wang X, Hu J, Zhang D** (2011) Rice MADS3 regulates ROS homeostasis during late anther development. *Plant Cell* **23**: 515-533
- Hurkman WJ, MccUE KF, Altenbach SB, Korn A, Tanaka CK, Kothari KM, Jonson EL, Bechtel DB, Wilson JD, Anderson OD, et al** (2003) Effect of temperature on expression of genes encoding enzymes for starch biosynthesis in developing wheat endosperm. *Plant Sci* **164**: 873-881
- Hutsch BW, Jahn D, Scubert S** (2018) Grain yield of wheat (*Triticum aestivum* L.) under long-term heat stress is sink-limited with stronger inhibition of kernel setting than grain filling. *J Agron Crop Sci* **205**: 22-32
- Ishiguro S, Kawai-Oda A, Ueda J, Nishida I, Okada K** (2001) The *DFECTIVE IN ANTHER DEHISCENCE1* gene encodes a novel phospholipase A1 catalyzing the initial step of jasmonic acid biosynthesis, which synchronizes pollen maturation, anther dehiscence, and flower opening in Arabidopsis. *Plant Cell* **13**: 2191-2209

- Jenner C** (1994) Starch synthesis in the kernel of wheat under high temperature conditions. *Aust J Plant Physiol* **21**: 791-806
- Kaur H, Ozga JA, Reinecke DM** (2021) Balancing of hormonal biosynthesis and catabolism pathways, a strategy to ameliorate the negative effects of heat stress on reproductive growth. *Plant Cell Environ* **44**: 1486-1503
- Kirby EJM** (2002) Botany of the wheat plant. *In* Curtis BC, Rajaram S, Macpherson HG, eds, Bread wheat. FAO of the UN, Rome, pp 2
- Koppolu R, Schnurbusch T** (2019) Developmental pathways for shaping spike inflorescence architecture in barley and wheat. *J Integr Plant Biol* **61**: 278-295
- Kumar R, Mukherjee S, Ayele BT** (2018) Molecular aspects of sucrose transport and its metabolism to starch during seed development in wheat: A comprehensive review. *Biotechnol Adv* **36**: 954-967
- Kumar S, Kumari P, Kumar U, Grover M, Singh AK, Singh R, Sengar RS** (2013) Molecular approaches for designing heat tolerant wheat. **22**: 359-371
- Kumar U, Joshi AK, Kumari M, Paliwal R, Kumar S, Order MS** (2010) Identification of QTLs for stay green trait in wheat (*Triticum aestivum* L.) in the ‘Chirya 3’ x ‘Sonalika’ population. *Euphytica* **174**: 437–445
- Kurusu T, Kuchitsu K** (2017) Autophagy, programmed cell death and reactive oxygen species in sexual reproduction in plants. *J Plant Res* **130**: 491-499
- Lancashire PD, Bleiholder H, Van-Den-Boom T, Langeluddke P, Stauss R, Weber E, Witzemberger A** (1991) A uniform decimal code for growth stages of crops and weeds. *Ann appl Biol* **119**: 561-601
- Lesk C, Rowhani P, Ramankutty N** (2016) Influence of extreme weather disasters on global crop production. *Nature* **529**: 84-87
- Li R, Hou L, Zhang A, Lu Y, Song W, Tadesse W, Wang X, Liu M, Zheng W, Xu S** (2018) Heat stress in filling stage confers distinct effect on starch granules formation in different thermotolerant wheat accessions. *Pak J Bot* **50**: 913-920

- Lindsey R and Dahlman L** (2021) Climate change: global temperature Available at <https://www.climate.gov/news-features/understanding-climate/climate-change-global-temperature> Access date 25th May, 2021.
- Liu B, Liu L, Asseng S, Zhang D, Ma W, Tang L, Cao W, Zhu Y** (2020) Modelling the effects of post-heading heat stress on biomass partitioning, and grain number and weight of wheat. *J Exp Bot* **71**: 6015-6031
- Liu P, Guo W, Jiang Z, Pu H, Feng C, Zhu X, Peng Y, Kuang A, Little CR** (2011) Effect of high temperature after anthesis on starch granules in grains of wheat (*Triticum aestivum* L.). *J Agric Sci* **149**: 159-169
- Lohani N, Singh MB, Bhalla PL** (2020) High temperature susceptibility of sexual reproduction in crop plants. *J Exp Bot* **71**: 555-568
- Maestri E, Klueva N, Perrotta C, Gullim, Nguyen HT, Marmioli N** (2002) Molecular genetics of heat tolerance and heat shock proteins in cereals. *Plant Mol Biol* **48**: 667-681
- McCallum BD, DePauw RM** (2008) A review of wheat cultivars grown in the Canadian prairies. *Can J Plant Sci* **88**: 649-677
- Muller F, Rieu I** (2016) Acclimation to high temperature during pollen development. *Plant Reprod* **29**: 107-118
- Nagpal P, Ellis CM, Weber H, Ploense SE, Barkawi LS, Guilfoyle TJ, Hagen G, Alonso JM, Cohen JD, Farmer EE, et al** (2005) Auxin response factors ARF6 and ARF8 promote jasmonic acid production and flower maturation. *Development* **132**: 4107-4118
- Narayanan S** (2018) Effects of high temperature stress and traits associated with tolerance in wheat. *Open Access J Sci* **2**: 177-186
- Okada K, Udea J, Komaki MK, Bell C, Shimura Y** (1991) Requirement of the Auxin Polar Transport System in Early Stages of *Arabidopsis* Floral Bud Formation. *Plant Cell* **3**: 677-684
- Oshino T, Miura S, Kikuchi S, Hamada K, Yano K, Watanabe M, Higashitani A** (2011) Auxin depletion in barley plants under high-temperature conditions represses DNA proliferation in organelles and nuclei via transcriptional alterations. *Plant Cell Environ* **34**: 284-290

Ozga JA, Kaur H, Savada RP, Reinecke DM (2017) Hormonal regulation of reproductive growth under normal and heat-stress conditions in legume and other model crop species. *J Exp Bot* **68**: 1885-1894

Pagnussat GC, Alandete-Saez M, Bowman JL, Sundaresan V, Ec A, Syn A (2009) Auxin-dependent patterning and *Arabidopsis* female gametophyte. *Science* **324**: 1684-1689

Palta JA, Kobata T, Turner NC, Fillery IR (1994) Remobilization of carbon and nitrogen in wheat as influenced by postanthesis water deficits. *Crop Sci* **34**: 118-124

Pandey GC, Mehta G, Sharma P, Sharma V (2019) Terminal heat tolerance in wheat: An overview. *J Cereal Res* **11**: 1-16

Parker ML (1985) The relationship between A-type and B-type starch granules in the developing endosperm of wheat. *J Cereal Sci* **3**: 271-278

Peng JR, Richards DE, Hartley NM, Murphy GP, Devos KM, Flintham JE, Beales J, Fish LJ, Worland AJ, Pelica F, et al (1999) Green revolution genes encode mutant gibberellin response modulators. *Nature* **400**: 256-261

Plackett ARG, Powers SJ, Fernandez-Garcia N, Urbanova T, Takebayashi Y, Seo M, Jikumaru Y, Benlloch R, Nilsson O, Ruiz-Rivero O, et al (2012) Analysis of the developmental roles of the *Arabidopsis* gibberellin 20-oxidases demonstrates that GA20ox1-2 and-3 are the dominant paralogs. *Plant Cell* **24**: 941-960

Pinto RS, Reynolds MP, Mathews KL, McIntyre CL, Olivares-Villegas JJ and Chapman SC (2010) Heat and drought adaptive QTL in a wheat population designed to minimize confounding agronomic effects. *Theor Appl Genet* **121**: 1001–1021

Pollar DA (2012) Design and construction of Recombinant Inbred Lines. *In* Rifkin SA, eds, Quantitative Trait Loci (QTL) methods and protocols. University of California, USA, pp 31-39

Porter JR, Gawith M (1999) Temperatures and the growth and development of wheat: a review. *Eur J Agron* **10**: 23-36

Prasad PVV, Djanaguiraman (2014) Response of floret fertility and individual grain weight of wheat to high temperature stress: sensitive stages and thresholds for temperature and duration. *Funct Plant Biol* **41**: 1261-1269

Raja MM, Vijayalakshmi G, Naik ML, Basha PO, Sergeant K, Hausman JF, Khan PSSV (2019) Pollen development and function under heat stress: from effects to responses. *Acta Physiol Plant* **41**: 1-20

Rampino P, Mita G, Pataleo S, DePascali M, DiFonzo N, Perrotta C (2009) Acquisition of thermotolerance and HSP gene expression in durum wheat (*Triticum durum* Desf.) cultivars. *Environ Exp Bot* **66**: 257-264

Reale L, Rosati A, Tedeschini E, Ferri V, Cerri M, Ghitarrini S, Timorato V, Ayano BE, Porfiri O, Frenguelli G, et al (2017) Ovary size in wheat (*Triticum aestivum* L.) is related to cell number. *Crop Sci* **57**: 914-925

Rebetzke GJ, Appels R, Morrison AD, Richards RA, McDonald G, Ellis MH, Spielmeier W, Bonnett DG (2001) Quantitative trait loci on chromosome 4B for coleoptile length and early vigour in wheat (*Triticum aestivum* L.). *Aust J Agric Res* **52**: 1221-1234

Rezaul IM, Baohua F, Tingting C, Weimeng F, Caixia Z, Longxing T, Guanfu F (2019) Abscisic acid prevents pollen abortion under high-temperature stress by mediating sugar metabolism in rice spikelets. *Physiol Plant* **165**: 644-663

Rijven AHGC (1986) Heat inactivation of starch synthase in wheat endosperm tissue. *Plant Physiol* **81**: 448-453

Rosewarne GM, Singh RP, Huerta-Espino J, Rebetzke GJ (2008) Quantitative trait loci for slow-rusting resistance in wheat to leaf rust and stripe rust identified with multi-environment analysis. *Theor Appl Genet* **116**: 1027-1034

Rudall PJ (1997) The Nucellus and chalaza in monocotyledons: structure and systematics. *The Bot Rev* **63**: 140-177

Saini HS, Aspinall D (1982) Abnormal sporogenesis in wheat (*Triticum aestivum* L.) induced by short periods of high temperature. *Ann Bot* **49**: 835-846

Saini HS, Sedgley M, Aspinall D (1983) Effect of heat stress during floral development on pollen tube growth and ovary anatomy in wheat (*Triticum aestivum* L.). Aust J Plant Physiol **10**: 137-144

Sakata T, Higashitani A (2008) Male sterility accompanied with abnormal anther development in plants-genes and environmental stresses with special reference to high temperature injury. Int J Plant Dev Bio **2**: 42-51

Sakata T, Ohino T, Miura S, Tomabechi M, Tsunaga Y, Higashitani N, Miyazawa Y, Takahashi H, Watanabe M, Higashitani A (2010) Auxins reverse plant male sterility caused by high temperatures. Proc Natl Acad Sci USA **107**: 8569-8574

Sakata T, Takahashi H, Nishiyama I, Higashitani A (2000) Effects of high temperature on the development of pollen mother cells and microspores in Barley *Hordeum vulgare* L. J Plant Res **113**: 395-402

Salinas-Grenet H, Herrera-Vasquez A, Parra S, Cortez A, Gutierrez L, Pollmann S, Leon G, Blanco-Herrera F (2018) Modulation of auxin levels in pollen grains affects stamen development and anther dehiscence in *Arabidopsis*. Int J Mol Sci **19**: 1-13

Sharma-Natu P, Sumesh KV, Ghildiyal MC (2010) Heat shock protein in developing grains in relation to thermotolerance for grain growth in wheat. J Agron Crop Sci **196**: 76-80

Shewry PR (2009) Wheat. J Exp Bot **60**: 1537-1553

Shirdelmoghanloo H, Lohraseb I, Rabie HS, Brien C, Parent B, Collins NC (2016) Heat susceptibility of grain filling in wheat (*Triticum aestivum* L.) linked with rapid chlorophyll loss during a 3-day heat treatment. Acta Physiol Plant **38**: 1-11

Shivanna KR (2003) Pollen biology and biotechnology. Science Publishers, Enfield

Skyllas DJ, Cordwell SJ, Hains PG, Larsen MR, Basseal DJ, Walsh BJ, Blumenthal C, Rathmell W, Copeland L, Wrigley CW (2002) Heat shock of wheat during grain filling: proteins associated with heat-tolerance. J Cereal Sci **35**: 175-188

- Spiertz JHJ, Hamer RJ, Xu H, Primo-Martin C, Don C, van der Putten PEL** (2006) Heat stress in wheat (*Triticum aestivum* L.): Effects on grain growth and quality traits. *Eur J Agron* **25**: 89-95
- Stintzi A, Browse J** (2000) The *Arabidopsis* male-sterile mutant, *opr3*, lacks the 12-oxophytodienoic acid reductase required for jasmonate synthesis. **97**: 10625-10630
- Stone PJ, Nicolas ME** (1995) Effect of heat stress during grain filling on two wheat varieties differing in heat tolerance. I. Grain growth. *Aust J Plant Physiol* **22**: 927-934
- Streck NA** (2005) Climate change and agroecosystems: the effect of elevated atmospheric CO₂ and temperature on crop growth, development, and yield. *Ciencia Rural* **35**: 730-740
- Suzuki K, Takeda H, Tsukaguchi T, Egawa Y** (2001) Ultrastructural study on degeneration of tapetum in anther of snap bean (*Phaseolus vulgaris* L.) under heat stress. *Sex Plant Reprod* **13**: 293-299
- Talukder ASMHM, Mcdonald GK, Gill GS** (2014) Effect of short-term heat stress prior to flowering and early grain set on the grain yield of wheat. *F Crop Res* **160**: 54-63
- Talukder ASMHM, McDonald GK and Gill GS** (2013) Effect of short-term heat stress prior to flowering and at early grain set on the utilization of water-soluble carbohydrate by wheat genotypes. *F Crops Res* **147**: 1-11
- Tang RS, Zheng JC, Jin ZQ, Zhang DD, Huang YH, Chen LG** (2008) Possible correlation between high temperature-induced floret sterility and endogenous levels of IAA, GAs and ABA in rice (*Oryza sativa* L.). *Plant Growth Regul* **54**: 37-43
- Tewolde H, Fernandez CJ, Erickson CA** (2006) Wheat cultivars adapted to post-heading high temperature stress. *J Agron Crop Sci* **120**: 111-120
- Tomas D, Rodrigues JC, Viegas W, Silva M** (2020) Assessment of high temperature effects on grain yield and composition in bread wheat commercial varieties. *Agronomy* **10**: 1-12
- Tshikunde NM, Mashilo J, Shimelis H, Odindo A** (2019) Agronomic and physiological traits, and associated Quantitative Trait Loci (QTL) affecting yield response in Wheat (*Triticum aestivum* L.): A review. *Front Plant Sci* **10**: 1-18

Varnier A-L, Mazeyrat-Gourbeyre F, Sangwan RS, Clement C (2005) Programmed cell death progressively models the development of anther sporophytic tissues from the tapetum and is triggered in pollen grains during maturation. *J Struct Biol* **152**: 118-128

Venske E, Dos Santos RS, Busanello C, Gustafson P, De Oliveira AC (2019) Bread wheat: a role model for plant domestication and breeding. *Hereditas* **156**: 1-11

Vijayalakshmi K, Fritz AK, Paulsen GM, Bai G, Pandravada S, Gill BS (2010) Modeling and mapping QTL for senescence-related traits in winter wheat under high temperature. *Mol Breed* **26**: 163-175

Vinh NT, Paterson AH (2005) Genome mapping and its implication for stress resistance in plants. In Ashraf M and Harris PJC, eds, *Abiotic Stresses: Plant Resistance through Breeding and Molecular Approaches*. Food Products Press, New York, pp 109-124

Wahid A, Gelani S, Ashraf M, Foolad MR (2007) Heat tolerance in plants: A overview. *Environ Exp Bot* **61**: 199-223

Wang A, Xia Q, Xie W, Datla R, Selvaraj G (2003) The classical Ubisch bodies carry a sporophytically produced structural protein (RAFTIN) that is essential for pollen development. *Proc Natl Acad Sci U S A* **100**: 14487-14492

Wang R, Estelle (2014) Diversity and specificity: auxin perception and signaling through the TIR1/AFB pathway. *Curr Opin Plant Biol* **21**: 51-58

Wang W, Vinocur B, Shoseyov O, Altman A (2004) Role of plant heat-shock proteins and molecular chaperones in abiotic stress response. *Trends Plant Sci.* **9**: 244-252

Wang X, Cai J, Liu F, Jin M, Yu H, Jiang D, Wollenweber B, Dai T, Cao W (2012) Pre-anthesis high temperature acclimation alleviates the negative effects of post-anthesis heat stress on stem stored carbohydrates remobilization and grain starch accumulation in wheat. *J Cereal Sci* **55**: 331-336

Wardlaw I, Sofield I, Cartwright P (1980) Factors limiting the rate of dry matter accumulation in the grain of wheat grown at high temperature. *Aust J Plant Physiol* **7**: 387-400

Wilhelm EP, Mackay IJ, Saville RJ, Korolev AV, Balfourier F, Greenland AJ, Boulton MI, Powell W (2013) Haplotype dictionary for the *Rht-1* loci in wheat. *Theor Appl Genet* **126**: 1733-47

Wilkinson LG, Tucker MR (2017) An optimised clearing protocol for the quantitative assessment of sub-epidermal ovule tissues within whole cereal pistils. *Plant Methods* **13**: 1-10

Won C, Shen X, Mashiguchi K, Zheng Z, Dai X, Cheng Y, Kasahara H, Kamiya Y, Chory J, Zhao Y (2011) Conversion of tryptophan to Indole-3-acetic acid by TRYPTOPHAN AMINOTRANSFERASES OF *ARABIDOPSIS* AND *YUCCAS* IN *ARABIDOPSIS*. *Proc Natl Acad Sci U S A* **108**: 18518-18523

Yang J, Sears RG, Gill BS, Paulsen GM (2002) Quantitative and molecular characterization of heat tolerance in hexaploid wheat. *Euphytica* **126**: 275-282

Yang J, Tian L, Sun MX, Huang XY, Zhu J, Guan YF, Jia QS, Yan ZN (2013) AUXIN RESPONSE FACTOR 17 Is Essential for Pollen Wall Pattern Formation in Arabidopsis. *Plant Physiol* **162**: 720-731

Yin X, Guo W Spiertz JH (2009) A quantitative approach to characterize sink-source relationships during grain filling in contrasting wheat genotypes. *Field Crops Res* **114**: 119-126

Youssefian S, Kirby EJM, Gale MD (1992) Pleiotropic effects of the GA insensitive *Rht* dwarfing genes in wheat: effects on leaf, stem, ear and floret growth. *Field Crops Res* **28**: 191-210

Zhang C, Jiang D, Liu F, Cai J, Dai T, Cao W (2010) Starch granules size distribution in superior and inferior grains of wheat is related to enzyme activities and their gene expressions during grain filling. *J Cereal Sci* **51**: 226-233

Zhang C, Li G, Chen T, Feng B, Fu W, Yan J, Islam MR, Jin Q, Tao L, Fu G (2018) Heat stress induces spikelet sterility in rice at anthesis through inhibition of pollen tube elongation interfering with auxin homeostasis in pollinated pistils. *Rice* **11**: 1-12

Zeng M, Morris CF, Batey IANL, Wrigley CW (1997) Sources of starch gelatinization, pasting, and gelation properties in wheat. *Cereal Chem* **74**: 63-71

Zhao Y (2012) Auxin Biosynthesis: A simple two-step pathway converts tryptophan to Indole-3-Acetic acid in plants. *Mol Plant* **5**: 334-338

Zou J, Semagn K, Iqbal M, Chen H, Asif M, N'Diaye A, Navabi A, Perez-Lara E, Pozniak C, Yang RC, et al (2017) QTL s associated with agronomic traits in the Attila x CDC Go spring wheat population evaluated under conventional management. *PLoS One* **12**: 1-20

Appendix

Appendix A

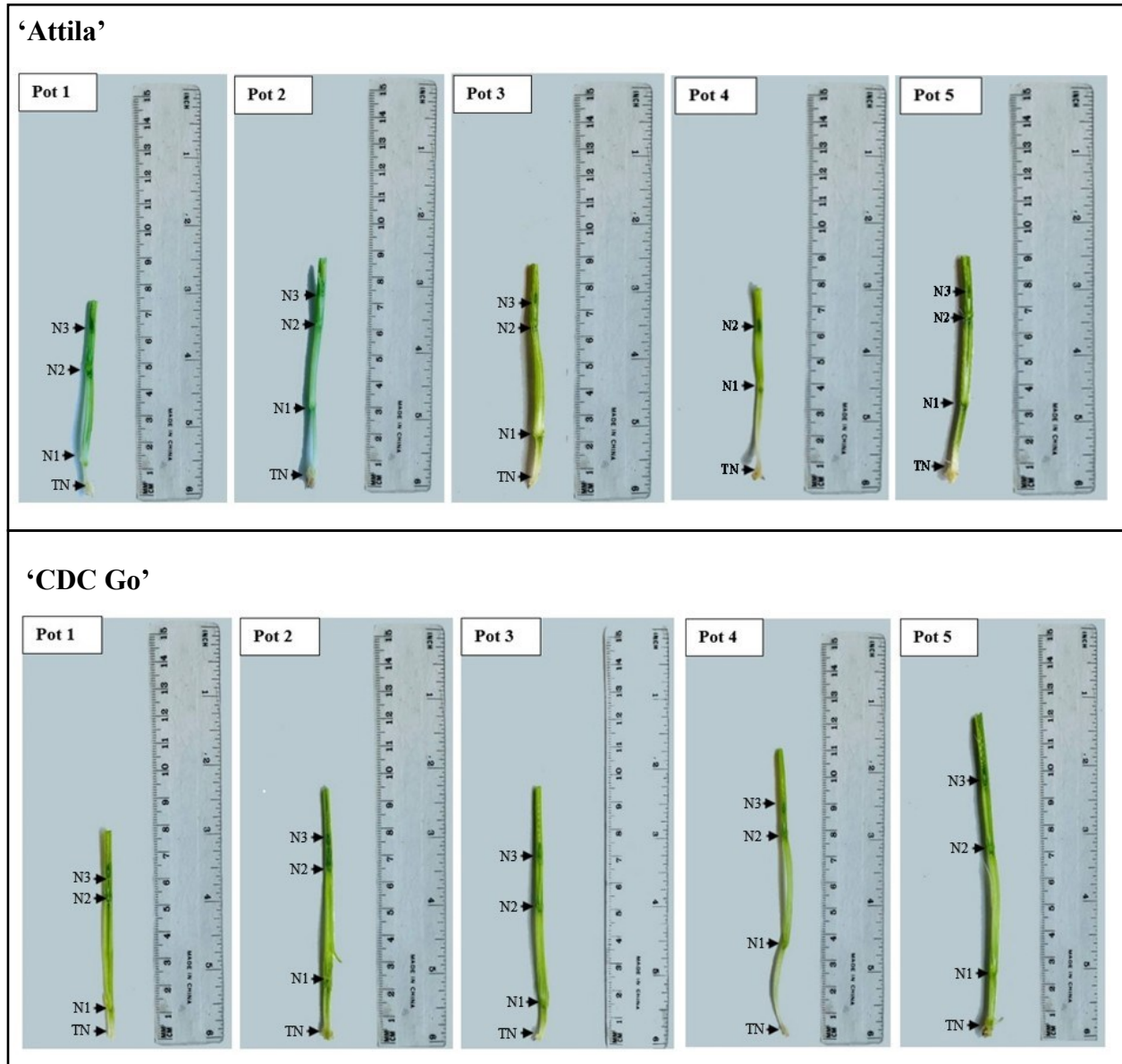


Figure A.1: Longitudinal sections of the main tiller of 'Attila' and 'CDC Go' plants at the flag-leaf emerging stage (BBCH 37). TN, Tillering Node; N1, Node1; N2, Node 2; N3, Node 3.

Table A.1: The internode length of the main tiller of ‘Attila’ and ‘CDC Go’ plants at the flag-leaf emerging stage.

Internode length (mm)				
Cultivar	Plant	Internode 1 (Tillering node to Node 1)	Internode 2 (Node 1 to Node 2)	Internode 3 (Node 2 to Node 3)
‘Attila’	1	7	29	15
	2	21	29	12
	3	15	40	7
	4	27	22	ND ^a
	5	24	31	31
	mean ^b	19±3.6	30±2.9	16±5.2
‘CDC Go’	1	9	39	7
	2	16	42	10
	3	11	34	17
	4	31	42	7
	5	15	43	21
	mean	16±3.9	40±1.6	12±2.8

^a ND, not determined.

^b Data are means ± standard error of the mean, n=4-5.

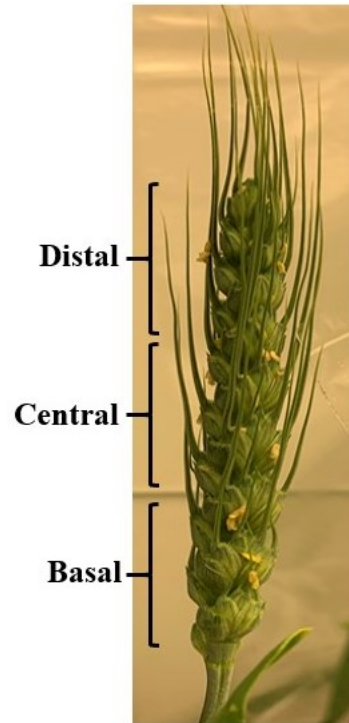


Figure A.2: The first floral spike at anthesis. The image represents the distal, central, and basal regions of the spike.

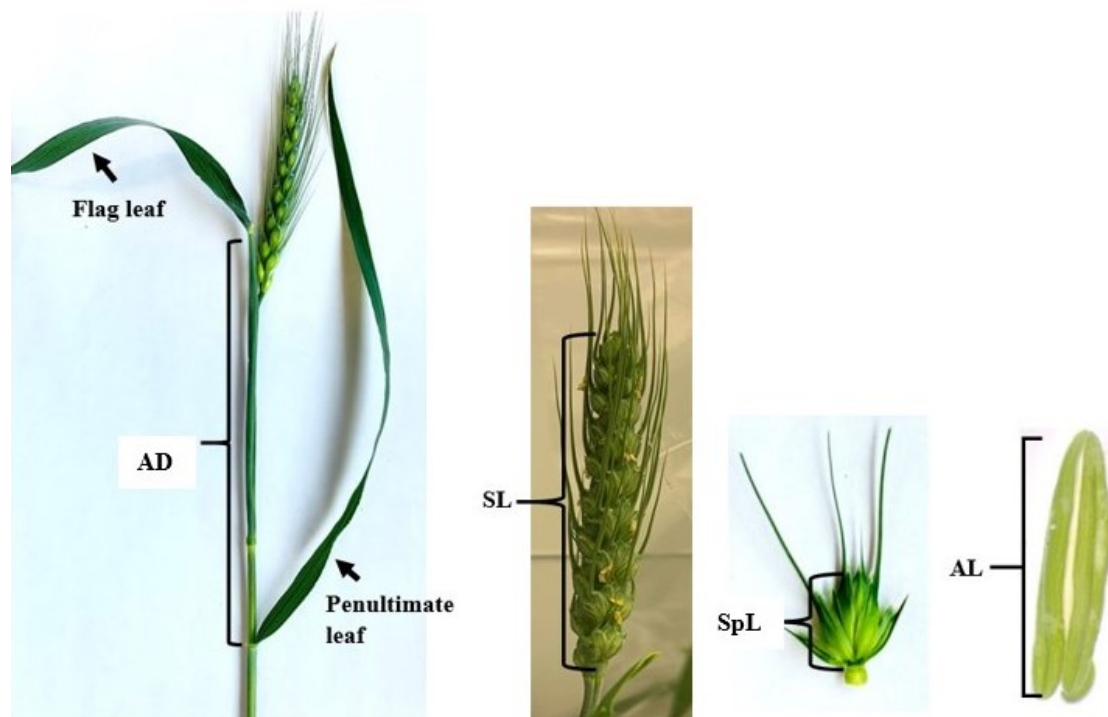


Figure A.3: Diagrams depicting the floral morphological measurements. **(A)** Auricle distance (AD) was measured between the attachment of the flag leaf and the attachment of the penultimate leaf. **(B)** Spike length (SL) was measured between attachment of the lowest spikelet to the rachis to the most distal spikelet excluding awns. **(C)** Spikelet length (SpL) was measured between base of the spikelet attached to the rachis to tip of the most distal floret excluding awns. **(D)** Anther length (AL) was measured using a dissecting microscope.

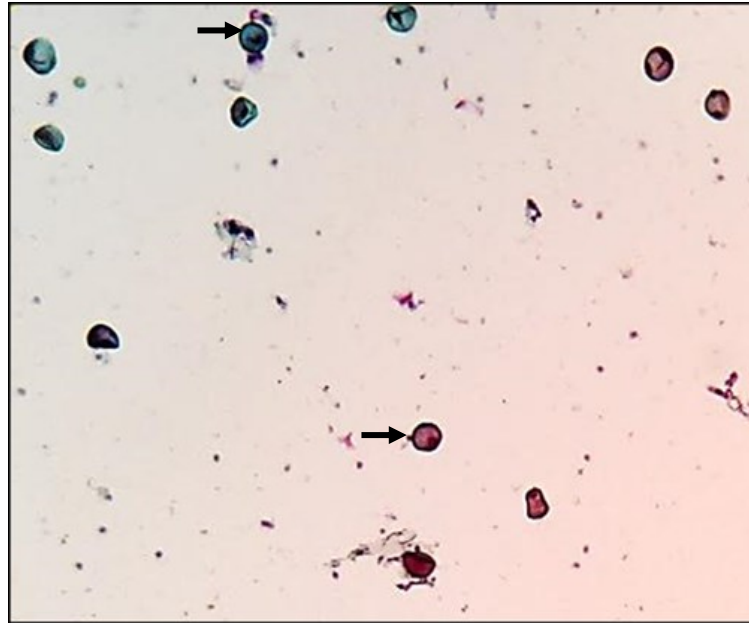


Figure A.4: Pollen grains imaged after staining with modified Alexander staining solution under a light microscope at 10X magnification. Black arrows indicate the viable (red color) and non-viable (green color) pollen grains.

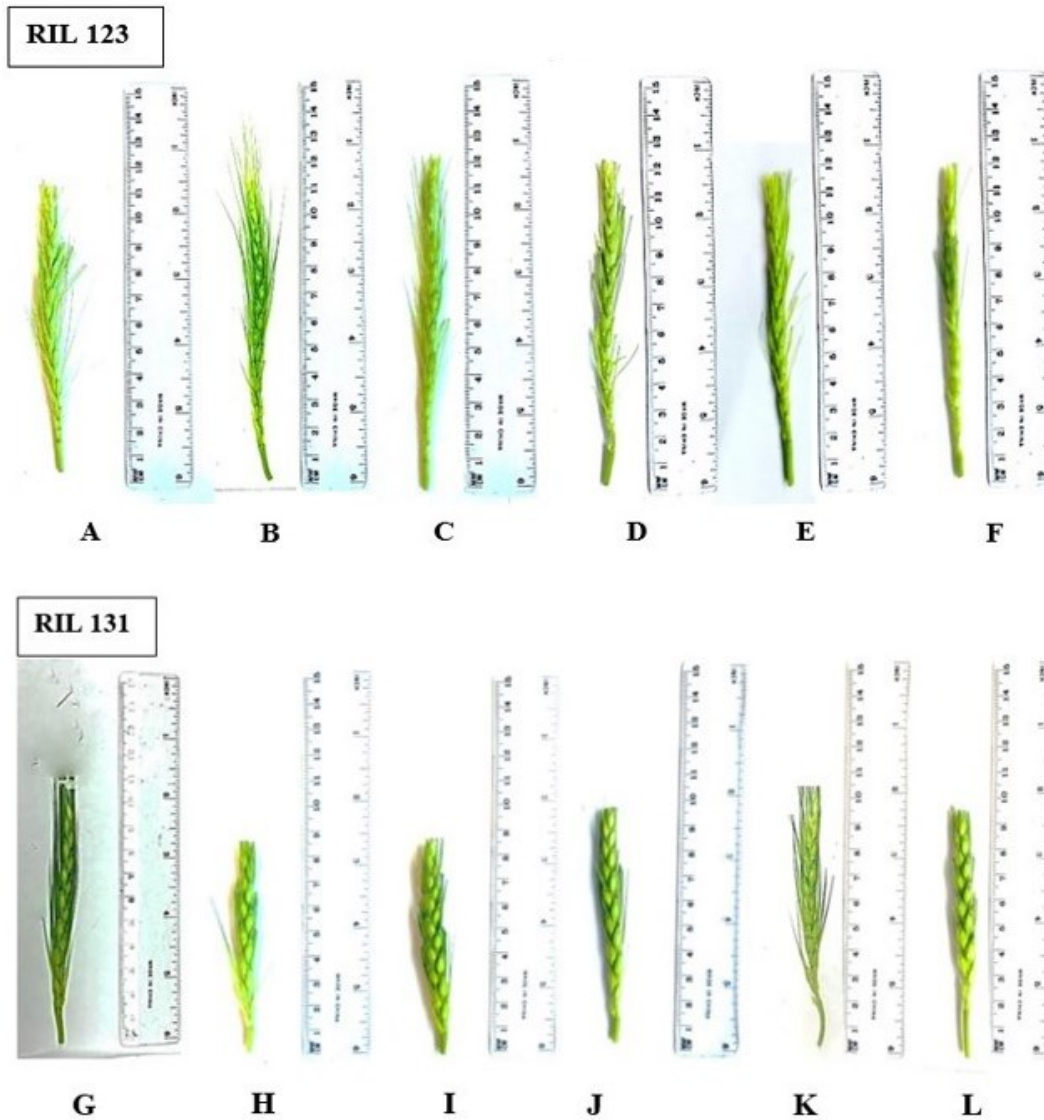


Figure A.5: Representative images of the developmental stage of the main tiller spike from the control and heat stress-treated plants of RIL 123 and RIL 131 at the time of tissue collection for histology. RIL 123 spikes ranged from BBCH 45-49 within each temperature treatment (A-C from heat stress-treated plants, spike length 101 ± 2.3 mm; D-F from control plants, spike length 100 ± 3.4 mm). RIL131 spikes ranged from BBCH 45-53 within each temperature treatment (G-I from heat stress-treated plants, spike length 79 ± 3.2 mm; J-L from control plants, spike length 78 ± 3.8 mm).

Table A.2 Auricle distance ANOVA analysis degrees of freedom, F values, and probability for the temperature and RIL ID main effects, and temperature x RIL ID interaction presented in Table 3.1 of the thesis.

Source of variation	Degrees of freedom	F value	Pr (>F)
Temperature	1	113.266	< 2.2e-16
RIL.ID	18	35.429	< 2.2e-16
Temperature x RIL ID	18	3.309	1.144e-05

Table A.3 Spike length ANOVA analysis degrees of freedom, F values, and probability for the temperature and RIL ID main effects, and temperature x RIL ID interaction presented in Table 3.1 of the thesis.

Source of variation	Degrees of freedom	F value	Pr (>F)
Temperature	1	1.0103	0.3158
RIL.ID	18	26.2146	<2e-16
Temperature x RIL ID	18	2.0921	0.0066

Table A.4 Spikelet length ANOVA analysis degrees of freedom, F values, and probability for the temperature and spike region main effects, and temperature x spike region interaction presented in Tables 3.2 and 3.3 of the thesis.

RIL ID	Temperature		Spike region		Temperature x Spike region	
	F value	Pr (>F)	F value	Pr (>F)	F value	Pr (>F)
Heat-resistant						
28	0.7784	0.3827	1.6748	0.1996	0.0311	0.9694
148	4.3591	0.0429	2.0866	0.1368	1.3810	0.2625
164	9.8	0.0033	3.5492	0.0384	1.0226	0.3691
123	36.0768	3.889e-07	8.0118	0.0011	0.7390	0.4837
174	0.2538	0.6170	4.5860	0.0158	0.0456	0.9555
143	0.0193	0.8903	2.2152	0.1217	0.3347	0.7175
36	12.7919	0.0009	17.8285	2.48e-06	0.2168	0.8060
'Attila'	3.9712	0.0528	1.4488	0.2464	0.9853	0.3818
Heat-sensitive						
153	0.7311	0.3974	25.9831	4.527e-08	0.0386	0.9622
46	0.1370	0.7131	36.0124	7.785e-10	0.6404	0.5321
140	0.4777	0.4933	7.5212	0.0016	0.1674	0.8464
116	3.5521	0.0664	45.3083	3.263e-11	0.9719	0.3867
145	1.1636	0.2869	24.0963	1.071e-07	0.2082	0.8128
52	8.6925	0.0052	44.4710	4.262e-11	1.0448	0.3607
26	0.5217	13.1765	0.0517	0.4741	3.617e-05	0.9497
131	9.8212	0.0031	10.8922	0.0002	0.2091	0.8122
40	0.1214	0.7293	17.4318	3.077e-06	0.0146	0.9855
13	1.7732	0.1902	33.5816	1.944e-09	0.1428	0.8673
'CDC Go'	0.2019	0.6555	37.7155	4.196e-10	1.2861	0.2870
Degrees of freedom	1		2		2	

Table A.5 Pollen viability ANOVA analysis degrees of freedom, F values, and probability for the temperature and spike region main effects, and temperature x spike region interaction presented in Tables 3.4 and 3.5 of the thesis.

RIL ID	Temperature		Spike region		Temperature x Spike region	
	F value	Pr (>F)	F value	Pr (>F)	F value	Pr (>F)
Heat-resistant						
28	11.0948	0.0018	1.0449	0.3607	2.3337	0.1094
148	0.4922	0.4868	2.3109	0.1116	1.4058	0.2565
164	8.2217	0.0066	2.8289	0.0712	2.6858	0.0808
123	1.0721	0.3065	0.6208	0.5425	0.8574	0.4317
174	10.9590	0.0019	0.5265	0.5945	1.3028	0.2825
143	1.4395	0.2371	1.4794	0.2397	1.6325	0.2079
36	2.5908	0.1150	0.7082	0.4983	0.0969	0.9079
‘Attila’	1.6095	0.2116	0.3449	0.7103	3.0080	0.0601
Heat-sensitive						
153	0.2864	0.5953	1.8578	0.1686	3.1759	0.0520
46	3.9264	0.0541	0.4808	0.6216	1.6654	0.2014
140	2.1833	0.1470	2.3069	0.1121	0.0758	0.9271
116	6.3687	0.0155	2.8096	0.0716	0.0727	0.9300
145	2.3923	0.1296	2.3907	0.1042	0.2230	0.8011
52	4.9529	0.0315	0.0588	0.9429	0.4792	0.6226
26	6.2975	0.0160	2.0432	0.1423	1.3826	0.2621
131	38.4098	2.06E-07	0.1848	0.8319	1.7099	0.1932
40	2.4682	0.1237	0.1893	0.8282	3.0231	0.0594
13	0.1204	0.7303	0.6577	0.5233	1.6845	0.1978
‘CDC Go’	0.7432	0.3935	3.1985	0.0509	0.2446	0.7841
Degrees of freedom	1		2		2	

Table A.6 Anther length ANOVA analysis degrees of freedom, F values, and probability for the temperature and spike region main effects, and temperature x spike region interaction presented in Tables 3.6 and 3.7 of the thesis.

RIL ID	Temperature		Spike region		Temperature x Spike region	
	F value	Pr (>F)	F value	Pr (>F)	F value	Pr (>F)
Heat-resistant						
28	37.5623	2.592e-07	8.6912	0.0007	1.5827	0.2174
148	11.9185	0.0013	6.2664	0.0042	1.7638	0.1839
164	22.8806	2.475e-05	7.6538	0.0016	0.9111	0.4105
123	37.5623	2.592e-07	8.6912	0.0007	1.5827	0.2174
174	0.1411	0.7090	1.9804	0.1507	0.0835	0.9200
143	19.0696	8.068e-05	0.8527	0.4335	0.0318	0.9687
36	1.8295	0.1840	0.4387	0.6480	1.0426	0.3622
‘Attila’	86.2210	9.779e-12	1.8171	0.1750	2.2684	0.1160
Heat-sensitive						
153	11.5713	0.0015	19.4381	1.057e-06	0.5454	0.5837
46	8.5909	0.0054	12.7538	4.697e-05	0.0795	0.9237
140	9.8174	0.0032	11.9623	7.731e-05	0.0228	0.9774
116	57.9417	1.962e-09	2.4520	0.0984	0.2498	0.7801
145	160.1896	6.354e-16	35.3246	1.004e-09	5.7749	0.0061
52	164.801	1.392e-15	12.4710	6.500e-05	0.0639	0.9382
26	2.8614	0.0989	5.1774	0.0103	2.0966	0.1369
131	45.192	3.63e-08	10.379	0.0002	0.9380	0.3994
40	24.2530	1.359e-05	17.6813	2.686e-06	0.8884	0.4189
13	56.8688	2.471e-09	8.4418	0.0008	0.0508	0.9506
‘CDC Go’	61.9190	8.537e-10	17.2820	3.340e-06	0.2670	0.7669
Degrees of freedom	1		2		2	

Table A.7 Ovule area and length ANOVA analysis degrees of freedom, F values, and probability for the temperature and spike region main effects, and temperature x spike region interaction presented in Table 3.8 of the thesis.

RIL ID	Temperature		Spike Region		Temperature x Spike Region	
	F value	Pr (>F)	F value	Pr (>F)	F value	Pr (>F)
Ovule area						
28	0.4398	0.5135	4.6138	0.0202	0.5781	0.5686
123	0.4433	0.5119	1.9163	0.1690	1.4507	0.2542
131	28.7208	1.678e-05	0.7345	0.4902	0.0413	0.9596
Ovule length						
28	0.1397	0.7118	2.8722	0.0762	0.8529	0.4387
123	0.7259	0.4026	1.0931	0.3513	0.6374	0.5374
131	34.2771	4.876e-06	0.9756	0.3914	0.1589	0.8540
Degrees of freedom	1		2		2	

Table A.8 Number of spikelets per spike ANOVA analysis degrees of freedom, F values, and probability for the temperature and RIL ID main effects, and temperature x RIL ID interaction presented in Table 3.9 of the thesis.

Source of variation	Degrees of freedom	F value	Pr (>F)
Temperature	1	2.5627	0.1111
RIL.ID	18	16.7119	<2e-16
Temperature x RIL ID	18	1.1688	0.2909

Table A.9 Number of fertile spikelets per spike ANOVA analysis degrees of freedom, F values, and probability for the temperature and RIL ID main effects, and temperature x RIL ID interaction presented in Table 3.9 of the thesis.

Source of variation	Degrees of freedom	F value	Pr (>F)
Temperature	1	9.1439	0.0028
RIL.ID	18	5.4639	3.348e-10
Temperature x RIL ID	18	2.1878	0.0049

Table A.10 Number of fertile spikelets per spike ANOVA analysis degrees of freedom, F values, and probability for the temperature and spike region main effects, and temperature x spike region interaction presented in Tables 3.10 and 3.11 of the thesis.

RIL ID	Treatment		Spike region		Treatment x Spike region	
	F value	Pr (>F)	F value	Pr (>F)	F value	Pr (>F)
Heat-resistant						
28	3.9512	0.0560	17.9024	7.637e-06	0.5854	0.5631
148	0.1128	0.7393	3.6591	0.0378	1.3534	0.2737
164	3.3383	0.0777	5.3858	0.0100	0.5786	0.5668
123	0.1163	0.7355	16.2500	1.654e-05	2.6453	0.0875
174	1.1502	0.2921	3.5446	0.0415	0.4460	0.6444
143	0.1220	0.7294	47.7744	4.727e-10	0.0305	0.9700
36	0.5479	0.4649	8.3562	0.0013	3.4247	0.0457
'Attila'	1.0305	0.3182	11.2341	0.0002	0.8015	0.4580
Heat-sensitive						
153	3.9474	0.0561	30.8596	5.247e-08	0.6842	0.5122
46	3.4774	0.0720	11.4403	0.0002	0.5761	0.5682
140	0.5590	0.4605	31.5062	4.253e-08	3.4006	0.0467
116	38.404	8.047e-07	18.617	5.533e-06	14.149	4.699e-05
145	9.3798	0.0046	23.9535	6.07e-07	1.0078	0.3771
52	1.3333	0.2573	5.7708	0.0076	0.5208	0.5993
26	0.7512	0.3930	1.9836	0.1552	3.5329	0.0419
131	0.5064	0.4828	0.5943	0.5590	0.6646	0.5227
40	2.2881	0.1408	16.0169	1.851e-05	0.7627	0.4752
13	0.2038	0.6552	13.0244	0.0001	1.0489	0.3642
'CDC Go'	0.8738	0.3574	5.3155	0.0106	1.5291	0.2331
Degrees of freedom	1		2		2	

Table A.11 Total grain weight ANOVA analysis degrees of freedom, F values, and probability for the temperature and RIL ID main effects, and temperature x RIL ID interaction presented in Table 3.12 of the thesis.

Source of variation	Degree of freedom	F value	Pr (>F)
Temperature	1	0.4145	0.5205
RIL.ID	18	5.6845	1.12e-10
Temperature x RIL ID	18	1.8748	0.0201

Table A.12 Total grain number ANOVA analysis degrees of freedom, F values, and probability for the temperature and RIL ID main effects, and temperature x RIL ID interaction presented in Table 3.12 of the thesis.

Source of variation	Degrees of freedom	F value	Pr (>F)
Temperature	1	0.3445	0.5580
RIL.ID	18	8.1577	9.162e-16
Temperature x RIL ID	18	1.5044	0.0920

Table A.13 Grain number ANOVA analysis degrees of freedom, F values, and probability for the temperature and spike region main effects, and temperature x spike region interaction presented in Tables 3.13 and 3.14 of the thesis.

RIL ID	Temperature		Spike region		Temperature x Spike region	
	F value	Pr (>F)	F value	Pr (>F)	F value	Pr (>F)
Heat-resistant						
28	3.7559	0.0621	45.2488	8.753e-10	0.4601	0.6356
148	0.0050	0.9442	4.1367	0.0259	0.4541	0.6393
164	0.0266	0.8716	10.3652	0.0004	0.2855	0.7536
123	0.6684	0.4200	25.1723	3.824e-07	1.3993	0.2624
174	2.2266	0.1461	11.7128	0.0002	0.6851	0.5117
143	2.9157	0.0981	29.2341	9.016e-08	0.3445	0.7113
36	0.3376	0.5656	9.7521	0.0005	2.1255	0.1370
'Attila'	0.4081	0.5278	12.4551	0.0001	0.1860	0.8312
Heat-sensitive						
153	1.6764	0.2053	41.0448	2.59e-09	0.9517	0.3974
46	1.2236	0.2775	14.3542	4.23e-05	0.1473	0.8637
140	0.9066	0.3486	30.7502	5.438e-08	2.1782	0.1308
116	9.9708	0.0036	22.1349	1.243e-06	4.5010	0.0195
145	12.4777	0.0014	32.3628	3.235e-08	0.3375	0.7162
52	0.3167	0.5778	20.0313	2.982e-06	1.4543	0.2496
26	0.8862	0.3540	15.3966	2.506e-05	0.5990	0.5558
131	3.2576	0.0823	6.7372	0.0042	1.2955	0.2902
40	2.3186	0.1383	41.7245	2.162e-09	0.2524	0.7786
13	0.1084	0.7446	14.1228	6.344e-05	0.9597	0.3957
'CDC Go'	6.6188	0.0153	16.4534	1.501e-05	1.8146	0.1803
Degrees of freedom	1		2		2	

Table A.14 Grain weight ANOVA analysis degrees of freedom, F values, and probability for the temperature and spike region main effects, and temperature x spike region interaction presented in Tables 3.15 and 3.16 of the thesis.

RIL ID	Temperature		Spike region		Temperature x Spike region	
	F value	Pr (>F)	F value	Pr (>F)	F value	Pr (>F)
Heat-resistant						
28	4.6094	0.0400	57.5408	5.403e-11	0.9168	0.4107
148	0.0681	0.7960	6.8714	0.0035	0.5377	0.5897
164	0.7709	0.3869	4.8980	0.0144	0.9945	0.3818
123	0.0068	0.9346	44.5163	1.052e-09	1.5421	0.2304
174	7.6425	0.0097	15.4213	2.476e-05	0.8596	0.4335
143	0.3351	0.5670	12.4305	0.0001	0.8891	0.4216
36	1.6467	0.2092	6.4452	0.0047	4.3458	0.0220
‘Attila’	0.0913	0.7646	13.8736	5.418e-05	0.2486	0.7814
Heat-sensitive						
153	1.0953	0.3037	35.3476	1.293e-08	1.1127	0.3419
46	0.4481	0.5084	21.4498	1.644e-06	0.0497	0.9516
140	0.5594	0.4603	31.2329	4.646e-08	1.6426	0.2104
116	5.6614	0.0239	24.3779	5.159e-07	2.2789	0.1198
145	8.0038	0.0082	36.7577	8.546e-09	0.2676	0.7670
52	0.0027	0.9588	28.9472	9.94e-08	1.2250	0.3080
26	1.0441	0.3150	19.8615	3.208e-06	0.7280	0.4912
131	10.3893	0.0033	13.4765	8.734e-05	1.3128	0.2857
40	1.7242	0.1991	66.8811	8.782e-12	0.3181	0.7299
13	0.0017	0.9675	22.6383	1.686e-06	0.8004	0.4595
‘CDC Go’	9.9172	0.0037	22.9477	8.986e-07	1.2692	0.2957
Degrees of freedom	1		2		2	

Table A.15 Total grain number and weight ANOVA analysis degrees of freedom, F values, and probability for the temperature and hormone treatment main effects, and temperature x hormone treatment interaction presented in Table 3.17 of the thesis.

RIL ID	Temperature		Hormone treatment		Temperature x hormone treatment	
	F value	Pr (>F)	F value	Pr (>F)	F value	Pr (>F)
Total grain number						
80	27.8885	3.615e-05	0.6778	0.4201	0.4939	0.4903
137	19.8112	0.0002	1.7259	0.2038	1.0800	0.3111
Total grain weight						
80	13.1623	0.0017	0.4503	0.5099	0.6795	0.4195
137	6.8644	0.0164	5.0329	0.0364	0.8398	0.3704
Degrees of freedom	1		1		1	

Table A.16 Auricle distance ANOVA analysis degrees of freedom, F values, and probability for the temperature and hormone treatment main effects, and temperature x hormone treatment interaction presented in Table 3.17 of the thesis.

RIL ID	Temperature		Hormone treatment		Temperature x hormone treatment	
	F value	Pr (>F)	F value	Pr (>F)	F value	Pr (>F)
80	7.2154	0.0120	0.0009	0.9765	0.0025	0.9608
137	4.7324	0.0382	8.4615	0.0070	1.8457	0.1851
Degrees of freedom	1		1		1	

Table A.17 Spike length ANOVA analysis degrees of freedom, F values, and probability for the temperature and hormone treatment main effects, and temperature x hormone treatment interaction presented in Table 3.17 of the thesis.

RIL ID	Temperature		Hormone treatment		Temperature x hormone treatment	
	F value	Pr (>F)	F value	Pr (>F)	F value	Pr (>F)
80	14.7781	0.0006	2.1262	0.1559	2.4467	0.1290
137	7.9013	0.0089	0.1814	0.6734	0.5877	0.4497
Degrees of freedom	1		1		1	

Table A.18 Number of spikelets per spike ANOVA analysis degrees of freedom, F values, and probability for the temperature and hormone treatment main effects, and temperature x hormone treatment interaction presented in Table 3.17 of the thesis.

RIL ID	Temperature		Hormone treatment		Temperature x hormone treatment	
	F value	Pr (>F)	F value	Pr (>F)	F value	Pr (>F)
80	27.2222	4.177e-05	1.8000	0.1947	0.5556	0.4647
137	2.0352	0.1691	0.2261	0.6396	0.0251	0.8756
Degrees of freedom	1		1		1	

Table A.19 Number of fertile spikelets per spike ANOVA analysis degrees of freedom, F values, and probability for the temperature and hormone treatment main effects, and temperature x hormone treatment interaction presented in Table 3.17 of the thesis.

RIL ID	Temperature		Hormone treatment		Temperature x hormone treatment	
	F value	Pr (>F)	F value	Pr (>F)	F value	Pr (>F)
80	37.7087	5.325e-06	1.6367	0.2154	0.4092	0.5297
137	10.4537	0.0042	0.8893	0.3569	0.2904	0.5959
Degrees of freedom	1		1		1	

Table A.20 Pollen viability ANOVA analysis degrees of freedom, F values, and probability for the temperature, hormone treatment, and spike region main effects, and temperature x hormone treatment, temperature x spike region, temperature x hormone treatment x spike region interaction presented in Tables 3.18 and 3.19 of the thesis.

RIL ID	Temperature		Hormone treatment		Spike region		Temperature x hormone treatment		Temperature x spike region		Temperature x hormone treatment x spike region	
	F value	Pr (>F)	F value	Pr (>F)	F value	Pr (>F)	F value	Pr (>F)	F value	Pr (>F)	F value	Pr (>F)
80	49.1233	6.485e-10	3.8038	0.0546	0.6376	0.5312	1.0348	0.3121	0.0295	0.9709	1.0820	0.3710
137	20.2934	2.154e-05	0.0357	0.8506	3.2066	0.0456	0.1252	0.7243	0.4640	0.6304	0.6323	0.6408
Degrees of freedom	1		1		2		1		2		4	

Table A.21 Anther length ANOVA analysis degrees of freedom, F values, and probability for the temperature, hormone treatment, and spike region main effects, and temperature x hormone treatment, temperature x spike region, temperature x hormone treatment x spike region interaction presented in Tables 3.18 and 3.19 of the thesis.

RIL ID	Temperature		Hormone treatment		Spike region		Temperature x hormone treatment		Temperature x spike region		Temperature x hormone treatment x spike region	
	F value	Pr (>F)	F value	Pr (>F)	F value	Pr (>F)	F value	Pr (>F)	F value	Pr (>F)	F value	Pr (>F)
80	90.7772	5.15 e-15	4.9230	0.0292	21.3926	3.096e-08	11.9973	0.0008	3.0001	0.0552	0.3679	0.83086
137	133.5386	< 2.2e-16	2.7843	0.0989	13.2899	9.668e-06	0.0130	0.9095	0.1780	0.8373	0.4773	0.7523
Degrees of freedom	1		1		2		1		2		4	

Table A.22 Spikelet length ANOVA analysis degrees of freedom, F values, and probability for the temperature, hormone treatment, and spike region main effects, and temperature x hormone treatment, temperature x spike region, temperature x hormone treatment x spike region interaction presented in Tables 3.18 and 3.19 of the thesis.

RIL ID	Temperature		Hormone treatment		Spike region		Temperature x hormone treatment		Temperature x spike region		Temperature x hormone treatment x spike region	
	F value	Pr (>F)	F value	Pr (>F)	F value	Pr (>F)	F value	Pr (>F)	F value	Pr (>F)	F value	Pr (>F)
80	162.8717	< 2.2e-16	1.0025	0.3196	29.2854	2.241e-10	12.7873	0.0006	1.4021	0.2518	0.6380	0.6368
137	74.3684	3.395e-13	2.7358	0.1019	13.5637	7.857e-06	2.2576	0.1367	0.2785	0.7576	0.3593	0.8369
Degrees of freedom	1		1		2		1		2		4	

Table A.23 Grain number ANOVA analysis degrees of freedom, F values, and probability for temperature, hormone treatment, and spike region main effects, and temperature x hormone treatment, temperature x spike region, temperature x hormone treatment x spike region interaction presented in Tables 3.18 and 3.19 of the thesis.

RIL ID	Temperature		Hormone treatment		Spike region		Temperature x hormone treatment		Temperature x spike region		Temperature x hormone treatment x spike region	
	F value	Pr (>F)	F value	Pr (>F)	F value	Pr (>F)	F value	Pr (>F)	F value	Pr (>F)	F value	Pr (>F)
80	57.4691	2.547e-10	1.1728	0.2832	35.2250	7.607e-11	1.1728	0.2832	1.7844	0.1767	0.0690	0.9911
137	42.6353	1.578e-08	3.7142	0.0587	26.9370	4.486e-09	2.3242	0.1326	4.0245	0.0229	0.1969	0.9391
Degrees of freedom	1		1		2		1		2		4	

Table A.24 Grain weight ANOVA analysis degrees of freedom, F values, and probability for the temperature, hormone treatment, and spike region main effects, and temperature x hormone treatment, temperature x spike region, temperature x hormone treatment x spike region interaction presented in Tables 3.18 and 3.19 of the thesis.

RIL ID	Temperature		Hormone treatment		Spike region		Temperature x hormone treatment		Temperature x spike region		Temperature x hormone treatment x spike region	
	F value	Pr (>F)	F value	Pr (>F)	F value	Pr (>F)	F value	Pr (>F)	F value	Pr (>F)	F value	Pr (>F)
80	16.6031	0.0002	0.4710	0.4955	33.8545	2.957e-10	0.8029	0.3742	1.1326	0.3297	0.1582	0.9585
137	13.7311	0.0005	10.0674	0.0024	30.9017	5.953e-10	1.6798	0.1999	1.5367	0.2234	0.3392	0.8505
Degrees of freedom	1		1		2		1		2		4	